Report No. FHWA-KS-03-8
FINAL REPORT

ACCELERATED TESTING FOR STUDYING PAVEMENT DESIGN AND PERFORMANCE (FY 2002)

Performance of Foamed Asphalt Stabilized Base in Full Depth Reclaimed Asphalt Pavement

Stefan Romanoschi, Ph.D., P.E.
Mustaque Hossain, Ph.D., P.E.
Paul Lewis
Octavian Dumitru
Kansas State University

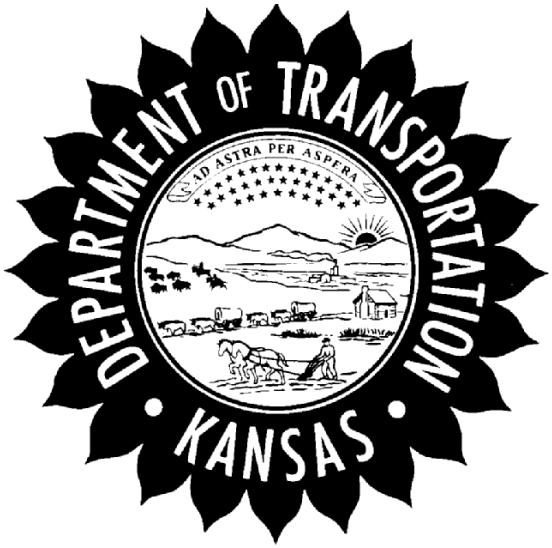

AUGUST 2004

KANSAS DEPARTMENT OF TRANSPORTATION

Division of Operations
Bureau of Materials and Research

1 Report No. FHWA-KS-03-8	**2 Government Accession No.**	**3 Recipient Catalog No.**
4 Title and Subtitle ACCELERATED TESTING FOR STUDYING PAVEMENT DESIGN AND PERFORMANCE (FY 2002) Performance of Foamed Asphalt Stabilized Base in Full Depth Reclaimed Asphalt Pavement		**5 Report Date** August 2004 **6 Performing Organization Code**
7 Author(s) Stefan Romanoschi, Ph.D., P.E.; Mustaque Hossain, Ph.D., P.E.; Paul Lewis and Octavian Dumitru		**8 Performing Organization Report No.**
9 Performing Organization Name and Address Kansas State University; Department of Civil Engineering 2118 Fiedler Hall Manhattan, Kansas 66506		**10 Work Unit No. (TRAIS)** **11 Contract or Grant No.** C1289
12 Sponsoring Agency Name and Address Kansas Department of Transportation Bureau of Materials and Research, Research Unit 2300 Southwest Van Buren Street Topeka, Kansas 66611-1195		**13 Type of Report and Period Covered** Final Report July 2001- November 2003 **14 Sponsoring Agency Code** RE-0165-01
15 Supplementary Notes For more information write to address in block 9.		

16 Abstract

This report covers the Fiscal Year 2002 project conducted at the Accelerated Testing Laboratory at Kansas State University. The project was selected and funded by the Midwest Accelerated Testing Pooled Fund Program , which includes Iowa, Kansas, Missouri and Nebraska.

The objective of this research was to determine the effectiveness of the use of foamed asphalt stabilized Recycled Asphalt Pavement from full-depth reclamation (FAS-FDR) as base material for flexible pavements. The experiment, conducted at the Accelerated Testing Laboratory (ATL) of Kansas State University, consisted of constructing four pavements, one with a nine inch conventional Kansas AB-3 granular base and three with six, nine and 12 inches of FAS-FDR, and subjecting them to full-scale accelerated pavement test. All four pavements sections were loaded with 500,000 ATL load repetitions, at room temperature and under moderate moisture levels in the subgrade soil. The measured stresses and strains as well as the permanent deformation (rutting) observed on the pavement sections indicated that FAS-FDR can be successfully used as a base material. The measured rut depths and compressive vertical stresses at the top of the subgrade suggest that one inch of FAS-FDR base shows performance equivalent to that of one-inch conventional Kansas AB-3 granular base. The effective structural number computed from the FWD deflection tests on the as-constructed pavements showed that average structural layer coefficient for the FAS-FDR base material is 0.18.

17 Key Words Accelerated Pavement Test, Pavement, Foamed Asphalt, Stabilized Base, Full-Depth Reclamation, Recycled Asphalt, Stress, Strain, Subgrade, Overlay		**18 Distribution Statement** No restrictions. This document is available to the public through the National Technical Information Service, Springfield, Virginia 22161	
19 Security Classification (of this report) Unclassified	**20 Security Classification (of this page)** Unclassified	**21 No. of pages** 148	**22 Price**

Form DOT F 1700.7 (8-72)

ACCELERATED TESTING FOR STUDYING PAVEMENT DESIGN AND PERFORMANCE (FY 2002)

Performance of Foamed Asphalt Stabilized Base in Full Depth Reclaimed Asphalt Pavement

Final Report

Prepared by

Stefan Romanoschi, Ph.D., P.E.
Associate Professor

Mustaque Hossain, Ph.D., P.E.
Professor

Paul Lewis

and

Octavian Dumitru

All with Kansas State University

A Report on Research Sponsored By

THE KANSAS DEPARTMENT OF TRANSPORTATION
TOPEKA, KANSAS

KANSAS STATE UNIVERSITY
MANHATTAN, KANSAS

August 2004

NOTICE

The authors and the state of Kansas do not endorse products or manufacturers. Trade and manufacturers names appear herein solely because they are considered essential to the object of this report.

This information is available in alternative accessible formats. To obtain an alternative format, contact the Office of Transportation Information, Kansas Department of Transportation, 915 SW Harrison Street, Room 754, Topeka, Kansas 66612-1568 or phone (785) 296-3585 (Voice) (TDD).

DISCLAIMER

The contents of this report reflect the views of the authors who are responsible for the facts and accuracy of the data presented herein. The contents do not necessarily reflect the views or the policies of the state of Kansas. This report does not constitute a standard, specification or regulation.

ABSTRACT

The objective of this research was to determine the effectiveness of the use of foamed asphalt stabilized Recycled Asphalt Pavement from full-depth reclamation (FAS-FDR) as base material for flexible pavements. The experiment, conducted at the Accelerated Testing Laboratory (ATL) of Kansas State University, consisted of constructing four pavements, one with a nine inch conventional Kansas AB-3 granular base and three with six, nine and 12 inches of FAS-FDR, and subjecting them to full-scale accelerated pavement testing. All four pavements sections were loaded with 500,000 ATL load repetitions, at room temperature and under moderate moisture levels in the subgrade soil. The measured stresses and strains as well as the permanent deformation (rutting) observed on the pavement sections indicated that FAS-FDR can be successfully used as a base material. The measured rut depths and compressive vertical stresses at the top of the subgrade suggest that one inch of FAS-FDR base shows performance equivalent to that of one-inch conventional Kansas AB-3 granular base. The effective structural number computed from the FWD deflection tests on the as-constructed pavements showed that average structural layer coefficient for the FAS-FDR base material is 0.18.

ACKNOWLEDGEMENTS

The research project was selected, designed and monitored by the members of the Midwest States Accelerated Pavement Testing Pooled Fund Technical Committee. The committee includes Mr. Andy Gisi, Kansas Department of Transportation (KDOT), Chair, Mr. George Woolstrum, Nebraska Department of Roads (NDOR), Mr. John Donahue, Missouri Department of Transportation (MDOT), and Mr. Mark Dunn, Iowa Department of Transportation (IADOT). The authors acknowledge the cooperation and supervision of all committee members in this study. Mr. Mike Heitzman of IADOT took personal interest in this research and designed the FAS-FDR mixture and supervised FAS-FDR base construction. The authors acknowledge his valuable contribution in this study. Contributions of Mr. Roger Swart, Mr. James Peterson, Ms. Jeniffer Hancock and Ms. Nicoleta Dumitru in various phases of this study are also gratefully acknowledged. The research team is also grateful to Sergeant Joe French from the Motor Vehicle Inspection Division of the Kansas Highway Patrol, for his help in the measurement and calibration of the ATL axle load.

TABLE OF CONTENTS

LIST OF TABLES

LIST OF FIGURES

Chapter 1
Introduction

1.1 Report Organization

This manuscript is the final report that describes the research project conducted under KDOT Contract C1355, "Accelerated Testing for Studying Pavement Design and Performance – FY 2002", (KSU Research Project No. 5-34257). This contract is funded by the Midwest States Accelerated Pavement Testing Pooled Fund Program. States participating in this program are Iowa, Kansas, Missouri and Nebraska.

The purpose of the project is to conduct the experiment selected by the Midwest States Accelerated Testing Pooled Funds Technical Committee for the Fiscal Year 2002 (FY-02). The experiment titled "Performance of Foamed Asphalt Stabilized Base in Full-Depth Reclaimed Asphalt Pavement " is the 11^{th} experiment conducted at the Civil Infrastructures Systems Lab (CISL), formerly known as the Accelerated Testing Lab (ATL), and is, therefore, now identified as CISL-Exp#11. The first two ATL experiments, ATL-Exp#1 and #2 were reported in reference [1], ATL-Exp#3 through #6 were reported in reference [2], ATL-Exp#7 is reported in reference [3], ATL-Exp#8 is reported in reference [4], CISL Exp #9 and 10 are reported in reference [5].

This report describes the following aspects of CISL-Experiment #11:

1. The test setup and testing strategies followed
2. The pavement structure and material used for pavement construction.
3. The executed monitoring plan.
4. A description of the experiment: This includes the experimental work performed in terms of the total number of load cycles applied to each

specimen, testing condition (load magnitude, temperature, etc.), and the testing activity and corresponding time schedule.

5. A summary of the data collected, results from instrumentation, variations (curves/histograms) of the response data with the number of load cycles applied, and comparison of the responses of different pavement constructions strategies.
6. The conclusions drawn from the results obtained and performance observed.
7. Recommendations to the participating highway agencies for practical implementation and future experiments.

1.2 Project Overview

The goal of this research was to evaluate the structural performance of foamed asphalt stabilized base layers obtained from full-depth reclamation of an existing asphalt pavement. The objective was accomplished by conducting full-scale accelerated pavement tests at the Civil Infrastructure Systems Laboratory on flexible pavements with foamed asphalt stabilized bases.

The work described in this report examines the experimental aspects of the research study. This mainly entails the application of full-scale axle loads on full-scale flexible pavements. The experimental work was conducted at the Civil Infrastructure Systems laboratory (CISL) of Kansas State University. The work also includes monitoring and recording deflection, strain, soil pressure, and temperature in the pavement structures tested. Mechanistic responses were calculated and compared with the observed data. The Falling Weight Deflectometer (FWD) deflection data were used to characterize the pavement layers.

This experimental investigation, together with the observed performance of similar situations on in-service highways and supplemented with additional analytical studies, can help the state highway agencies establish special provisions/standards for the use of foamed asphalt in

full-depth reclamation to construct stabilized base layers. It may also lead to standard guidelines for instrumentation of in-service highway pavements in the states participating in the Pooled Fund Program. Further work could include numerical modeling, and comparative studies with other research in the United States and abroad.

Chapter 2

Background

2.1 Foamed Asphalt Stabilized Reclaimed Asphalt Pavement (RAP) Material

Cold recycling is gaining recognition and popularity worldwide as a cost effective method of rehabilitating distressed asphalt pavements [6]. In the in-plant recycling method, the asphalt surface layer of the distressed pavement is milled and the resulting material, commonly known as RAP, is transported to a storage site and stockpiled. The material from the stockpiles is later mixed with a stabilizing agent (asphalt emulsion, foamed asphalt, cement slurry, lime or fly ash) and aggregates in a conventional pug mill. The resulting mix is then transported to the construction site, placed and compacted. The major advantage of this recycling method is that it allows a good control of the quantities of aggregates, stabilizing agent and RAP in the mix, and the resulting mix is usually very uniform.

In-situ recycling requires the use of specially designed recycling machines with a mixing chamber. While the milling operation is taking place in the front part of the machine, the milled material passes through a mixing chamber where it is mixed with the stabilizing agent (lime, fly ash, bitumen emulsion, foamed bitumen or cement slurry). After mixing, the material is placed on the milled pavement and compacted. The process is carried out in a single-pass operation. The main advantage of the process is that the milled material is not transported and stockpiled, thus costs are reduced. The main disadvantage is that the stabilized material is less uniform than that obtained through in-plant mixing.

The use of foamed bitumen as a stabilizing agent is not a new idea. In 1956, Dr. Ladis H. Csanyi, Professor at the Engineering Experiment Station of Iowa State University, investigated

the possibility of using the foamed asphalt as a binder for soil stabilization [7]. Foaming of the asphalt reduces its viscosity considerably and has shown to increase adhesion properties making it well suited for mixing with cold and moist aggregates. No chemical reaction is involved, only the physical properties of the asphalt are temporarily altered. When the cold water comes into contact with the hot asphalt, it turns into steam and in turn, gets trapped in the asphalt as thousands of tiny steam bubbles. After a few minutes, the asphalt will regain its original properties once the steam evaporates. Figure 2.1 shows the schematic of the asphalt foaming process.

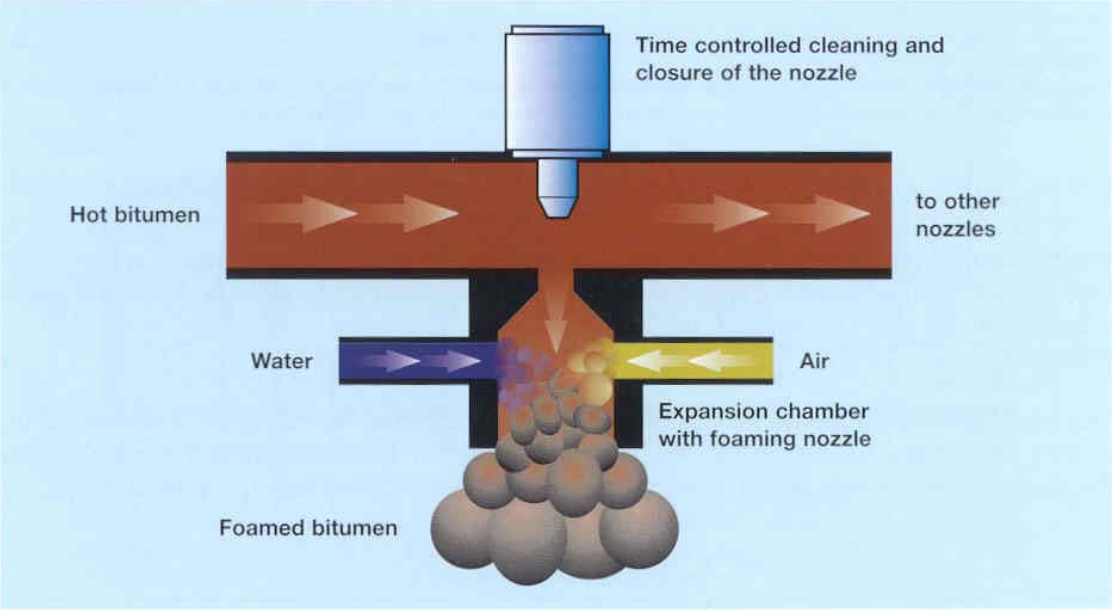

FIGURE 2.1: Schematic of the Foamed Asphalt Production [8]

Foamed asphalt is generally characterized in terms of expansion ratio and half-life. The expansion ratio of the foam is defined as the ratio between the maximum achieved volume of the foamed asphalt and the original volume of the non-foamed asphalt. This expansion is approximately 15 to 20 times the volume of the original asphalt. The half-life is the time elapsed from the moment the foamed asphalt was at its maximum volume to the time it reached half of

this volume. The half-life is measured in seconds and usually lies in between 10 and 15 seconds. Figure 2.2 explains these parameters to define foamed asphalt quality. As a rule, the larger the expansion and the longer the half-life, the better the quality of the foamed asphalt.

2.2 Prior Reported Use of Foamed Asphalt

The first reported use of foamed asphalt dates back to 1957 on an Iowa county road. Several other field applications were also reported including projects in Arizona (1960) and in Nipawin, Canada (1960-1962). However, the original process consisted of injecting high-pressure steam, at controlled pressure and temperature, into a heated penetration grade asphalt cement. This required special equipment on the job site such as a boiler and was not very practical.

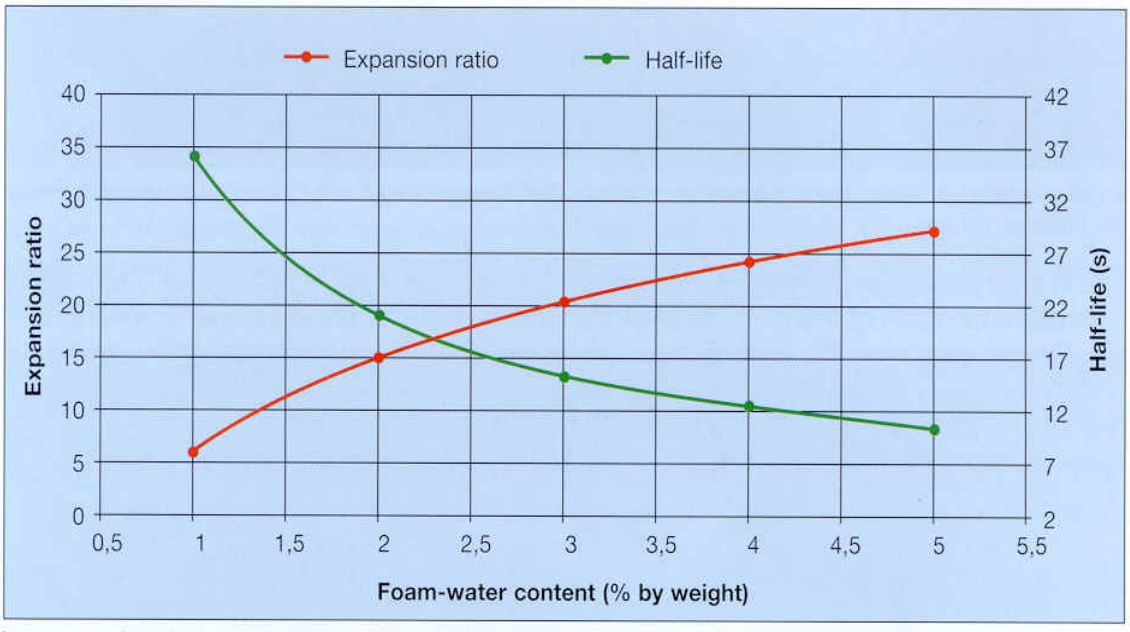

FIGURE 2.2: Parameters to Determine the Quality of Foamed Asphalt [8]

In 1968, Mobil Oil Australia modified the original process by adding cold water rather than steam, into a stream of hot asphalt in a low-pressure system [9]. This made the process much more practical and economical. The foam was created within an expansion chamber after which it was dispersed through a series of nozzles, onto the aggregate mass. However, the

nozzles were prone to blockage and the manufacturer could not control the foam characteristics. Recently, Wirtgen GmbH of Germany, Soter of Canada, and CMI of the United States have developed new equipment for producing foamed asphalt. The Soter system is very suitable for a Caterpillar RR-250 or RR-350 system used in full-depth reclamation [10]. A list of reference publications of foamed asphalt technology is assembled in Appendix A.

Stabilization of RAP material with foamed asphalt has been tried in the United States and abroad. In a laboratory study, Roberts et al. [11] compared the performance of stabilized RAP material with foamed asphalt with those treated with cut-back asphalt and asphalt emulsion. An important finding was that the engineering properties of the foamed-asphalt stabilized RAP materials were equal or superior to the cut back and emulsion stabilized RAP materials. Macaronne [12], [13], Lancaster [14] and Ramanujam [15] reported successful stabilization with foamed asphalt of RAP material, both in-plant and in-place, in Australia. Muthen [16], Lewis [17] and Van der Walt [18] have reported the use of foamed asphalt to stabilize RAP material in South Africa. All these studies have shown that foamed asphalt stabilization of the RAP is effective but do not clearly indicate the structural contribution of the stabilized layer or a comparative performance of this layer and that of a conventional granular base.

Van der Walt [18] has compared different methods of obtaining the foamed asphalt that will be later used to stabilize the materials obtained from full-depth reclamation of an asphalt pavement. The RAP material in this case would be contaminated with aggregates and soil from the subgrade layers. Unfortunately, this laboratory study does not provide any information on the field performance of the stabilized material.

Van Wijk [19], [20] reported the successful use of foamed asphalt stabilization of the RAP material on two road sections in Indiana. The study estimated the structural layer

coefficient of the stabilized material between 0.19 and 0.32. The road sections showed a satisfactory performance during the first few years of life, indicating that this recycling method is promising. However, it is important to note that only 'clean' RAP material was used. The RAP material was obtained by milling only the top five inches of a distressed asphalt pavement. Therefore, the RAP was not contaminated with aggregates or soil.

In full-depth recycling of asphalt pavements, a common recycling procedure nowadays, the salvaged material would contain not only RAP material, but also aggregates from the granular base and in some case, soil from the subgrade. Thus it would be useful to determine if the foamed-asphalt stabilization is effective, and what are the structural properties of this new material as bases in a pavement system.

Chapter 3

Description of the Test Experiment

This section gives a detailed description of the test, CISL experiment #11 including the design of the foamed asphalt stabilized RAP mixture, pavement construction, loading conditions, sensor installation and data acquisition, and the performance monitoring plan.

3.1 Laboratory Mix Design of Foamed Asphalt Stabilized Mixture

The laboratory mix design was conducted by the IADOT Central Materials Laboratory in Ames, Iowa. Sample aggregates, reclaimed asphalt pavement (RAP), soil, and the PG binder to be used in this project were shipped to IADOT to develop the mixture design. A Wirtgen Foamed Bitumen Laboratory Plant (WLB 10) (Figure 3.1) was used in the mix design process.

3.1.1 Determination of the Foaming Characteristics of the Asphalt

The objective of this part of the mix design was to determine the temperature and percentage of water injection that will optimize the foaming properties of the binder selected for this project by maximizing the expansion ratio and half-life of the foamed asphalt. In this mixture design, a PG 64-28 binder was used. The binder was selected based on the consideration that this is one of the most common PG binder grades used in Kansas. The steps followed in mixture design are as follows:

1. Calibrate the asphalt and water flow rates;
2. Select three temperatures at which the foaming characteristics are to be measured, typically 160˚C, 170˚C and 180˚C (320˚F, 356˚F and 392˚F). Bring the temperature of the asphalt to the required temperature and maintain that temperature for at least 10 minutes before commencing the foam production. Then, for each temperature measure the foaming

characteristics of five samples of foamed asphalt at water injection rates ranging from 1 % to 5 % by mass of the asphalt, in increments of 1 %, as follows:

a. For each sample, allow 500g (1.12lbs) of foam to discharge into a 20litre (5gal)steel drum;
b. Mark the maximum volume to which the foam expands, using a marking pencil on the side of the drum. Using a stopwatch, measure the time in seconds that the foam takes to dissipate to half of its maximum volume. This is defined as the half-life. Calculate the expansion ratio of the foamed asphalt by dividing the maximum foamed volume by the volume of asphalt in the drum after the foam has completely dissipated (allow at least 3 minutes); and
c. Plot a graph of the expansion ratio and half-life versus moisture content for all the samples on the same set of axes. This will enable the foam- water content to be optimized.
d.

The optimum water content for foaming of the asphalt cement was found to be at 3% water injection rate at a binder temperature of 160˚C (320˚F) (Figure 3.2).

FIGURE 3.1: Wirtgen Mobile Foamed Bitumen Laboratory Plant

3.1.2 Aggregate Preparation

As mentioned before, a crushed limestone aggregate, RAP and soil were used in the mixture design. The following steps were followed in aggregate preparation:

- Carry out standard tests to determine the grading and plasticity index (PI) of the aggregates;
- Carry out any blending of more than one aggregate if required to provide the required grading. In this step, the crushed limestone rock, RAP, soil and Portland cement were blended at 50%, 37%, 12% and 1%, respectively. A typical Kansas asphalt pavement that is a candidate for FDR would consist of 6 in. HMA, 8 in. aggregate base. In the FDR process, the milled material may consist of 2 in. of subgrade soil. Table 3.1 tabulates the individual and combined gradation. Figure 3.3 shows the combined gradation.

- Determine the Optimum Moisture Content (OMC) as per the modified moisture-density relationship test, AASHTO designation T180;
- Oven-dry the material to constant mass at 105˚C (221˚F). For RAP, drying should be carried out at a lower temperature to prevent the particles from sticking together;

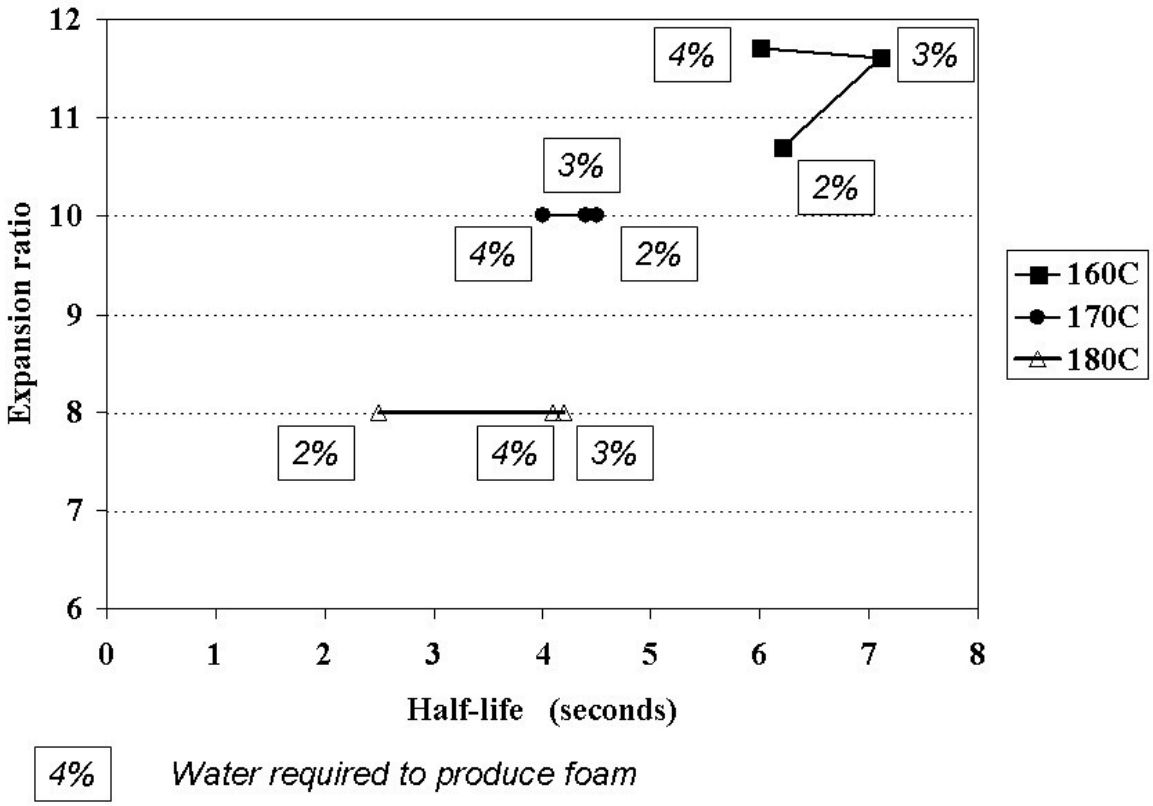

- Split the sample into five 10 kg (2.25 lbs) batches.

FIGURE 3.2: Asphalt Cement Foaming Characteristics

TABLE 3.1: Gradation of the Materials Used in the Construction of Foamed Asphalt Stabilized RAP Base (% passing)

Sieve #	Sieve Size (mm)	Crushed Rock	RAP	Soil	Combined	Tolerance
1"	25	99.0	100.0	100.0	99.5	100 – 76
3/4"	19	90.0	100.0	100.0	95.0	92 – 70
1/2"	12.5	62.0	92.0	100.0	78.0	86 – 62
3/8"	9.5	48.0	84.0	100.0	68.0	80 – 56
#4	4.75	29.0	61.0	100.0	50.0	67 – 45
#8	2.36	19.0	36.0	100.0	36.0	57 – 35
#16	1.18	14.0	18.0	100.0	27.0	48 – 26
#30	0.6	12.0	7.0	100.0	22.0	40 – 19
#50	0.3	11.0	1.7	100.0	19.0	30 – 12
#100	0.15	9.7	0.4	100.0	18.0	25 – 8
#200	0.075	8.8	0.1	99.0	17.3	20 - 5

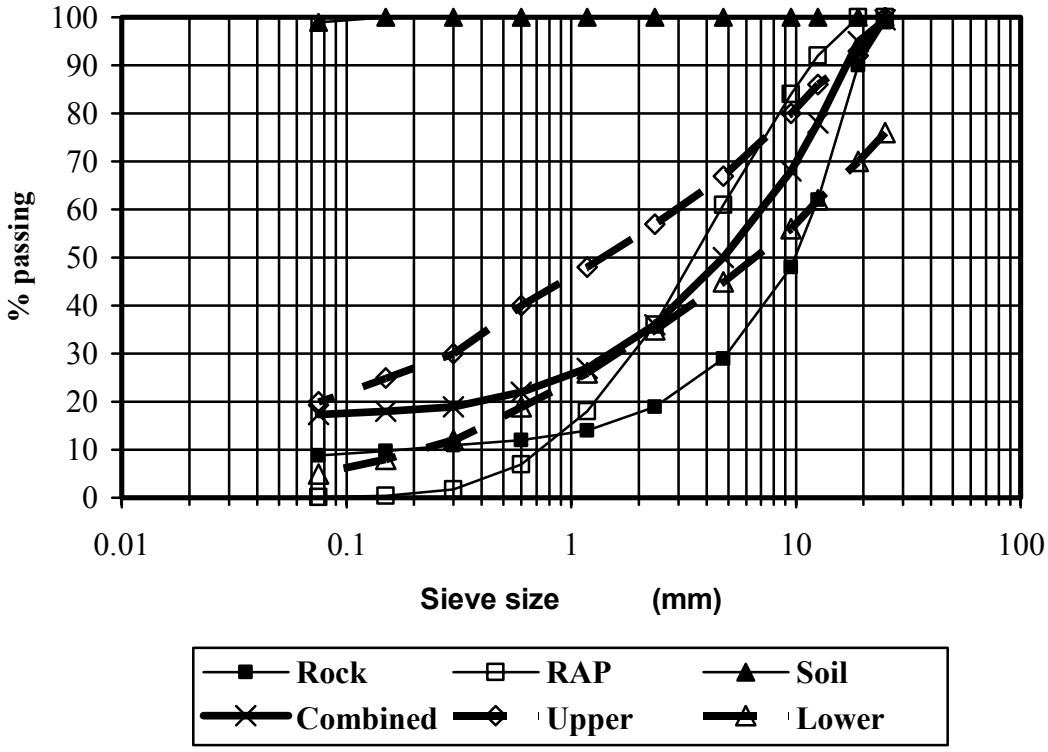

FIGURE 3.3: Combined Aggregate, RAP and Soil Gradation

3.1.3 Determination of Optimum Asphalt Content

3.1.3.1 Sample Preparation and Stabilizing with Foamed Asphalt

To determine the optimum asphalt content, mixture samples were prepared by injecting with foamed asphalt. All five 10kg (2.25lb.) aggregate samples were injected with foamed asphalt at different bitumen contents, 1% apart. For each batch, the following procedure was carried out:

a. Place the entire 10 kg (2.25lb.) batches into the bowl of the mechanical mixer (WLB 10 laboratory foamed bitumen unit/mixer);

b. Add the required percentage (by mass) of Portland cement as per the formula:

$M_{CEM} = [P_{CEM} / 100]* [10000 * (1 + P_{CEM} /100)]$ - metric
(3.1)
$M_{CEM} = 2.25 [P_{CEM} * (1 + P_{CEM} /100)]/100$ -U.S. customary

Where:
M_{CEM} = mass of cement to be added in g *(lbs)*; and
P_{CEM} = percentage of Portland cement (and/or lime) required in %;

c. Add sufficient water to bring the sample to 90% of OMC as per the following formula:

$M_{WATER} = 0.9 * (OCM / 100) * (1000 * M_{CEM})$
(3.2)

Where:
M_{WATER} = mass of water to be added in g *(lbs)*;
OMC = optimum moisture content in %;
M_{CEM} = mass of Portland cement added in g *(lbs)*;

d. Position the mechanical mixer adjacent to the WLB10 unit so that the foamed asphalt can be discharged directly into the mixing bowl;

e. Mix the aggregates and moisture in the mixer for one minute;

f. Without stopping the mixer, discharge the required mass of foamed asphalt into the mixing bowl;

g. Continue mixing the foamed asphalt into the moistened aggregate for a further 30 seconds;

h. Repeat this procedure to obtain five samples of foamed asphalt stabilized material at the different asphalt contents. These samples are now ready for the manufacture of briquettes in the Marshall molds.

3.1.3.2 Sample Compaction

The sample briquettes were prepared following these steps:

a. Prepare the Marshall mold and hammer by cleaning the mold, collar, base-plate and face of the compaction hammer;

b. Place a round plastic or paper disc at the bottom of the mold;

c. Weigh enough material to achieve a compacted height of 63.5 ± 1.5mm (2.5 ± 0.05in.) Usually 115 g (0.25 lbs) is sufficient.

d. Rod the mixture with a spatula 15 times around the perimeter and rod the rest of the surface 10 times leaving the surface slightly rounded;

e. Compact the mixture by applying 75 blows with the compaction hammer. Care must be taken to ensure the free fall of the hammer;

f. Remove the mold and collar from the pedestal, invert (turn over), then replace it and press it down so that it rests firmly on the base plate;

g. Compact the other face of the briquette with a further 75 blows.

3.1.3.3 Sample Curing

The curing was accomplished following these steps:

a. After compaction, remove the mold from the base-plate and extrude it by means of an extrusion jack;

b. Pace the samples on a smooth flat tray and cure in a forced draft oven for a further 72 hours at 40˚C (104˚F).

3.1.3.4 Dry Density Calculation

The Dry Density of the compacted specimens was calculated using the following formula:

$$D = [100/(d + 100)]*[W/(3.1415*r^2*h)]*1000 \quad (3.3)$$

Where:

D = dry density in kg/m3 ;
h = height of specimen in cm (1.0 in = 2.54 cm);
W = mass of sample in g (1.0 lbs = 453.6 g);
r = radius of specimen in cm (1.0 in = 2.54 cm);
d = moisture content of sample in % .

The densities obtained are shown below:

Binder Content (%)	**Compacted (Wet) Density (pcf)**
2	135.2
3	134.1
3.5	133.5
4	132.9

3.1.3.5 Determination of Indirect Tensile Strength

The standard indirect tensile strength (ITS) test was used to test the briquettes under both dry and soaked conditions. The ITS was determined by measuring the ultimate load to failure of a specimen which is subjected to a constant deformation rate of 2 in/minute on its diametrical axis. The procedure followed is as follows:

a. Leave the cured briquettes overnight at room temperature before testing;
b. Measure the height of each briquette at four evenly spaced places around the circumference and calculate the average height, L (in);
c. Measure the diameter of each specimen, D (in);
d. Place the briquettes in the air cabinet at 25˚C ± 1˚C (77˚F ± 2˚F) for at least 1 hour, but not for longer than 2 hours before testing;
e. Remove a specimen from the air cabinet and place it into the loading apparatus;
f. Position the sample such that the loading strips are parallel and centered on the vertical diametrical plane;

g. Place the transfer plate on the top bearing strip and position the assembly centrally under the loading ram of the compression testing device;

h. Apply the load to the specimen, without shock, at a rate of advance of 2 in. per minute until the maximum load is reached;

i. Record this load, P (in lbs), accurate to 0.1 lb.

j.

The ITS of the soaked samples were used following the procedure as below:

- Place the cured specimen in a vacuum desiccator and cover with water at 25˚C ± 1˚C (77˚F ± 2˚F);
- Apply a vacuum of 50 mm of mercury for 60 ± 1 minutes. For this mixture design, no vacuum desiccator is available and the samples were soaked for 24 hours at 25˚C ± 1˚C (77˚F ± 2˚F);
- Remove the specimen, surface dry and test for the ultimate tensile load, as described above.

The ITS for each specimen was calculated using the following formula:

$$ITS = 2 * P / (3.1415 * L * D) \quad (3.4)$$

Where:

ITS = Indirect Tensile Strength in psi;

P = maximum applied load in lbs;

L, D = average height and diameter of the specimen in inches

The ITS results for both dry and soaked samples are shown in Table 3.2. For 3% binder content, the measured Tensile Strength Ratio was 66.9%, lower than 80% considered as the minimum value for a moisture insensitive material. This indicates that the foamed asphalt stabilized base material is sensitive to the action of water. Measures needs to be adopted to limit the moisture levels in the foamed asphalt stabilized base so its durability will not be affected.

TABLE 3.2: Indirect Tensile Strength Test Results

Binder Content (%)	Indirect Tensile Strength (psi)		Tensile Strength Ratio
	Dry	Soaked	(%)
2.0	89.2	40.7	45.6
3.0	98.1	65.6	66.9
3.5	93.9	47.6	50.7
4.0	89.5	47.8	53.4

3.1.4 Determination of the Design Asphalt Content

A graph of the measured ITS versus asphalt content (added asphalt) for all samples (both dry and soaked) was plotted. The added asphalt content at which the soaked ITS was maximum was taken as the design asphalt content. For this mixture, the design asphalt content was found to be 3%.

3.2 Test Bed and Construction

The test bed consists of two six feet deep pits, the North Pit (approx. 15 x 20 feet square) and the South pit (approx. 20 x 20 feet square). The pits are surrounded by the reinforced concrete walls. There is no integral drainage system for the pits. An 8 -12 in. layer of pea gravel was placed at the bottom of the pits and was covered by geotextiles to intrusion of fines from the subgrade layer.

In this study, four pavement sections were constructed in the pits, two in the North pit ((NN & NS) and two in the South pit (SN and SS). Figure 3.4 shows the schematic of the pavement cross sections. The subgrade and the base layers were placed in the second part of November in 2001. The asphalt concrete surface layer was constructed on the same day in both pits during the first week of December 2001.

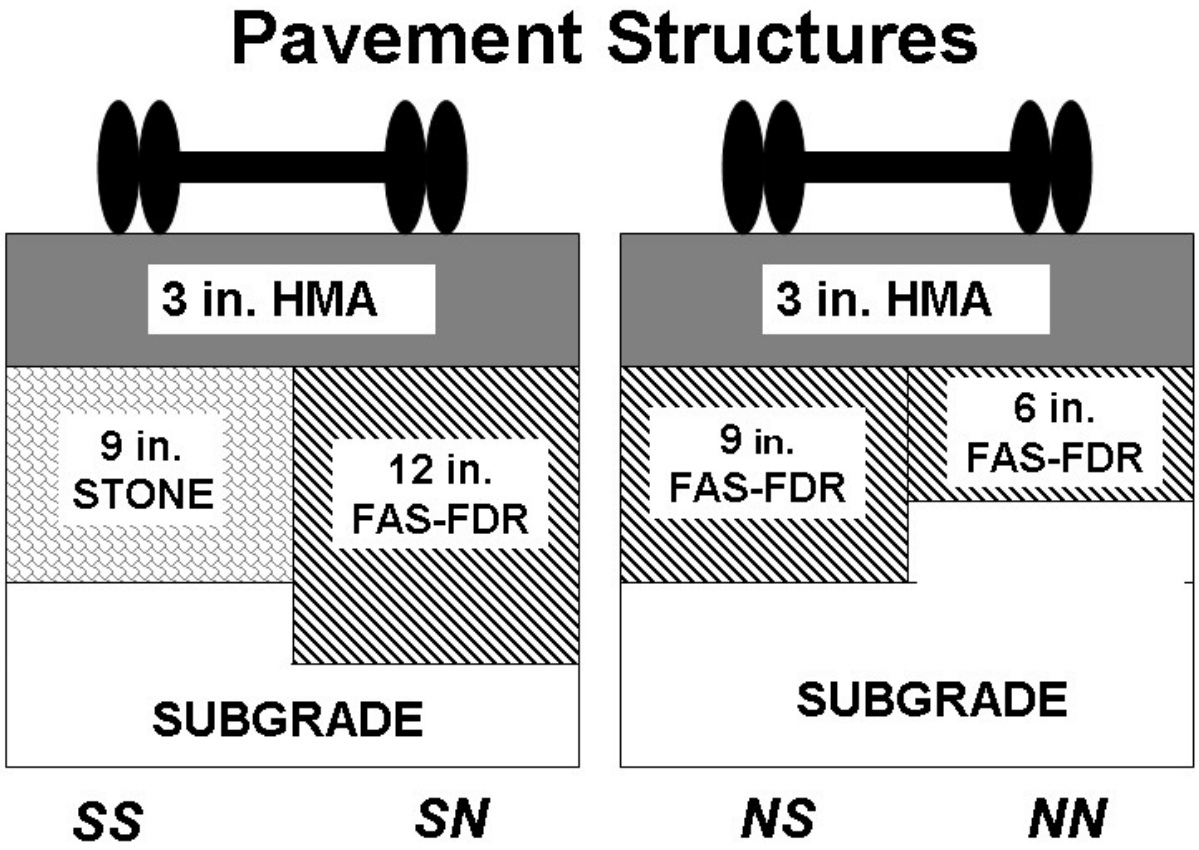

FAS-FDR: Foamed Asphalt Stabilized RAP from Full Depth Reclamation

FIGURE 3.4: Cross Section of the Pavement Sections

3.2.1 Subgrade Soil

The existing subgrade material was silty clay. Figure 3.5 shows the gradation curve for this material. The moisture-density curve for this soil, obtained from the standard Proctor test, is illustrated in Figure 3.6. The Atterberg limit test results are given in Figure 3.7. After removal and drying, the subgrade soil was recompacted in the pit to a density greater than 90% of the maximum dry density (MDD) (Table 3.1 and Figure 3.8), at near optimum moisture content. This compaction was done manually with a "jumping jack-type" vibratory compactor resulting in

densities of the order of 97.2 – 102.9 % of MDD. This subgrade was brought up to the required depth in four to six inch lifts.

3.2.2 Granular Base – Lane SS

Lane SS was constructed with a nine-inch granular base. The material used in this base is classified as an AB-3 by the current KDOT specifications and consists of crushed limestone materials. The gradation curve for the AB-3 material is given in Figure 3.9. The material has an MDD of 128 pcf at optimum moisture content of 10%. The as compacted density for the granular base, measured with the Troxler Nuclear Density gauge is given in Figure 3.10 and Table 3.4. The granular base was compacted in three lifts, each having a thickness of three inches. Compaction was done using the vibratory plate compactor and very high densities were obtained.

3.2.3 Foamed Asphalt Stabilized RAP Bases

3.2.3.1 Production of Foamed Asphalt Stabilized Material

The foamed asphalt stabilized base material was produced on the grounds of CISL in a portable plant of Wirtgen GmbH. of Germany. The general view of the plant is shown in Figure 3.11. The plant was operated by one technician from Wirtgen and supervised by an engineer from Wirtgen - UK (Mr. Mike Marshall). Mr. Mike Heitzman of IADOT supervised the full-depth reclamation and base construction process. The plant consisted of a two-bin aggregate blending system and a chamber for mixing foamed asphalt with the full depth reclamation material blend. The RAP, aggregate and soil were stockpiled at the site. Figure 3.12 shows the RAP stockpile. The PG asphalt was pumped from the tanker truck into the plant (Figure 3.13).

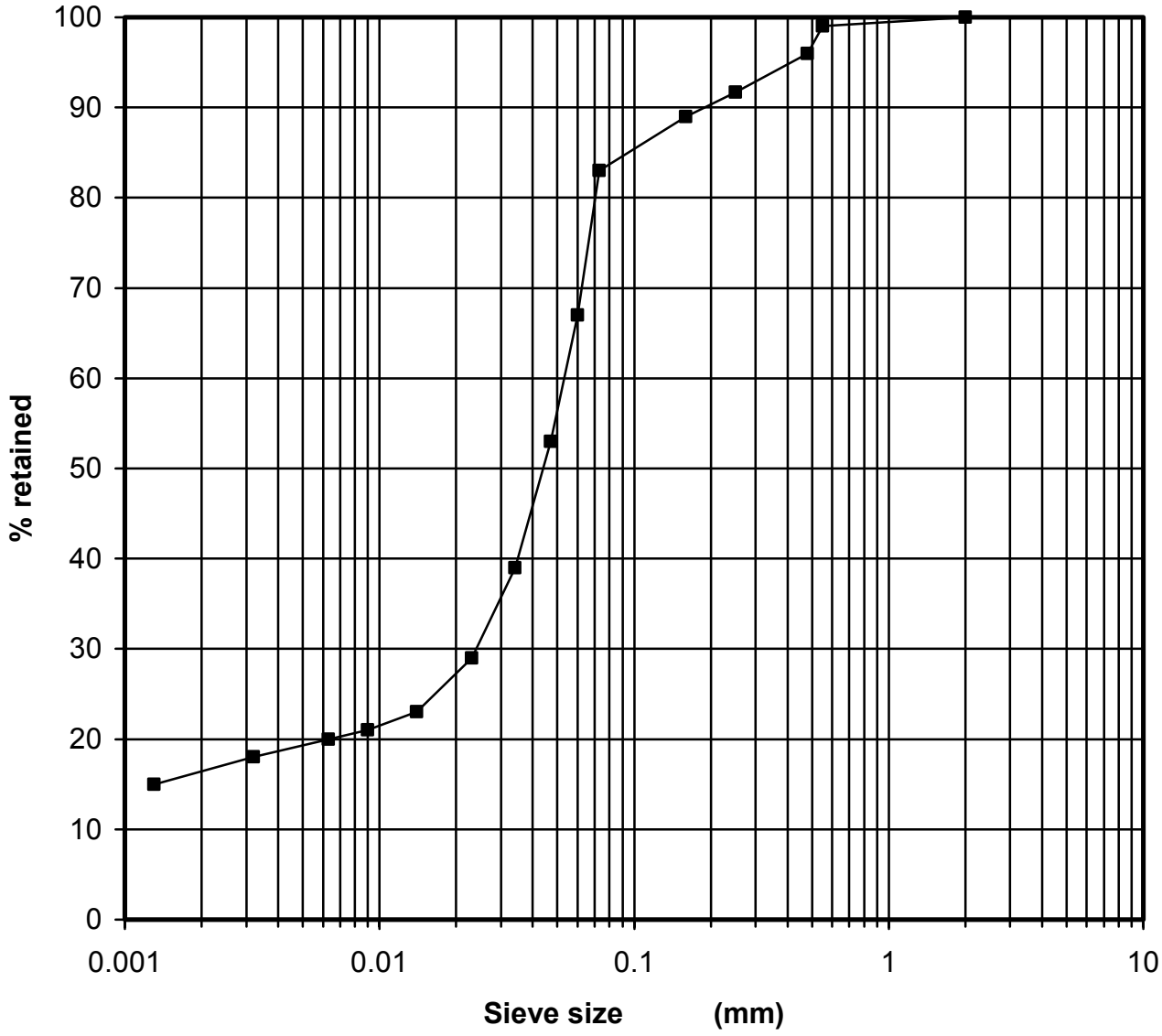

FIGURE 3.5: Gradation Curve for the Existing Subgrade Soil

MOISTURE CONTENT (%)	16.81	19.41	21.77	23.15	25.35
DRY DENSITY (lb/cu.ft)	93.02	97.59	99.77	99.4	95.65

Test results:
Optimum moisture content: 22.2%
Maximum dry density: 99.95 lb/cu ft

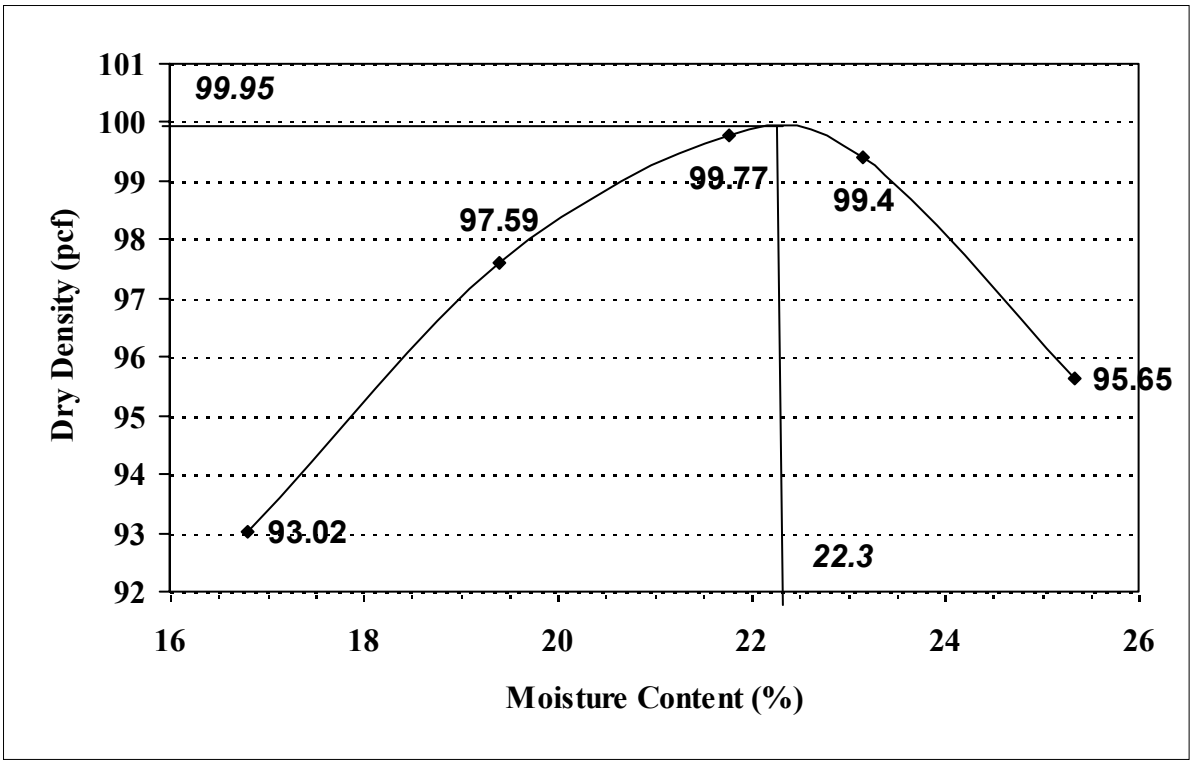

FIGURE 3.6: Moisture-Density Curve for the Subgrade Soil

Test results: Liquid limit = 43%
Plastic limit = 21 %
Plasticity index = 43 – 21 = 22%

FIGURE 3.7: Plasticity Characteristics of the Subgrade Soil

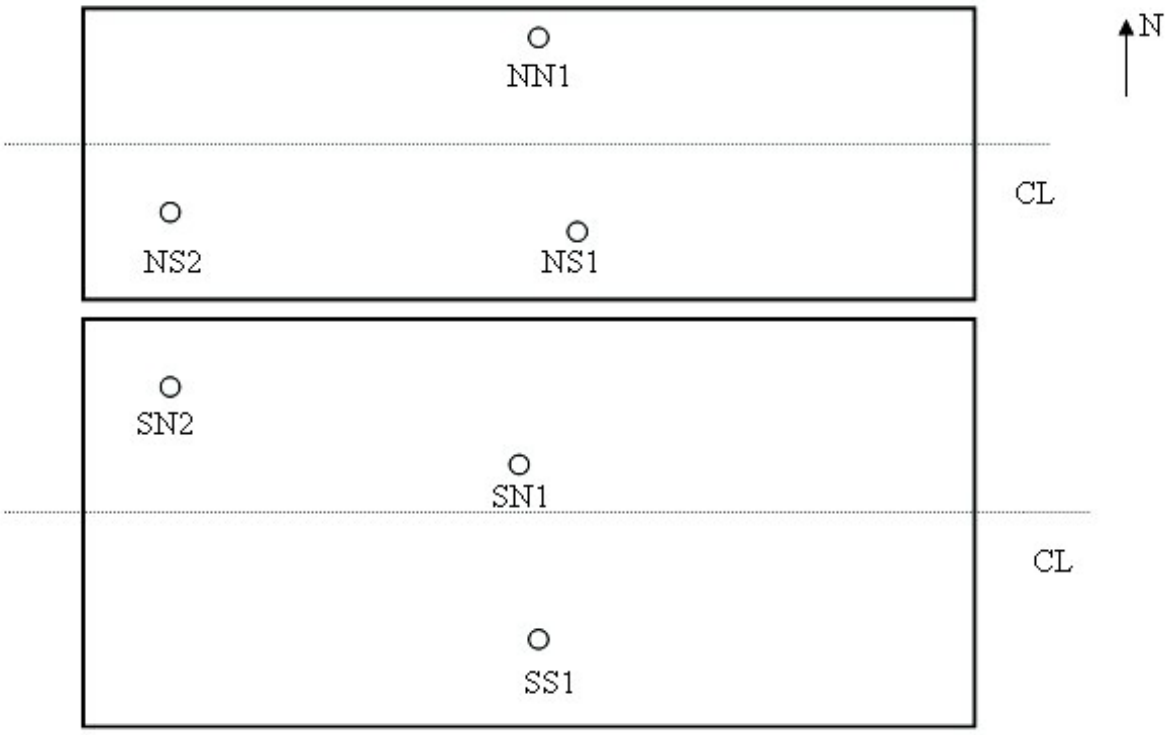

FIGURE 3.8: Soil Nuclear Density Measurement Locations

TABLE 3.3: Measured As-Constructed Densities on the Top Lift of Subgrade Soil

Location	In-Situ Dry Density (lb/cu.ft)	In-Situ Moisture (%)	Maximum Dry Density (lb/cu.ft)	Compaction (%)
SS1	99.13	15.5	99.95	99.2
SN1	102.8	15.3	99.95	102.9
SN2	101.6	17.2	99.95	101.7
NS1	98.36	14.4	99.95	98.4
NS2	97.14	16.0	99.95	97.2
NN1	100.4	15.5	99.95	100.5

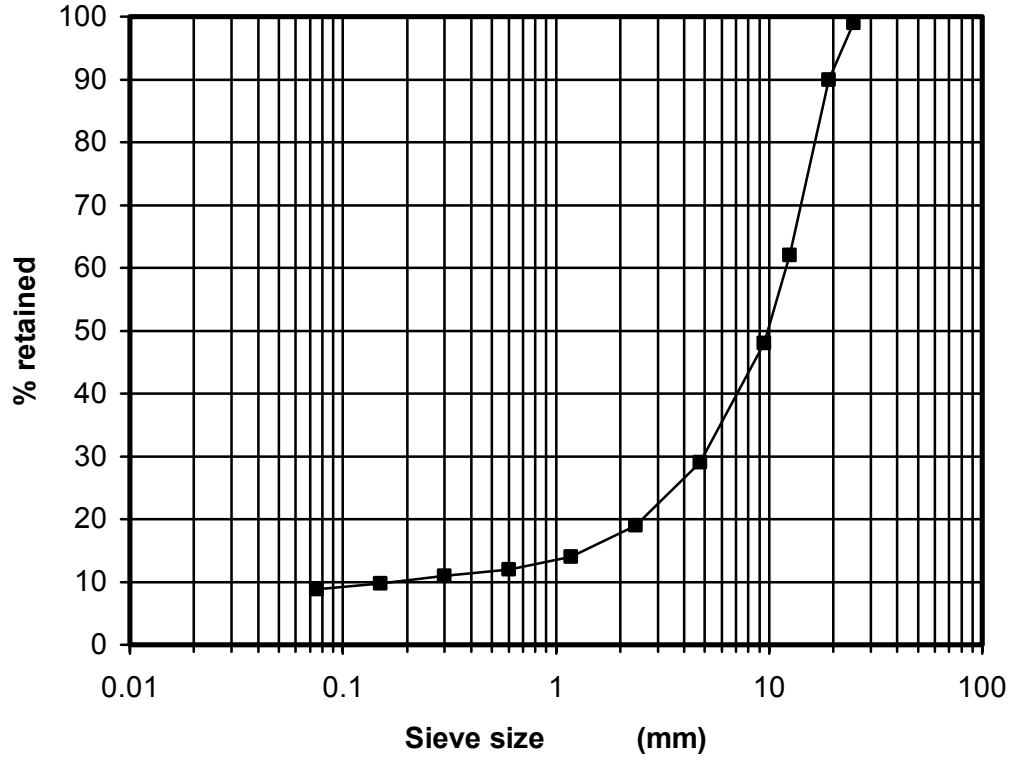

FIGURE 3.9: Gradation Curve for the AB-3 Granular Base

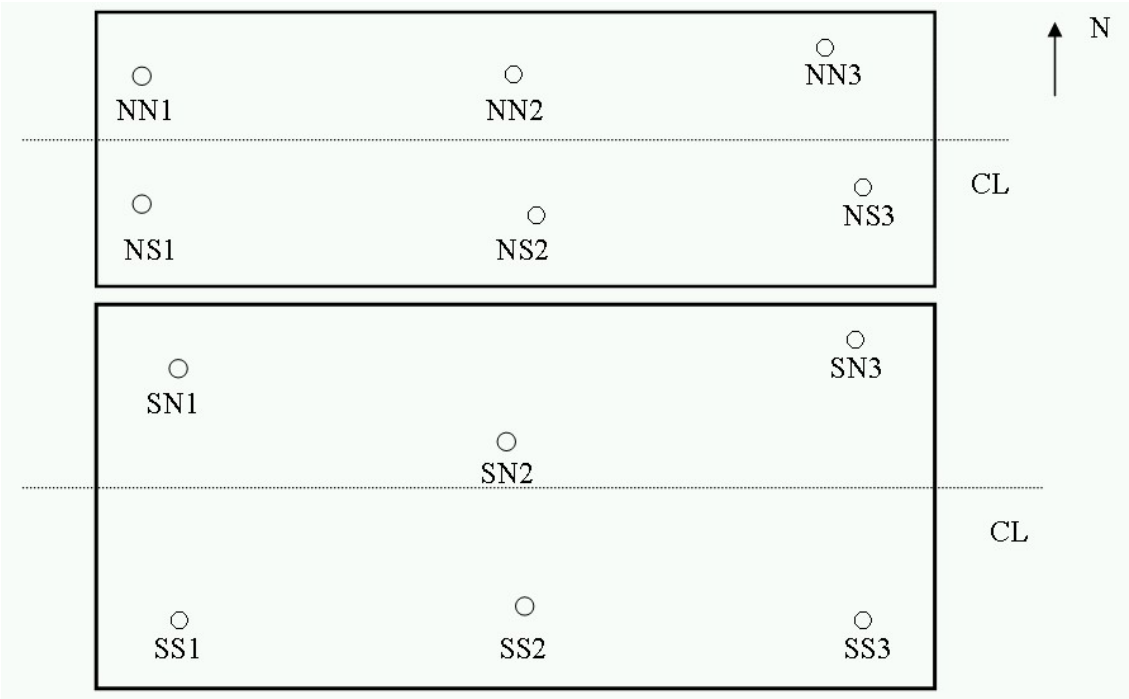

FIGURE 3.10: Location of Nuclear Density Measurements on the Base Layer

TABLE 3.4: Measured As-Constructed Densities on the Base Layer

Location	Wet Density (pcf)	Dry Density (pcf)	Total Moisture Asphalt & Water (%)	Moisture Water (%)	Compaction (%)
NN1	125.6	119.4	11.3	5.2	89.0
	125.9	120.3	10.8	4.7	89.7
	126	119.8	11.3	5.2	89.3
NN2	122.1	117.9	9.7	3.6	87.9
	121.8	116.8	10.4	4.3	87.1
	122.2	117.9	9.8	3.7	87.9
NN3	124.7	117.7	12.1	6.0	87.7
	125.4	117.9	12.5	6.4	87.9
	124.7	117.2	12.5	6.4	87.4
NS1	127.7	121.7	11	4.9	90.8
	126.7	120.8	11	4.9	90.1
	126.8	120.8	11.1	5.0	90.1
NS2	128.4	120.9	12.3	6.2	90.2
	128	120.3	12.5	6.4	89.7
	128.3	121.5	11.7	5.6	90.6
NS3	130.6	124.6	10.9	4.8	92.9
	130.2	124.1	11	4.9	92.6
	131.1	125.2	10.8	4.7	93.4
SN1	127	123.4	9	2.9	92.0
	127.7	123.4	9.6	3.5	92.0
	127.4	123.6	9.2	3.1	92.2
SN2	128.7	120.9	12.6	6.5	90.1
	128.4	120.9	12.3	6.2	90.2
	128.3	121.0	12.1	6.0	90.3
SN3	123.8	117.0	11.9	5.8	87.3
	122.7	116.8	11.2	5.1	87.1
	123.7	117.5	11.4	5.3	87.6
SS1	136	128.8	5.6	5.6	100.6
	136.8	129.3	5.8	5.8	101
	136.2	129.4	5.3	5.3	101.1
SS2	134.4	128.6	4.5	4.5	100.5
	134.7	128.8	4.5	4.5	100.6
	134.6	128.7	4.5	4.5	100.5
SS3	138.2	132.1	4.6	4.6	103.2
	137.9	131.9	4.6	4.6	103
	138	131.6	4.9	4.9	102.8

Reference G_{mb} for FAS-FDR= 2.149
Reference Wet Density for FAS-FDR =134.1 pcf

The soil and the aggregate were pre-blended, and then that mixture and RAP were fed with a front-end loader as shown in Figure 3.14. The whole process was carefully controlled with a control panel on the plant. The produced material was collected on a dump truck (Figure 3.15) and stockpiled for later use (Figure 3.16).

3.2.3.2 Construction of Foamed Asphalt Stabilized Base

The stockpiled stabilized material was transferred into the pit in the CISL with a bucket (Figure 3.17). Enough material was transferred at a time so that, after compaction, a three-inch layer of compacted FAS-FDR will result. The material was raked to have a plane surface (Figure 3.18). Compaction was done first with a vibratory sheepsfoot utility trench roller (Figure 3.19). This method proved unsuccessful, so the compaction was repeated with a jumping jack-type compactor. The in-place density was monitored with a nuclear gage (Figure 3.20) that measured the wet density and the total moisture content (water + asphalt cement). The percent compaction obtained has been shown in Table 3.4. It is to be noted that the nuclear gage reading for moisture contents on the sections with FAS-FDR contained contribution from both moisture and asphalt in the FAS-FDR. The FAS-FDR sample was tested in ignition oven to find out the asphalt content. The asphalt content from the burn-off was 6.36%. A correction factor of 0.25% was for 100% limestone aggregates common in northeast Kansas. Thus the resulting asphalt content was 6.11%. This value was subtracted from the moisture content readings of the nuclear gage for the FAS-FDR lanes, and the corresponding dry densities were calculated.

The data in Table 3.4 indicates that the percent compaction obtained for the FAS–FDR base ranged between 87.1 and 93.4 percent, while for the AB-3 granular base varied between 100.5 and 103.2, even though the same compaction effort was applied. This suggests that the

foamed asphalt stabilized RAP base requires a higher compaction effort than the AB-3 granular base to reach the same percent compaction level.

FIGURE 3.11: Wirtgen Plant

FIGURE 3.12: RAP Stockpile

FIGURE 3.13: Asphalt Transfer from Tanker to the Plant

FIGURE 3.14: Feeding of Aggregates into the Plant

FIGURE 3.15: Foamed Asphalt Stabilized Material Production

FIGURE 3.16: Foamed Asphalt Stabilized RAP Stockpile

FIGURE 3.17: Placement of the Foamed Asphalt Stabilized Material

FIGURE 3.18: Foamed Asphalt Stabilized RAP Material Raking

FIGURE 3.19: Sheepsfoot Roller Compaction

FIGURE 3.20: Nuclear Gage Density Measurement

3.2.4 Construction of the Asphalt Concrete Surface Layer

The 3-inch asphalt layer above the base was placed in one lift on all lanes in two pits. During construction, paving was done by Shilling Construction Co. of Manhattan, Kansas, and the compaction was done with a steel-wheeled vibratory roller. The asphalt layer consisted of a 12.5 mm nominal maximum size Superpave mixture. The combined aggregate gradation (dry) of this mixture, designated as SM-12.5B in Kansas, passes below the maximum density line in the sand sizes. The mixture was being used as an overlay material on a PCCP project on I-70. Some trucks were diverted during regular production for construction of these test sections. At least 100 tons of mixture was produced before building the test sections at the CISL. The mixture consisted of 18% Big Springs Quarry crushed limestone (CA-5), 17% Ozawkie Fine Asphalt Screening (FAS), 26% Ozawkie and Ervine Creek ledge Manufactured Sand, 6% Meier's Asphalt Sand, 9% ¼" Ozawkie chips and 24% Ozawkie and Ervine Creek Combined Chips. The asphalt binder was a PG 64-22. The mixture design requirements and the quality control results are shown in Table 3.5. The mixture has a higher air voids at N_{des} than allowed but also has higher than required minimum VMA. This, however, resulted in lower VFA too. Other properties are within the allowable limits. Good compaction was achieved on almost all sections (Figure 3.21 and Table 3.6).

TABLE 3.5: Properties of the Superpave Mixture
(N_{design} = 100)

Mixture/Aggregate Blend Property	Target / Read./ Criteria	Test Result (As-Built)
Asphalt Content (%)	6.3	6.43
Air Voids (%) at N_{des}	4.0 ± 2%	6.49
VMA (%)	13.0 % min. (14% - 1%)	15.0
VFA (%)	65-76	56.7
Dust-Binder Ratio	0.8 - 1.6	1.1
%Gmm at N_{ini}	89% max.	88.6
%Gmm at N_{max}	98% max.	96.5
Fine Aggregate Angularity (%)	45	45.3

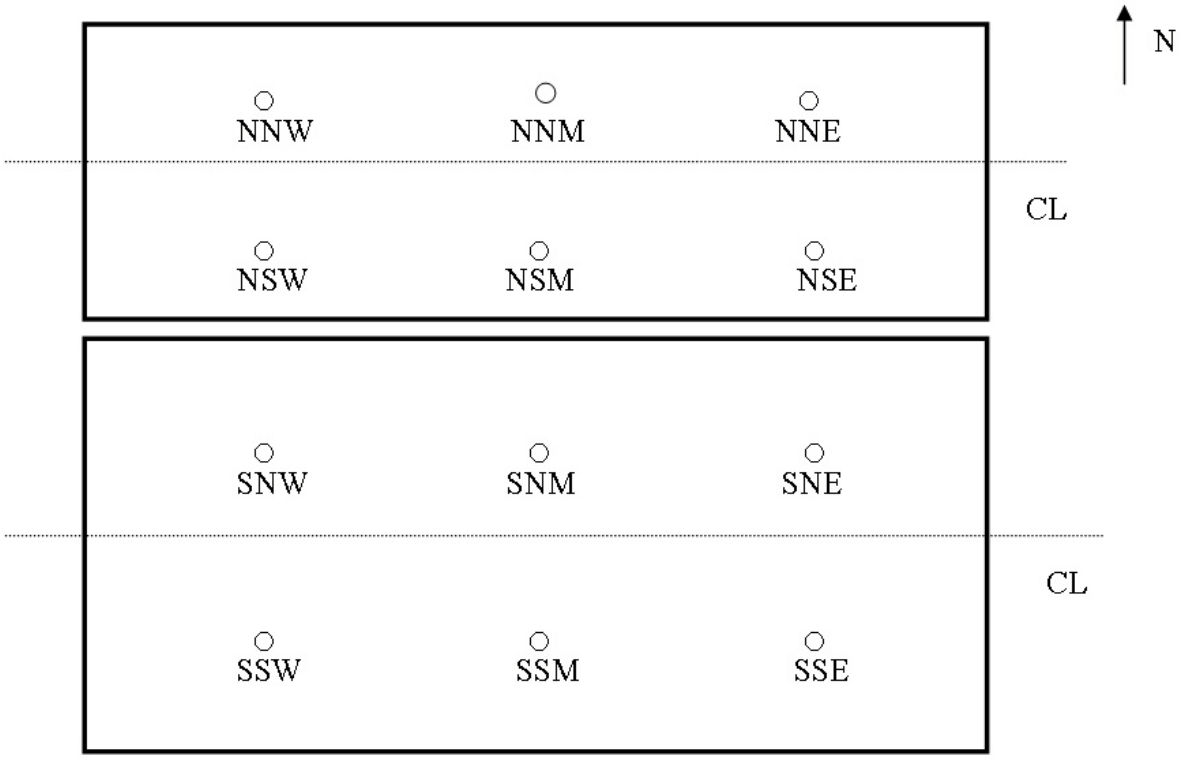

FIGURE 3.21: Location of Nuclear Density Measurements on the Asphalt Surface Layer

TABLE 3.6: Measured As-Constructed Densities on the Asphalt Surface Layer

Location		As-Constructed Density (pcf)				% Gmm			
		Lane				Lane			
		NN	NS	SN	SS	NN	NS	SN	SS
W	1	143.6	138.0	143.5	147.0	93.9	90.2	93.8	96.1
	2	143.0	137.6	143.3	147.8	93.5	90.0	93.7	96.6
	3	143.1	137.0	145.3	145.5	93.6	89.6	95.0	95.1
M	1	144.9	140.5	142.1	140.6	94.8	91.9	92.9	91.9
	2	143.4	142.4	143.5	140.5	93.8	93.1	93.8	91.9
	3	144.9	140.7	141.5	139.3	94.8	92.0	92.5	91.1
E	1	144.6	143.9	143.0	140.3	94.6	94.1	93.5	91.7
	2	143.6	143.3	142.0	140.3	93.9	93.7	92.9	91.7
	3	144.2	143.1	142.1	139.3	94.3	93.6	92.9	91.1

G_{mm} = 2.451;
Reference Density = 152.9 pcf

3.3 Instrumentation and Pavement Condition and Response Monitoring

Several sensors were placed in the test sections to monitor pavement behavior. In addition to complement measurements obtained from these sensors, Falling Weight Deflectometer (FWD) and weight drop deflections were also recorded.

3.3.1 Pressure Cells

Two Pressure cells (Geokon) were placed at the bottom of the base layer in the centerline of each pavement section to measure the vertical compressive stress at the top of the soil subgrade. The relative locations of the pressure cells are shown in Figure 3.22. One cell was placed in the western part of the lane and the other one in the eastern part. These 6-inch diameter Geokon pressure cells were successfully used in previous projects and have shown good performance and acceptable results. These sensors were installed according to the manufacture's

guidelines. After the subgrade was compacted, holes were drilled to place the pressure cells. After the horizontal alignment was checked with a level, the cells were covered with a thin layer of sand.

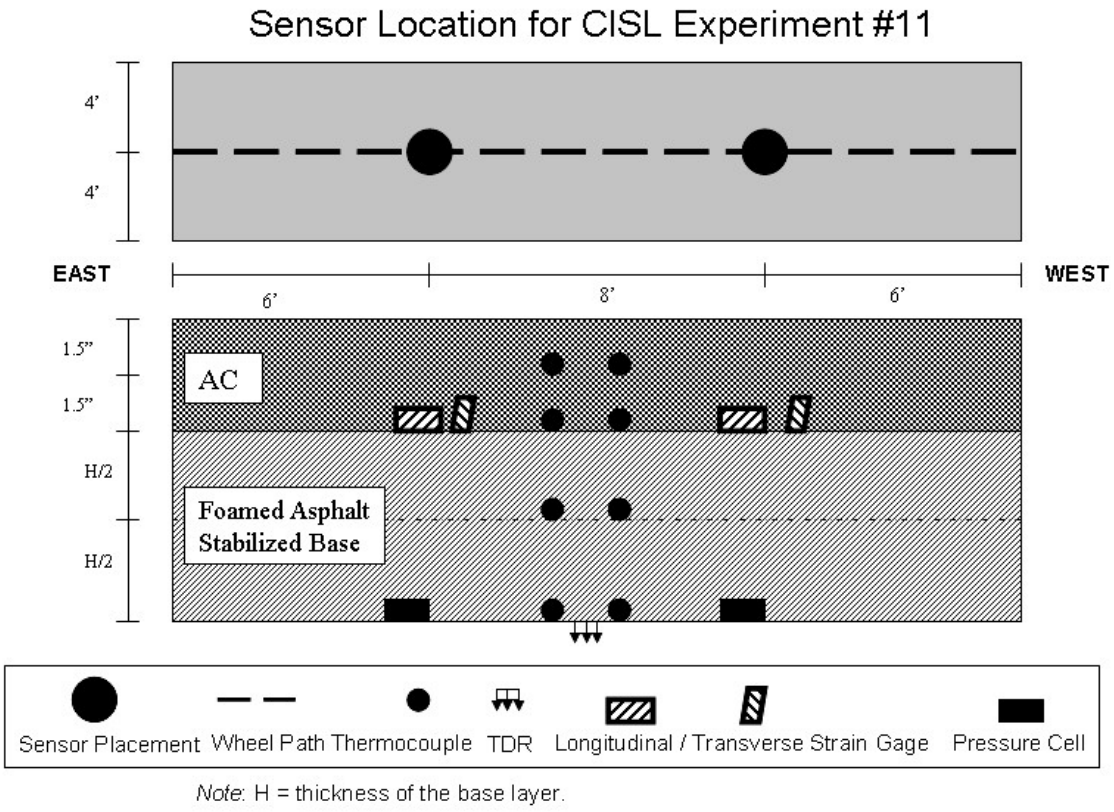

FIGURE 3.22: Location of Sensors Embedded in the Pavement Structure

3.3.2 Strain Gages

Strain gages were installed at the bottom of the asphalt surface layer to measure transverse and longitudinal tensile strains. In each section, four strain gages were installed on the centerline of the lane as shown in Figure 3.22. One gage was placed in the longitudinal direction and one in the transverse direction in the western part of the lane. Similarly one gage was placed

in the longitudinal direction and one in the transverse direction in the eastern part of the lane.

The gages were constructed by attaching aluminum bars at the two ends of Tokyo Sokkai Kenkyujo (TML) strain gages. The H-Bars formed this way were fixed with short nails on top of the base layer after the layer was compacted, and before paving the asphalt concrete surface layer. During paving, asphalt mix was shoveled on top of the strain gages and the connection wires, and then lightly compacted to prevent deterioration of gages and wires during the paving operation. Five out of total sixteen gages were lost during construction. It was presumed that the gages became inoperable when the hot asphalt mix melted the connection wires of these gages.

3.3.3 Longitudinal Position of the ATL Load Assembly

A linear positioning gage, fixed to the East-North pole of the frame of the ATL machine, was used to record the longitudinal position of the ATL load assembly when the strain/pressure measurements were performed. The gage provided accurate measurement only when the load assembly was traveling West, away from the gage, since the cable of the linear positioning gage was properly stretched. When the load assembly was traveling toward the gage, the cable was not stretched to its entire length, and the readings were erroneous- somewhat higher than the true position of the load assembly. However, the use of the linear positioning gage for the measurement of longitudinal position of the ATL load assembly was abandoned in this experiment, and a new measuring system was installed.

The ATL load assembly position reading, horizontal strains at the bottom of the asphalt surface layer and vertical stress at the top of the subgrade were taken at a frequency of 100Hz by the same data acquisition system. The use of a single data acquisition system allowed all recording to be recorded on the same time basis in a single file.

3.3.4 Thermocouples

Four thermocouples were placed in each pavement structure, in the center location of each lane as shown in Figure 3.22. Two sensors were placed at the bottom of the asphalt layer (3 inches from the surface) and two at the bottom of the base layer.

The thermocouples were manufactured in-house and their precision was verified before installation. Similar thermocouples were used in previous ATL experiments and produced acceptable results when compared to other conventional temperature measurement devices. Temperature readings were taken monthly.

3.3.5 Falling Weight Deflectometer (FWD) Testing

FWD testing was performed by KDOT personnel at three different time periods:

- Before loading was started on the ATL sections, on December 6 and 19, 2001.
- After the first 100,000 ATL passes on the SS and SN lanes on January 24, 2002
- On all four lanes on April 9, 2002

The FWD tests were performed at six stations on each test lane as shown in Figure 3.23. For stations 1, 2 and 3 the geophones were oriented toward the East. For stations 4, 5 and 6 the geophones were oriented toward the West. Stations 3 and 4 were at the same location, in the center of the lane, but the geophones were directed to the East for station 3 and to the West for station 4.

Strain and pressure measurements were performed when the FWD loads were dropped at stations 1 and 6 to investigate if predicted strains, computed using the backcalculated elastic moduli, matched the measured strains. Stations 2 and 5 were added to stations 1 and 6 to investigate the effect of load position on the strain magnitudes. Therefore, stations 2 and 5 were

selected six inches off the center of the lane from stations 1 and 6, respectively.

The FWD testing sequence consisted of three drops at 6,000 lbs load level followed by five drops at 9,000 lbs load level. The seven geophones were placed at: 0.0, 8.0, 12.0, 18.0, 24.0, 36.0 and 60.0 inches from the center of the FWD loading plate. The deflections recorded for the last drop at 6,000-lb load level and the last two drops at the 9,000 lb-load level were used to backcalculate the elastic moduli of the pavement layers. These drops were selected since for these drops the deflection measurements are the most reliable because the FWD loading plate has the optimum contact with the pavement surface.

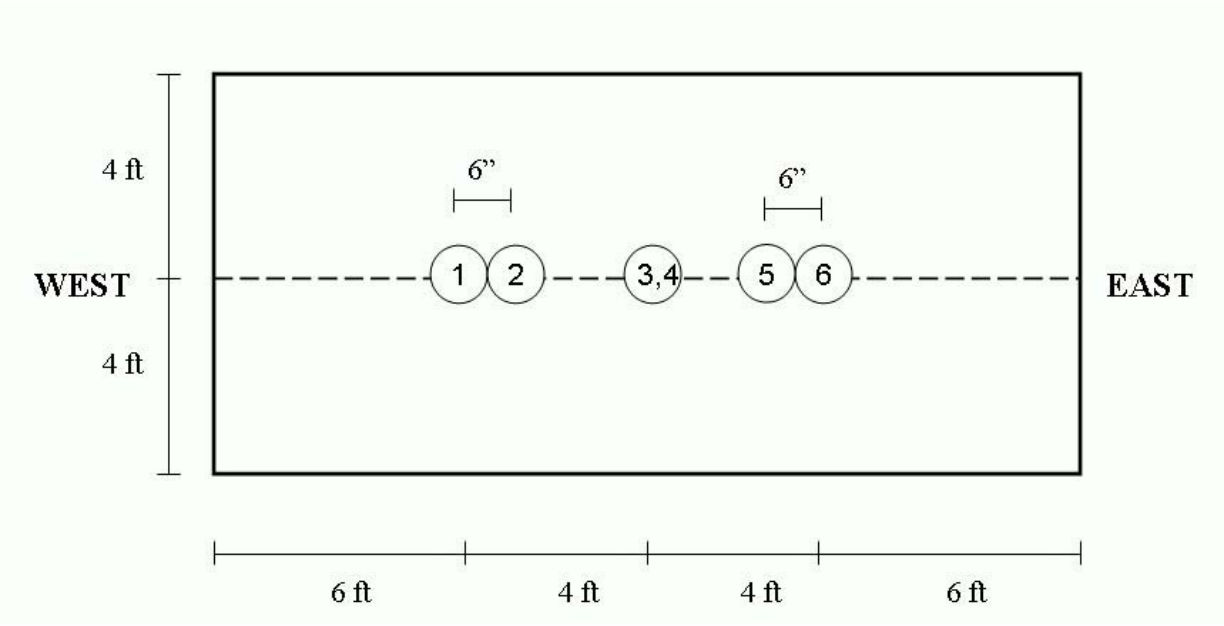

FIGURE 3.23: Location of the FWD Test Stations

3.3.6 Weight Drop Device

Weight drop tests were performed on the same day profile measurements were made at four stations for each lane. Figure 3.24 shows the station locations. Station W was at the West side of the lane, and station V at the center of the lane with the Linear Variable Differential Transformer (LVDT) beam directed to the East. Station E was at the East side of the lane, and

station M at the center of the lane with the LVDT beam directed to the West. Stations V and M were at the same location, in the center of the lane, but the LVDT beam was directed to the East for station V and to the West for station M.

The weight drop test consisted of dropping a weight of 60 lbs on a set of rubber plates that transmitted the load to a circular steel plate, nine inches in diameter. The plate was placed at the top of the pavement. The dynamic impact load was measured with a load cell under the rubber plates. The pavement surface deflections were measured by seven LVDTs fixed on a reference plastic beam oriented radially, at six-inch intervals. The first LVDT is located at the center of the loading plate. The plastic beam holding the LVDTs was attached to the frame of the ATL machine so that it will not move when the weight was dropped.

The principle of the weight drop device is very similar to that of the FWD but the dropped weight, diameter of the loading plate and the spacing between the geophones are larger for the FWD. A typical load applied by the FWD is between 6,000 and 12,000 lbs, while the load applied by the weight drop device ranges between 2,000 and 2,500 lbs.

The vertical impact force and the seven sensor deflections were measured and recorded at a sampling frequency of 10,000Hz. The time traces of the load and deflections are recorded. For backcalculation of layer moduli based on a linear elastic layered theory algorithm, only the maximum load and the maximum deflections were used.

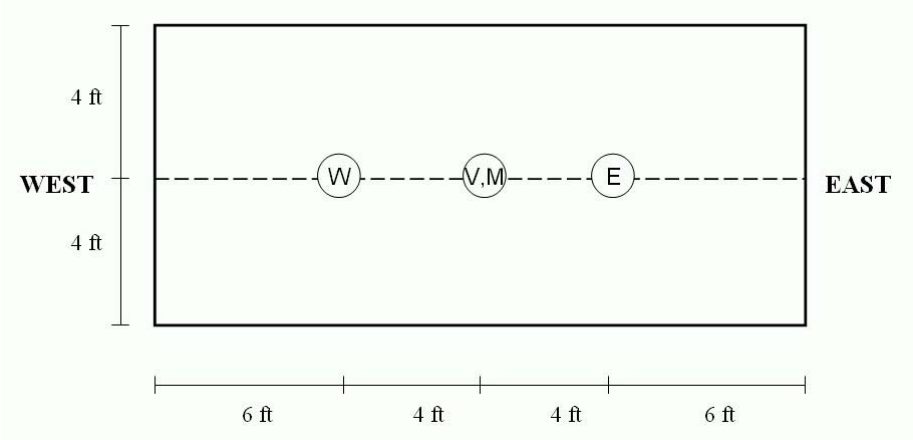

FIGURE 3.24: Location of Weight Drop Stations

3.4 Accelerated Pavement Testing Conditions

Loading was applied using a single axle with dual wheel with a total load of 17 kips (75.7 kN) for the first 100,000 passes. After that, additional 400,000 passes of a tandem axle with dual wheel with a total load of 30 kips (133.6 kN) were applied. A fixed wheel path (zero lateral wander) was maintained and loading was bi-directional traffic throughout the experiment. The tire inflation pressure was maintained at 100 psi and was verified weekly.

All testing was performed at room temperature. The pavement structures were not subjected to any special heating or cooling conditions. Thermocouples embedded in the pavement structure (Figure 3.22) recorded the temperature data tabulated in Table 3.7. Figures 3.25 and 3.26 show the tabulated values reported in Table 3.7. These figures indicate that the two pairs of pavement structures (NN-NS and SN-SS) were tested under very similar temperature regimes.

No water was added to the pavements. Since the pavements were constructed in pit and the asphalt concrete surface layer was paved wall-to-wall, the moisture content in the subgrade

soil remained relatively constant during the accelerated testing. However, the measured volumetric moisture contents, reported in Table 3.8, indicated that the values were significantly higher for the SN and SS pavements. No explanation can be given for this difference, since the top layer of the subgrade soil was placed in all pavements on the same day, and the sand-and-cone measured values were very similar for all four pavements.

TABLE 3.7: Temperature Measured During Testing

Date	Top of Base Layer				Base of Base Layer			
	NN	NS	SN	SS	NN	NS	SN	SS
12/20/2001	67.22	66.89	67.24	67.10	67.67	67.07	67.37	68.12
1/23/2002	68.05	68.23	69.12	69.46	67.79	67.90	68.49	68.88
3/15/2002	70.21	70.51	70.10	70.10	70.40	70.74	70.43	70.38
4/5/2002	71.86	72.20	72.27	72.11	70.71	71.10	70.56	70.70
5/31/2002	84.80	84.97	82.03	81.61	79.35	79.12	76.23	77.65
6/26/2002	90.05	90.15	87.85	87.86	87.73	87.57	84.66	85.85
7/17/2002	89.58	89.25	88.75	88.37	88.99	87.94	85.80	88.45
8/6/2002	89.34	89.08	90.52	90.66	89.30	89.05	89.9	91.28
8/23/2002	86.89	87.27	88.96	88.94	86.71	86.92	87.68	88.90
9/4/2002	85.78	85.95	86.97	87.11	86.23	86.36	87.06	88.18
9/12/2002	82.53	82.77	84.16	84.41	83.46	83.61	85.34	86.17
9/17/2002	80.10	80.31	81.56	81.80	81.45	81.96	83.64	84.19
9/25/2002	76.66	77.21	78.53	78.62	78.26	78.58	80.10	80.20
10/2/2002	82.22	82.47	82.73	82.65	82.1	82.36	82.45	82.76

TABLE 3.8: Moisture Content (Volumetric) in the Subgrade Soil During Testing

Date	NN	NS	SN	SS
1/18/2002	8.63	9.49	13.81	15.54
2/12/2002	8.46	8.63	12.08	15.54
4/10/2002	8.24	8.93	12.36	15.10
6/27/2002	8.80	9.66	12.60	15.71
10/3/2002	5.69	6.38	7.25	7.25

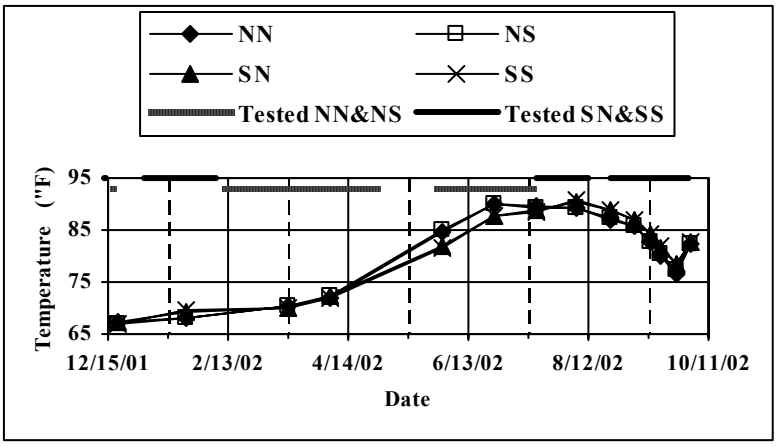

FIGURE 3.25: Temperature Measured at the Top of the Base Layer

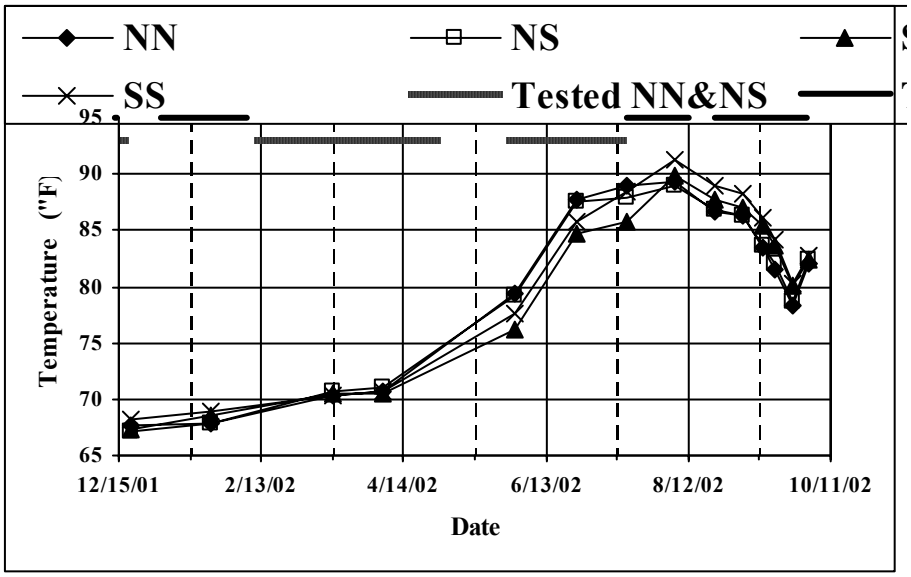

FIGURE 3.26: Temperature Measured at the Bottom of the Base Layer

3.5 Operating Schedule and Recording of Data

Table 3.9 shows the operating schedule of the project, when test data was collected. In May 2002, breakdowns of the control unit of the ATL machine caused delays in the planned operating schedule.

TABLE 3.9: Summary of Loading and Data Acquisition Dates for CISL # 11

Date	Load Repetitions	Test Section	Remarks
12-06-01	0	South & North	FWD
12-13-01	0	South	Start single axle loading
12-14-01	5,000	South	Stop
12-17-01	0	North	Start single axel loading
12-18-01	5,000	North	Stop
12-19-01	5,000	South	Resume loading & FWD
01-03-02	25,000	South	25K data*
01-11-02	45,000	South	45K data*
01-24-02	71,000	South	71K data* & FWD
01-31-02	82,570	South	82K data*
02-07-02	100,130	South	100K data*
02-11-02	5,000	North	Resume loading
02-28-03	60,298	North	60K data*
03-07-02	82,138	North	82K data*
03-14-02	99,898	North	100K data*
03-26-02	99,898	North	Start tandem axle loading
04-04-02	130,752	North	130K data*
04-09-02	149,152	North	FWD
04-11-02	149,152	North	150K data*
04-25-02	208,374	North	208K data*
04-29-02	214,236	North	Inverter failure
05-28-02	214,236	North	Resume testing
06-10-02	276,404	North	276K data*
06-20-02	341,240	North	341K data*
07-01-02	407,420	North	408K data*
07-10-02	459,848	North	460K data*
07-16-02	500,068	North	500K data*
07-17-02	100,130	South	Start tandem axle loading
07-25-02	156,754	South	157K data*
08-02-02	201,422	South	201K data*
08-12-02	245,694	South	Inverter failure, 246K data*
08-23-02	245,649	South	Resume loading
09-04-02	327,652	South	328K data*
09-17-02	421004	South	420K data*
09-25-02	467,410	South	468K data*
10-01-02	500,000	South	Finish loading, 500K data*

* Data taken consisted of strain gage readings, soil pressure readings, transverse and longitudinal profiles, and weight drop data.

Chapter 4

Test Results and Observations

4.1 Transverse Profiles

Transverse profile measurements were performed periodically, at the same time with the longitudinal profile, strain/stress and weight drop measurements (Table 3.9). On each pair of pavements, transverse profiles were measured at three different spatial locations: at the middle of the lane, five feet West from the middle, and five feet East of the mid location. Each profile consists of elevation data at 210 points spaced at 0.5 in. intervals. Two nails were driven in the pavement in the areas not trafficked by the ATL machine, at transverse position of 36 and 72 inches. These nails were used as reference since their elevations did not change during the entire experiment. The movement of these nails was checked every time profile measurements were made using a reference elevation point at the base of the steel pole near the East gate of the CISL laboratory.

The elevation data for the transverse profiles was assembled in a database in an Excel spreadsheet format. Because of the large quantity of data, the transverse profiles are archived on a CD-ROM that is available on request from the Kansas DOT or the author.

Figure 4.1 illustrates two typical transverse profiles obtained from the elevation data on the NN and NS pavements. The initial profile is the profile measured before any ATL load was applied. The profile showing larger elevation variation is the profile after ATL passes have been made on the pavements. The ruts caused by the passage of the ATL load assembly at the pavement surface are clearly visible. Since no lateral wander was applied in this experiment, the

ruts formed underneath each tire. Between the tires of the dual wheel, the asphalt concrete surface exhibited some heaving due to upward shoving of the materials.

Two major parameters were derived from the elevation data:

- *Permanent Deformation* at the pavement surface was calculated first in each of the 105 (210/2) points of the profile by subtracting measured elevation after a given number of ATL passes from the initial elevation data. The permanent deformation was positive when the current elevation of the point was lower. Then, for each pavement, and for a particular transverse profile (West, Middle and East), the permanent deformation (PD) was computed as the maximum value obtained from the 105 points. The permanent deformation data is reported in Tables 4.1 and 4.2.
- *Rut Depth* (RD) for each pavement, and for a particular transverse profile (West, Middle and East), was computed as the difference between the elevation of the highest and lowest points of that profile. The rut depth data is reported in Tables 4.3. and 4.4.

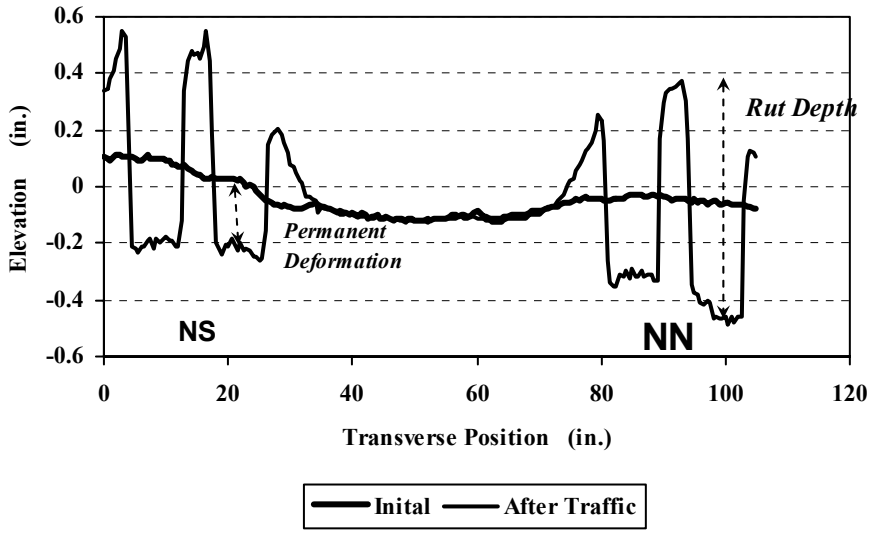

FIGURE 4.1: Example of Transverse Profile

The evolution of permanent deformation with the number of ATL load assembly passes is plotted in Figure 4.2. The chart clearly indicates that the evolution of the permanent deformation is similar for the pavement structures with nine and six inches foamed asphalt stabilized RAP bases (NS and SN) and for the pavement structure with a nine inch granular base (SS).

The evolution of rut depth with the number of applied ATL load assembly passes is plotted in Figure 4.3. The figure shows that at the end of loading the rut depth for the flexible pavement with a nine- inch granular base (SS) is slightly higher than for the pavement with a 12-inch foamed asphalt stabilized RAP base (SN) and lower than that of the pavement with a nine-inch foamed asphalt stabilized RAP base (NS).

Table 4.1 Evolution of Permanent Deformation (in.) - Lanes NN and NS

Date	Passes (x 1,000)	NN-W	NN-M	NN-E	NN-Avg	NS-W	NS-M	NS-E	NS-Avg
12/14/01	**0**	0.000	0.000	0.000	*0.000*	0.000	0.000	0.000	*0.000*
02/15/02	**23**	0.105	0.105	0.131	*0.114*	0.096	0.079	0.088	*0.088*
02/22/02	**42**	0.131	0.116	0.188	*0.145*	0.127	0.102	0.096	*0.108*
03/01/02	**60**	0.112	0.178	0.143	*0.144*	0.213	0.177	0.093	*0.161*
03/08/02	**82**	0.116	0.162	0.127	*0.135*	0.139	0.192	0.092	*0.141*
03/14/02	**100**	0.210	0.163	0.135	*0.169*	0.096	0.252	0.115	*0.154*
04/05/02	**130**	0.132	0.291	0.158	*0.194*	0.167	0.142	0.119	*0.143*
04/12/02	**150**	0.117	0.176	0.156	*0.150*	0.109	0.089	0.135	*0.111*
04/19/02	**176**	0.164	0.217	0.181	*0.187*	0.125	0.118	0.119	*0.120*
04/26/02	**208**	0.147	0.211	0.171	*0.177*	0.140	0.152	0.087	*0.126*
06/20/02	**341**	0.220	0.239	0.290	*0.250*	0.134	0.178	0.216	*0.176*
07/01/02	**408**	0.311	0.338	0.373	*0.341*	0.181	0.188	0.300	*0.223*
07/10/02	**460**	0.310	0.313	0.406	*0.343*	0.196	0.242	0.315	*0.251*
07/17/02	**500**	0.309	0.377	0.425	*0.370*	0.201	0.208	0.328	*0.246*

TABLE 4.2: Evolution of Permanent Deformation (in.) - Lanes SN and SS

Date	Passes (x 1,000)	SN-W	SN-M	SN-E	SN-Avg	SS-W	SS-M	SS-E	SS-Avg
11/11/01	**0**	0.000	0.000	0.000	*0.000*	0.000	0.000	0.000	*0.000*
01/04/02	**25**	0.061	0.051	0.094	*0.068*	0.115	0.120	0.057	*0.097*
01/11/02	**45**	0.118	0.064	0.116	*0.099*	0.076	0.117	0.073	*0.089*
01/25/02	**71**	0.049	0.086	0.097	*0.078*	0.125	0.113	0.034	*0.091*
02/01/02	**82**	0.026	0.067	0.078	*0.057*	0.125	0.131	0.093	*0.116*
02/07/02	**100**	0.143	0.081	0.092	*0.105*	0.067	0.159	0.115	*0.114*
07/25/02	**157**	0.188	0.155	0.247	*0.197*	0.189	0.222	0.198	*0.203*
08/02/02	**201**	0.219	0.184	0.263	*0.222*	0.261	0.261	0.225	*0.249*
08/12/02	**246**	0.210	0.192	0.288	*0.230*	0.286	0.266	0.239	*0.264*
09/04/02	**328**	0.234	0.197	0.302	*0.244*	0.278	0.279	0.241	*0.266*
09/17/02	**420**	0.221	0.198	0.316	*0.245*	0.282	0.285	0.260	*0.276*
09/25/02	**468**	0.236	0.203	0.313	*0.251*	0.283	0.283	0.272	*0.279*
10/01/02	**500**	0.218	0.198	0.315	*0.244*	0.295	0.279	0.257	*0.277*

TABLE 4.3: Evolution of Rut Depth (in.) - Lanes NN and NS

Date	Passes (x 1,000)	NN-E	NN-M	NN-W	NN-Avg	NS-E	NS-M	NS-W	NS-Avg
12/14/01	**0**	0.000	0.000	0.000	*0.000*	0.000	0.000	0.000	*0.000*
02/15/02	**23**	0.140	0.136	0.118	*0.131*	0.133	0.097	0.082	*0.104*
02/22/02	**42**	0.169	0.137	0.123	*0.143*	0.136	0.097	0.111	*0.115*
03/01/02	**60**	0.130	0.122	0.129	*0.127*	0.128	0.096	0.114	*0.113*
03/08/02	**82**	0.136	0.139	0.123	*0.132*	0.132	0.123	0.112	*0.122*
03/14/02	**100**	0.136	0.163	0.152	*0.150*	0.135	0.140	0.102	*0.126*
04/05/02	**130**	0.160	0.203	0.142	*0.168*	0.153	0.144	0.128	*0.142*
04/12/02	**150**	0.164	0.180	0.161	*0.168*	0.164	0.117	0.113	*0.131*
04/19/02	**176**	0.197	0.234	0.211	*0.214*	0.171	0.144	0.152	*0.156*
04/26/02	**208**	0.229	0.254	0.212	*0.232*	0.195	0.154	0.149	*0.166*
06/20/02	**341**	0.422	0.473	0.447	*0.448*	0.398	0.308	0.283	*0.330*
07/01/02	**408**	0.642	0.716	0.655	*0.671*	0.638	0.451	0.431	*0.507*
07/10/02	**460**	0.762	0.817	0.758	*0.779*	0.726	0.545	0.484	*0.585*
07/17/02	**500**	0.841	0.962	0.833	*0.878*	0.848	0.591	0.520	*0.653*

TABLE 4.4: Evolution of Rut Depth (in.) - Lanes SN and SS

Date	Passes (x 1,000)	SN-E	SN-M	SN-W	SN-Avg	SS-E	SS-M	SS-W	SS-Avg
11/11/01	**0**	0.000	0.000	0.000	*0.000*	0.000	0.000	0.000	*0.000*
01/04/02	**25**	0.077	0.059	0.065	*0.067*	0.094	0.087	0.093	*0.091*
01/11/02	**45**	0.102	0.078	0.077	*0.085*	0.098	0.089	0.087	*0.091*
01/25/02	**71**	0.110	0.090	0.048	*0.083*	0.113	0.095	0.097	*0.102*
02/01/02	**82**	0.090	0.098	0.077	*0.088*	0.115	0.107	0.110	*0.111*
02/07/02	**100**	0.099	0.091	0.086	*0.092*	0.120	0.129	0.088	*0.112*
07/25/02	**157**	0.275	0.225	0.239	*0.246*	0.364	0.257	0.281	*0.301*
08/02/02	**201**	0.347	0.314	0.283	*0.314*	0.458	0.331	0.367	*0.385*
08/12/02	**246**	0.382	0.306	0.297	*0.328*	0.482	0.337	0.382	*0.400*
09/04/02	**328**	0.397	0.330	0.320	*0.349*	0.524	0.363	0.407	*0.431*
09/17/02	**420**	0.439	0.347	0.312	*0.366*	0.543	0.377	0.418	*0.446*
09/25/02	**468**	0.451	0.346	0.323	*0.373*	0.533	0.371	0.416	*0.440*
10/01/02	**500**	0.439	0.323	0.311	*0.358*	0.538	0.374	0.409	*0.441*

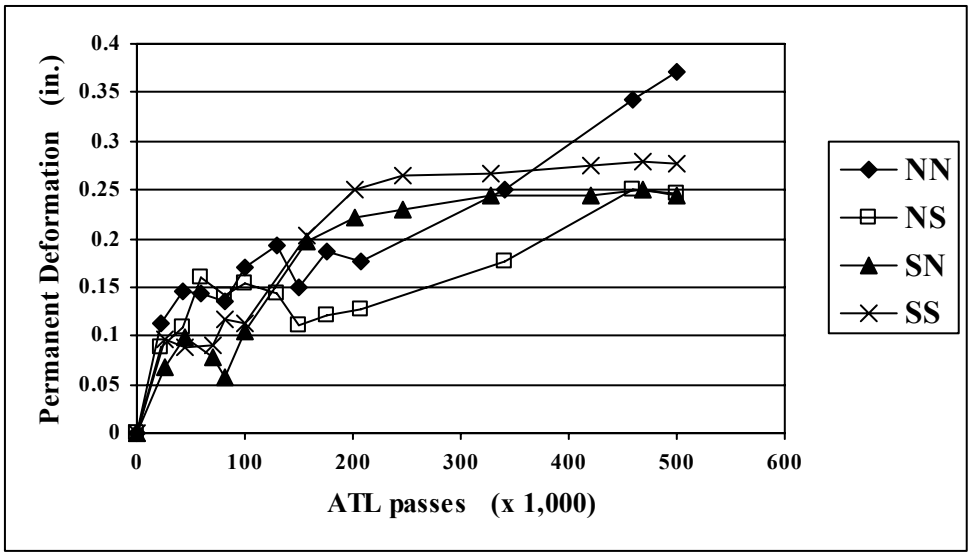

FIGURE 4.2: Evolution of Permanent Deformation

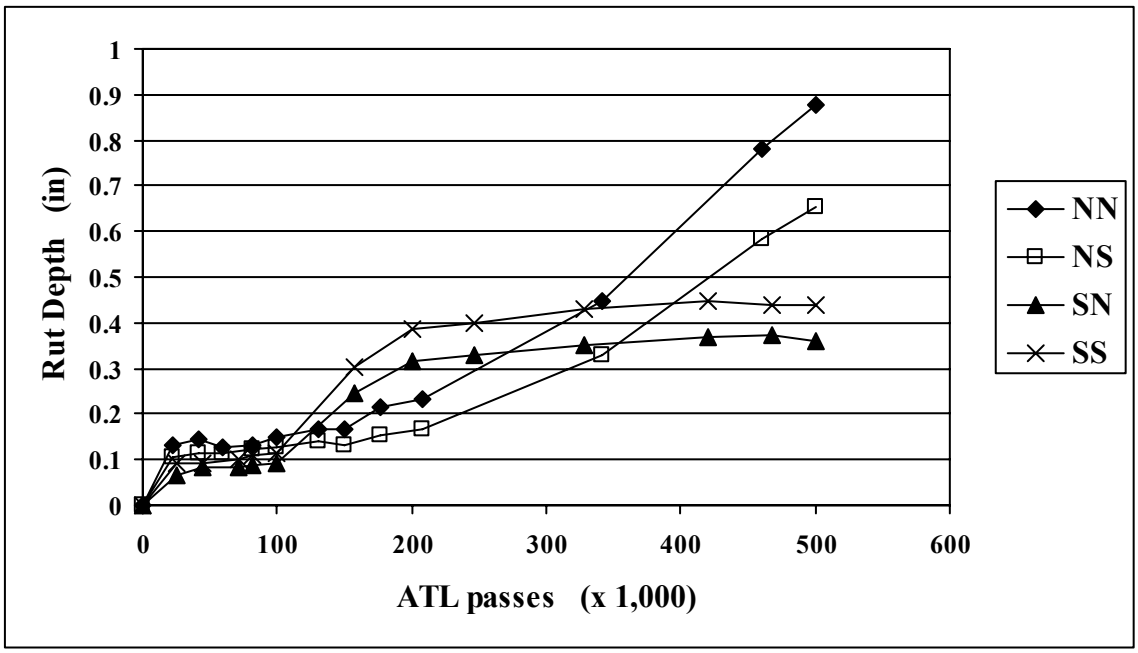

FIGURE 4.3: Evolution of Rut Depth

4.2. Longitudinal Profiles

The longitudinal profile of a pavement section was recorded by measuring the elevation of 19 points spaced at one-foot intervals on the outside wheel path with surveying equipment. The points were numbered from East to West, with the first point being at one foot West of the East wall of the pit. A fixed point at the base of a steel pole near the East gate of the CISL laboratory was used as reference. The longitudinal profile data is reported in Appendix C.

The roughness of the longitudinal profile was estimated from the elevation data, with the Slope Variance (SV) as the roughness statistic. SV was selected for this project because of its simplicity. Other indexes that are computed based on elevation data require a minimum length of pavement section. For example, to compute the International Roughness Index (IRI), the road section must be at least 33 feet (11 meters) long. The slope variance (SV) can be computed as:

$$SV = [\ SUM\ (S_i - S_{avg})^{2}\ ] / (N-1) \qquad (4.1)$$

Where:

N – number of segments where the slope is computed (N=18 for the CISL sections);

$S_i = 100*(h_{i+1} – h_i) / d$ - slope in point i, in percent;

h – elevation (in); and

d – spacing between points (d = 12 in).

It is important to note that the roughness statistic derived from the longitudinal profile is not a good indicator of pavement performance for the 20-ft long pavement sections subjected to full scale accelerated testing at CISL, and it does not correlate well with the roughness of in-service pavement. The main reason is that the variability of material properties and layer thickness are much smaller for such a small section than for an in-service pavement. Also, the environmental factors are carefully controlled in CISL.

However, the slope variance was computed here only to compare its evolution for the four pavement structures under study. The Slope Variance values are reported in the Appendix B.

Figure 4.4 shows the evolution of Slope Variance and clearly indicates that the SV values did not change with the number of accumulated ATL load assembly passes. This can be explained by the very uniform dynamic loading provided by the ATL machine. The uniformity of loading was in part due to the fact that the pavements did not exhibit distresses other than rutting in the wheel path.

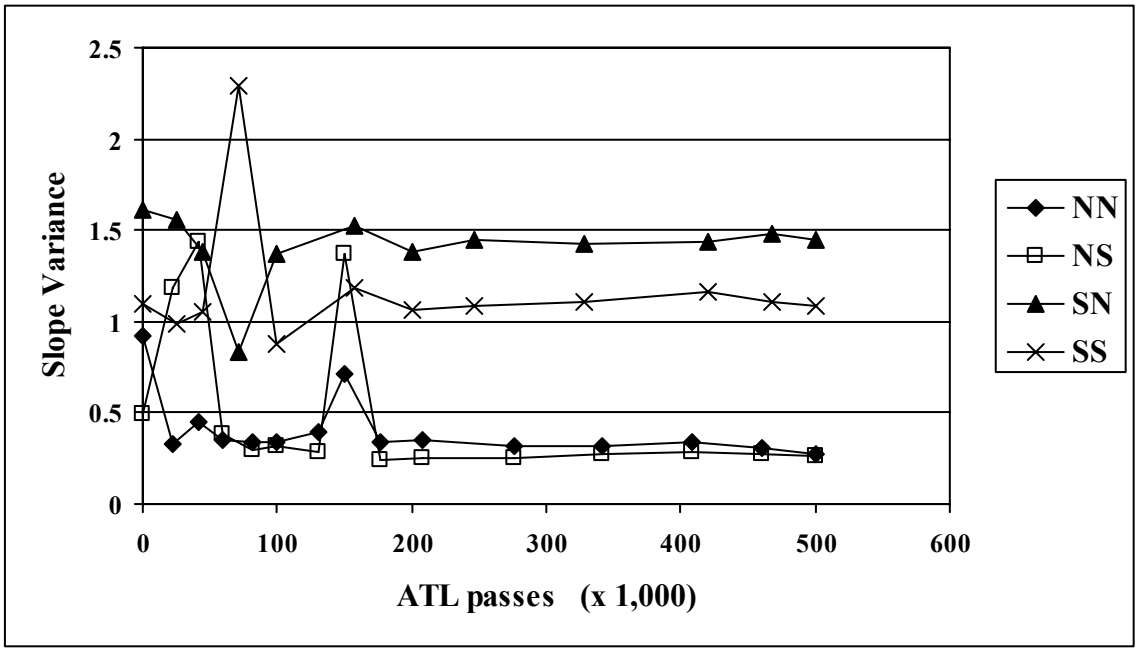

FIGURE 4.4: Evolution of Roughness

4.3. Horizontal Strains at the Bottom of the Asphalt Concrete Layer

The strain and pressure values were recorded for at least four cycles (eight passes) of the ATL load assembly, at a sampling frequency of 100Hz. Recording was started when the ATL load assembly was at the West end of the travel and started traveling East. All strain measurements were made with the wheel centered right above the gages. When the wheel was passing on the pavement, the tires were straddling the gage (Figure 4.5). Since no lateral wander of the ATL load assembly was used in this experiment, no strain measurements were performed with one tire passing right above the strain gages. Higher strains may have induced at the bottom of the three-inch thick asphalt layer at right underneath the tire.

The stress and strain data was stored in the same electronic file, in a spreadsheet format, along with the load assembly position data. Figure 4.6 presents the six typical shapes of the strain signal that were observed for a complete ATL test cycle (from the time the load assembly

leaves and arrives at the West end of travel position). The values A to G recorded on the strain signals are given in Appendix D.

As mentioned earlier, five strain gages failed during placement of the asphalt concrete layer, possibly due to high temperature of the asphalt mixture. The failed gages are:

- Both gages measuring longitudinal strain in section SS;
- Both gages measuring transverse strain in section SN;
- The gage measuring transverse strain in section NS, the West side. The gage at the East side of the same lane, NS, gave unreliable strain data after first 100,000 ATL passes.

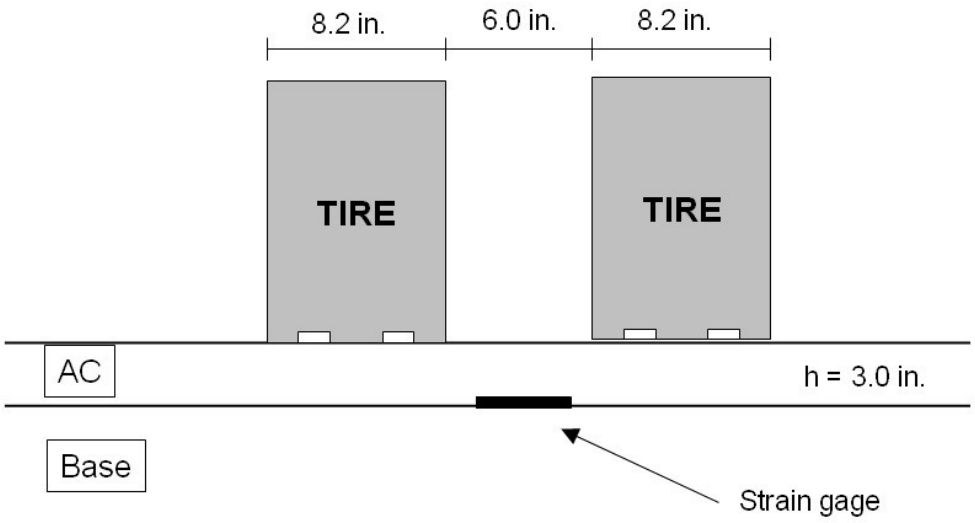

FIGURE 4.5: Position of the Wheel During Strain Measurements

From the recorded strain signals, six signal shape types were identified. Strain signal shapes 1, 2, 3 and 4 were observed when the single axle loads were applied to the pavement structures. The strain values (S) were computed with the following formulas:

Shape type 1, 2 and 3: $S = (A+C)/2 - B$

Shape type 4: $S = (A-B) / 2$

Shape type 4 was observed only for the strain gauge measuring transverse strain, placed on the East side of Lane NS. Because the shape of the strain signal for this gage was not consistent, it is very likely that this gage did not provided reliable data after the first 100,000 ATL load assembly passes. However, the measured values have been reported in the Appendix D.

Strain signal type 5 and 6 were observed when tandem axle loads were applied to the pavement structures. The strain values were computed with the following formula:

$$S = (A + B + C + D)/4 - E$$

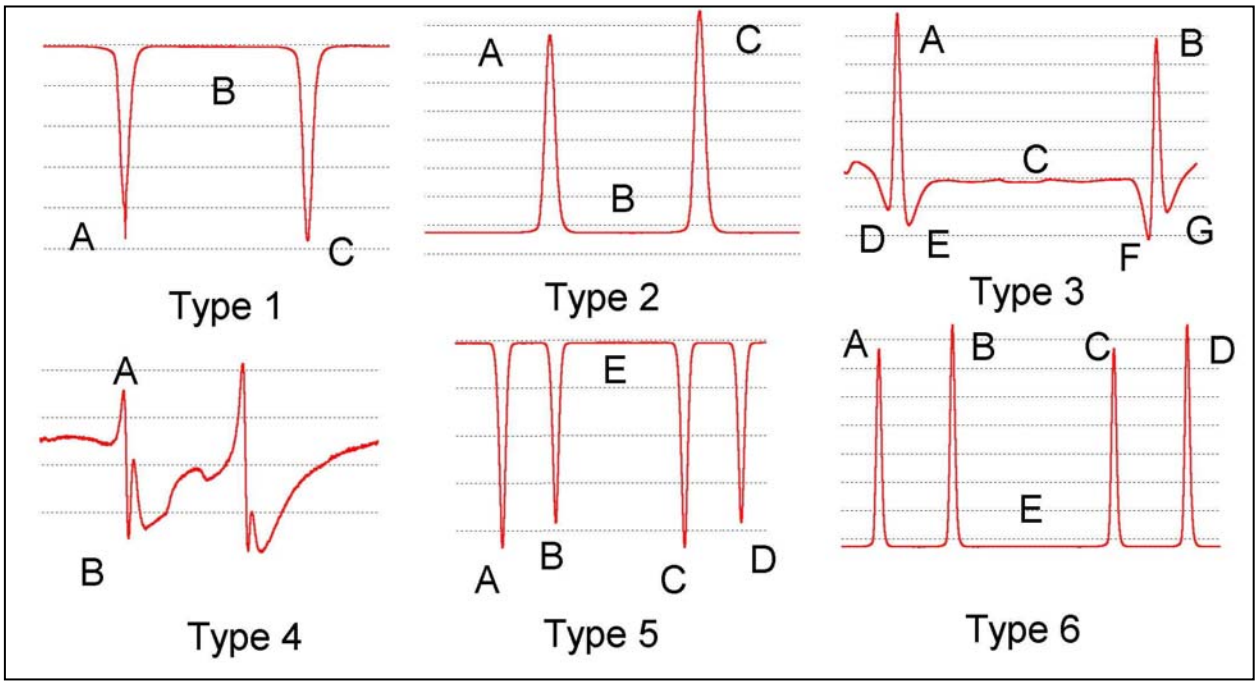

FIGURE 4.6: Types of Strain Signal Shapes

The values of measured strains are given for all working strain gages in the Appendix D. Tables 4.5 and 4.6 tabulate the average values of the measured strains, when both gages measuring the same strain (longitudinal or transverse) on the same pavement sections were

recorded. The average strain values are plotted in Figures 4.7 and 4.8. Figure 4.7 indicates that the longitudinal strains decrease with the increasing number of load repetitions. A surprising result is that the transverse strain at the bottom of the asphalt layer was higher for the pavement with nine inches of foamed asphalt stabilized RAP base (NS) than for the pavement with six inches of foamed asphalt stabilized RAP base (NN). Unfortunately, both gages measuring longitudinal strain in the lane with crushed stone AB-3 base (SS) failed during the construction of the asphalt concrete layer.

Figure 4.8 indicates that with the exception of the gage in the pavement with six inches of foamed asphalt stabilized RAP base (NN), the gages measuring transverse strains were not giving reliable data after the first 100,000 ATL passes. In fact, four gages for measuring transverse strain failed during construction. When the values measured in the first 100,000 ATL passes are compared, the measured transverse strains in the pavements with six and nine inches of foamed asphalt stabilized RAP base (NN and NS) are smaller than the strains measured in the pavement with nine inches of conventional crushed stone AB-3 base (SS). Figures 4.7 and 4.8 also indicate that the measured longitudinal strains are higher than the transverse strains, up to 12 times higher for the pavement with nine inches of foamed asphalt stabilized RAP base (NS).

4.4. Vertical Stresses at the Top of the Subgrade

Vertical compressive stresses at the top of the subgrade were measured in each pavement structure at two locations (West and East) as shown in Figure 3.4. The stress measurements were performed on the dates indicated in the pavement monitoring plan given in Table 3.9.

The measured compressive stresses are reported in the Appendix E. The average values of the stresses measured by the two pressure cells in the same lane are reported in Table 4.7 and have been plotted in Figure 4.9. As expected, for the stabilized base, the compressive stresses at

the top of the subgrade remained almost constant for the first 100,000 single axle load repetitions, and started to increase when the tandem axle loads were applied. Also, the stress values were higher for the six-inch base pavement (NN), lower for the nine-inch base pavement (NS) and the lowest for the 12-inch base pavement (SN).

The stress values for the pavement with the granular base (SS) are very similar to those for the pavement with the nine-inch foamed asphalt stabilized RAP base (NS). This clearly indicates that the foamed asphalt stabilized RAP base provides the same level of protection to the subgrade soil as the conventional granular base. Therefore, to limit the permanent deformation at the top of the subgrade soil layer, it is reasonable to consider that one inch of foamed asphalt stabilized RAP material is equivalent to one inch of conventional (AB-3) crushed stone when used as a base layer material.

TABLE 4.5: Longitudinal Strains at the Bottom of the Asphalt Concrete Layer

Direction	Date	Passes (x 1,000)	Lane		
			NN	NS	SN
L	17-Dec-01	0	836	1188	
L	15-Feb-02	23	806	1150	
L	19-Feb-02	26	707	1073	
L	25-Feb-02	42	704	1047	
L	26-Feb-02	47	734	1064	
L	1-Mar-02	60	679	1034	
L	5-Mar-02	67	680	1033	
L	8-Mar-02	82	684	1024	
L	15-Mar-02	100	639	994	
L	5-Apr-02	130	568	858	
L	12-Mar-02	150	593	840	
L	19-Mar-02	176	636	932	
L	26-Apr-02	208	652	936	
L	10-Jun-02	276	566	759	
L	20-Jun-02	341	527	632	
L	10-Jul-02	460	571	697	
L	17-Jul-02	500	669	717	
L	13-Dec-01	0			671
L	7-Jan-02	25			365
L	11-Jan-02	45			200
L	28-Jan-02	71			207
L	8-Feb-02	100			240
L	24-Jul-02	150			99
L	29-Jul-02	171			144
L	2-Aug-02	201			128
L	6-Aug-02	224			185
L	23-Aug-02	247			107
L	27-Aug-02	273			97
L	4-Sep-02	328			111
L	12-Sep-02	386			111
L	17-Sep-02	420			148
L	25-Sep-02	468			107
L	2-Oct-02	500			115

TABLE 4.6: Transverse Strains at the Bottom of the Asphalt Concrete Layer

Direction	Date	Passes (x 1,000)	Lane		
			NN	NS	SS
T	17-Dec-01	0	273	109	
T	15-Feb-02	23	280	78	
T	19-Feb-02	26	226	72	
T	25-Feb-02	42	266	52	
T	26-Feb-02	47	289	32	
T	1-Mar-02	60	244	55	
T	5-Mar-02	67	231	63	
T	8-Mar-02	82	211	61	
T	15-Mar-02	100	221	52	
T	5-Apr-02	130	69		
T	12-Mar-02	150	101		
T	19-Mar-02	176	102		
T	26-Apr-02	208	88		
T	10-Jun-02	276	43		
T	20-Jun-02	341	-7	696	
T	10-Jul-02	460		618	
T	17-Jul-02	500		556	
T	13-Dec-01	0			378
T	7-Jan-02	25			381
T	11-Jan-02	45			408
T	28-Jan-02	71			410
T	8-Feb-02	100			378

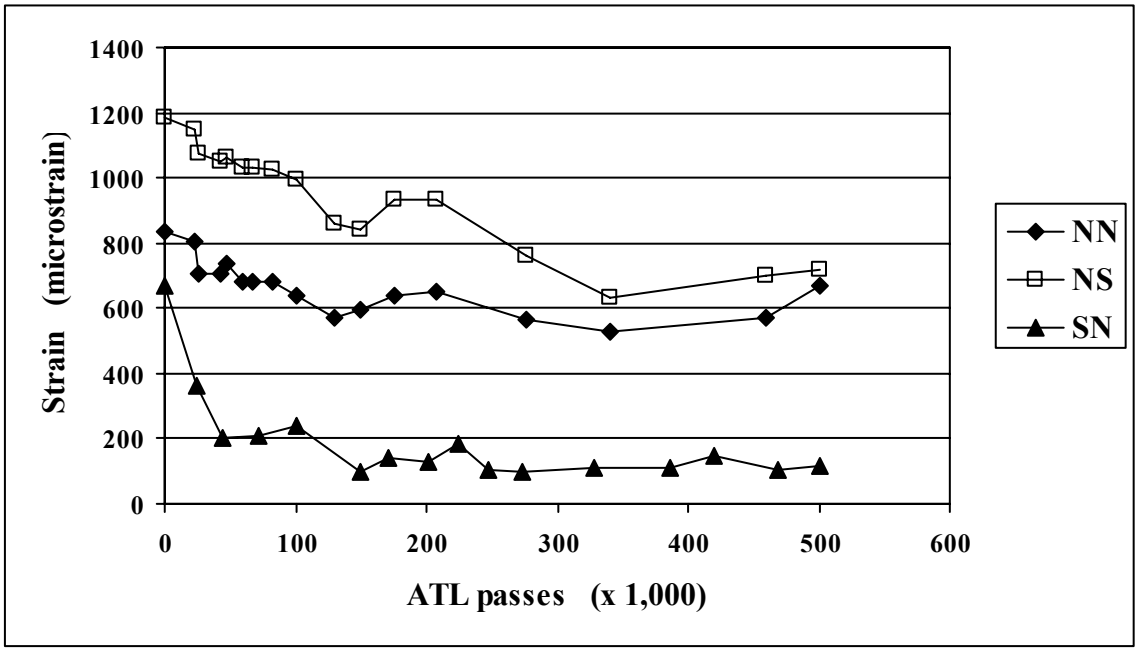

FIGURE 4.7: Longitudinal Strains at the Bottom of the Asphalt Concrete Layer

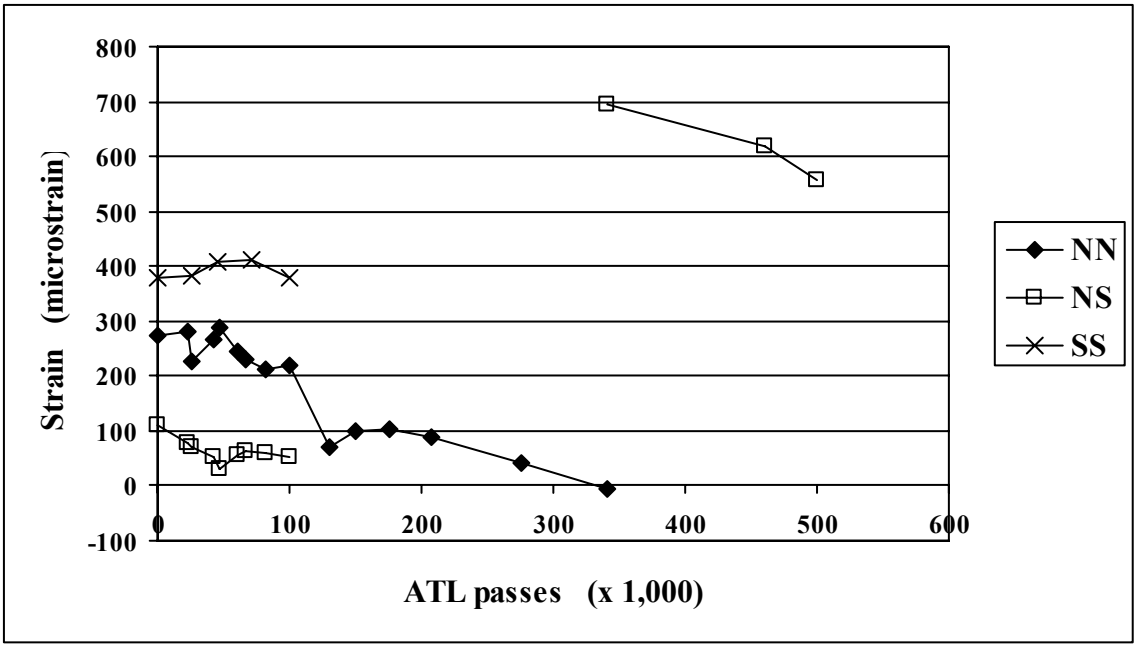

FIGURE 4.8: Transverse Strains at the Bottom of the Asphalt Concrete Layer

TABLE 4.7: Average Vertical Compressive Stresses (psi) at the Top of Subgrade

Date	ATL Passes (x 1,000)	NN	NS	Date	ATL Passes (x 1,000)	SN	SS
17-Dec-01	0	6.693	4.143	13-Dec-01	0	0.168	1.255
15-Feb-02	23	7.583	4.200	7-Jan-02	25	0.135	1.990
19-Feb-02	26	6.788	3.690	11-Jan-02	45	0.278	3.445
25-Feb-02	42	6.220	3.248	28-Jan-02	71	0.235	2.855
26-Feb-02	47	6.030	3.133	8-Feb-02	100	0.240	3.130
1-Mar-02	60	5.673	2.730	24-Jul-02	150	0.963	5.170
5-Mar-02	67	5.920	3.048	29-Jul-02	171	0.899	5.120
8-Mar-02	82	7.305	3.008	2-Aug-02	201	1.148	4.300
15-Mar-02	100	6.095	2.820	6-Aug-02	224	1.160	4.315
5-Apr-02	130	5.785	2.729	23-Aug-02	247	0.923	5.790
12-Mar-02	150	6.248	2.455	27-Aug-02	273	1.061	5.823
19-Mar-02	176	7.489	3.756	4-Sep-02	328	0.978	5.260
26-Apr-02	208	6.749	2.946	12-Sep-02	386	0.910	3.575
10-Jun-02	276	8.898	4.655	17-Sep-02	420	0.418	2.965
20-Jun-02	341	10.029	5.631	25-Sep-02	468	0.689	4.000
10-Jul-02	460	10.448	5.868	2-Oct-02	500	0.456	3.068
17-Jul-02	500	9.983	4.901				

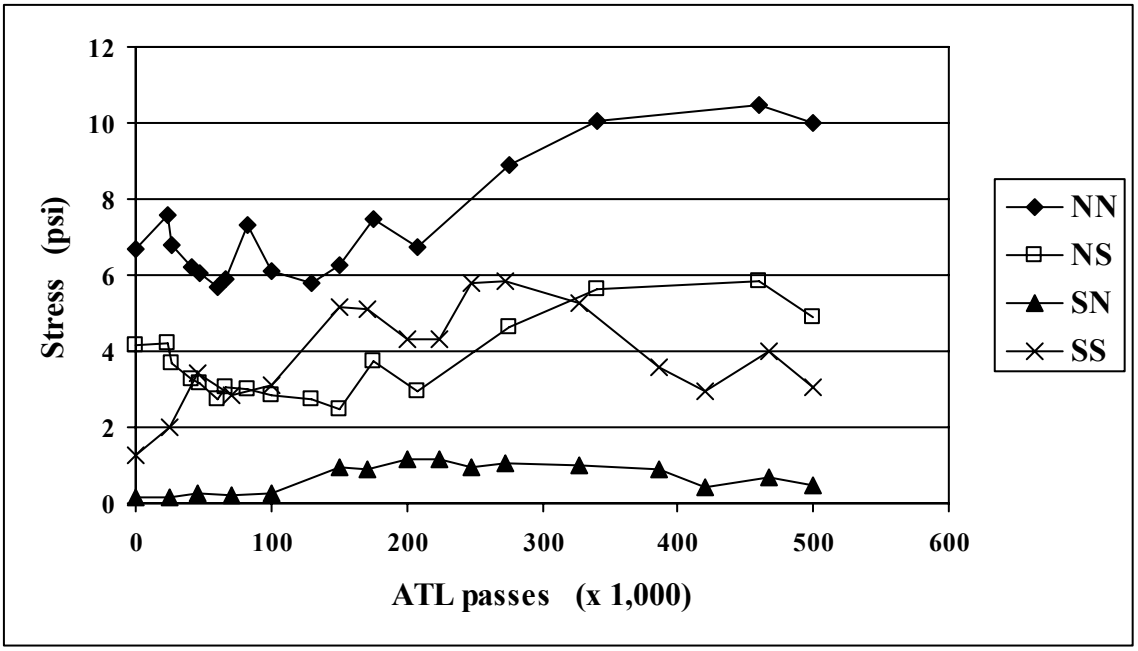

FIGURE 4.9: Average Vertical Stress at the Top of the Subgrade

4.5 Backcalculation of Layer Moduli from the FWD Deflections

The backcalculation analysis was performed using MODULUS 4.0 backcalculation program. The measured FWD deflections along with the backcalculated layer moduli are reported in the Appendix F. The backcalculated asphalt layer moduli were not corrected to the standard temperature of 68°F, because the temperature at the bottom of the asphalt layer varied between 67°F and 72° F during FWD tests, close to the reference temperature of 68°F (Table 3.7). The backcalculated moduli for the last drop at the 9,000 lbs load level (Drop 3) are reported in Table 4.8. The average values of the backcalculated moduli for the six FWD stations are plotted for each pavement layer in Figures 4.10, 4.11 and 4.12 for all three FWD test sessions.

Figure 4.10 and Table 4.8 indicate that the backcalculated asphalt layer moduli had large variabilities for the six FWD test stations. Moduli are also quite different for the four pavement sections, despite the fact that the same HMA mix was used in paving. This large variation can be attributed to the fact that the asphalt layer thickness of the constructed pavements varied along the pavement sections and thus may be different from the thickness values used in the backcalculation process. However, the thickness variation alone cannot explain the difference in the backcalculated moduli obtained from the deflections measured on December 6 and 19, 2001. The backcalculated moduli should be similar because on both occasions FWD tests were done before any ATL loading was applied, and the recorded temperatures at the bottom of the asphalt layer were similar.

Figure 4.11 and Table 4.8 indicate that the backcalculated modulus for the foamed asphalt stabilized RAP base remained relatively unchanged during the experiment, and was always higher that the backcalculated moduli for the AB-3 granular base material. This indicates that the stiffer foamed asphalt stabilized RAP base may assure a better protection to the soil

subgrade than the conventional AB-3 granular base.

Table 4.8 and Figure 4.12 indicate that the backcalculated subgrade soil moduli remained unchanged during the experiment, and was close to 15,000 psi for lanes NN, NS and SS. Higher values of around 20,000 psi were obtained for the lane SN.

TABLE 4.8: Backcalculated Moduli from the FWD Deflections

Section	Date	Passes (x1,000)	Station	Drop Nr.	E(AC) (psi)	E(Base) (psi)	Mr subgrade (psi)
NN	12/06/01	0	1	3	1,466,621	99,761	14,880
NN	12/06/01	0	2	3	1,664,273	82,385	14,956
NN	12/06/01	0	3	3	794,320	79,990	14,783
NN	12/06/01	0	4	3	604,185	96,493	14,826
NN	12/06/01	0	5	3	791,633	76,949	14,702
NN	12/06/01	0	6	3	739,434	82,748	14,609
Average					**1,010,078**	**86,388**	**14,793**
NN	12/19/01	5	1	3	2,199,995	62,528	14,467
NN	12/19/01	5	2	3	2,199,995	54,906	14,552
NN	12/19/01	5	3	3	1,159,546	54,635	14,020
NN	12/19/01	5	4	3	1,033,350	59,159	14,243
NN	12/19/01	5	5	3	1,033,920	52,067	14,170
NN	12/19/01	5	6	3	1,056,204	52,423	14,079
Average					**1,447,168**	**55,953**	**14,255**
NN	04/06/02	149	1	3	1,999,995	69,921	14,060
NN	04/06/02	149	2	3	1,999,995	60,165	14,395
NN	04/06/02	149	3	3	1,576,328	40,894	13,718
NN	04/06/02	149	4	3	1,337,851	47,719	14,054
NN	04/06/02	149	5	3	990,655	63,504	13,449
NN	04/06/02	149	6	3	1,095,927	56,854	13,559
Average					**1,500,125**	**56,510**	**13,873**
NS	12/06/01	0	1	3	814,250	79,745	15,875
NS	12/06/01	0	2	3	954,782	77,554	15,883
NS	12/06/01	0	3	3	654,088	69,424	16,428
NS	12/06/01	0	4	3	505,584	81,465	16,074
NS	12/06/01	0	5	3	666,317	66,452	15,698
NS	12/06/01	0	6	3	493,972	63,477	15,973
Average					**681,499**	**73,020**	**15,989**

TABLE 4.8: Backcalculated Moduli from the FWD Deflections
(continued)

Section	Date	Passes (x1,000)	Station	Drop Nr.	E(AC) (psi)	E(Base) (psi)	Mr subgrade (psi)
NS	12/19/01	5	1	3	1,214,564	60,163	15,351
NS	12/19/01	5	2	3	1,174,081	62,590	15,351
NS	12/19/01	5	3	3	998,732	46,176	15,657
NS	12/19/01	5	4	3	656,704	60,179	15,492
NS	12/19/01	5	5	3	1,027,315	38,280	15,326
NS	12/19/01	5	6	3	797,728	40,861	15,302
Average					**978,187**	**51,375**	**15,413**
NS	04/06/02	149	1	3	1,497,737	74,144	15,369
NS	04/06/02	149	2	3	1,563,479	77,889	15,149
NS	04/06/02	149	3	3	1,417,438	44,774	15,274
NS	04/06/02	149	4	3	853,398	63,181	15,096
NS	04/06/02	149	5	3	1,271,880	35,103	14,904
NS	04/06/02	149	6	3	842,532	43,403	14,486
Average					**1,241,077**	**56,416**	**15,046**
SN	12/06/01	0	1	3	560,531	138,245	22,066
SN	12/06/01	0	2	3	586,136	131,626	21,941
SN	12/06/01	0	3	3	1,007,605	106,092	21,963
SN	12/06/01	0	4	3	717,908	125,773	21,641
SN	12/06/01	0	5	3	601,373	104,387	22,573
SN	12/06/01	0	6	3	561,135	98,144	23,259
Average					**504,336**	**88,033**	**16,680**
SN	12/19/01	5	1	3	760,041	131,653	21,589
SN	12/19/01	5	2	3	921,148	116,909	21,724
SN	12/19/01	5	3	3	1,343,135	95,231	21,715
SN	12/19/01	5	4	3	1,078,745	107,539	21,530
SN	12/19/01	5	5	3	818,686	96,420	21,642
SN	12/19/01	5	6	3	752,204	93,478	21,944
Average					**945,660**	**106,872**	**21,691**
SN	01/24/02	71	1	3	1,430,716	114,216	20,655
SN	01/24/02	71	2	3	1,699,996	96,664	20,784
SN	01/24/02	71	3	3	1,699,996	88,618	20,271
SN	01/24/02	71	4	3	1,464,856	90,244	20,739
SN	01/24/02	71	5	3	1,467,630	82,613	21,178
SN	01/24/02	71	6	3	1,312,098	85,337	21,045
Average					**1,512,549**	**92,949**	**20,779**

TABLE 4.8: Backcalculated Moduli from the FWD Deflections (continued)

Section	Date	Passes (x1,000)	Station	Drop Nr.	E(AC) (psi)	E(Base) (psi)	Mr subgrade (psi)
SN	04/06/02	100	1	3	950,975	198,010	21,759
SN	04/06/02	100	2	3	1,073,149	177,954	21,454
SN	04/06/02	100	3	3	1,555,869	131,029	21,774
SN	04/06/02	100	3	3	1,699,996	115,234	22,594
SN	04/06/02	100	4	3	1,086,798	150,108	22,123
SN	04/06/02	100	4	3	1,178,324	148,586	21,871
SN	04/06/02	100	5	3	1,113,196	142,980	22,603
SN	04/06/02	100	6	3	998,584	147,020	22,994
Average					**1,272,128**	**139,160**	**22,327**
SS	12/06/01	0	1	3	703,239	34,570	16,528
SS	12/06/01	0	2	3	766,176	33,640	16,663
SS	12/06/01	0	3	3	690,185	36,204	16,638
SS	12/06/01	0	4	3	737,515	31,043	17,087
SS	12/06/01	0	5	3	800,298	31,141	16,926
SS	12/06/01	0	6	3	781,479	30,194	16,732
Average					**746,482**	**32,799**	**16,762**
SS	12/19/01	5	1	3	922,727	29,822	15,831
SS	12/19/01	5	2	3	880,967	32,810	15,806
SS	12/19/01	5	3	3	811,682	36,367	15,525
SS	12/19/01	5	4	3	845,523	31,446	15,834
SS	12/19/01	5	5	3	904,088	30,971	15,813
SS	12/19/01	5	6	3	915,570	29,631	15,673
Average					**880,093**	**31,841**	**15,747**
SS	01/24/02	71	1	3	1,022,371	24,868	15,108
SS	01/24/02	71	2	3	1,009,966	25,100	15,369
SS	01/24/02	71	3	3	948,135	27,531	14,806
SS	01/24/02	71	4	3	963,839	26,748	14,966
SS	01/24/02	71	5	3	947,535	27,502	14,800
SS	01/24/02	71	6	3	945,545	28,909	14,554
Average					**972,899**	**26,776**	**14,934**
SS	04/06/02	100	1	3	1,012,684	36,453	17,099
SS	04/06/02	100	2	3	998,497	37,254	17,248
SS	04/06/02	100	3	3	944,307	37,322	16,738
SS	04/06/02	100	4	3	984,563	33,935	17,381
SS	04/06/02	100	5	3	1,008,850	34,709	16,888
SS	04/06/02	100	6	3	1,041,664	34,611	17,243
Average					**998,428**	**35,714**	**17,100**

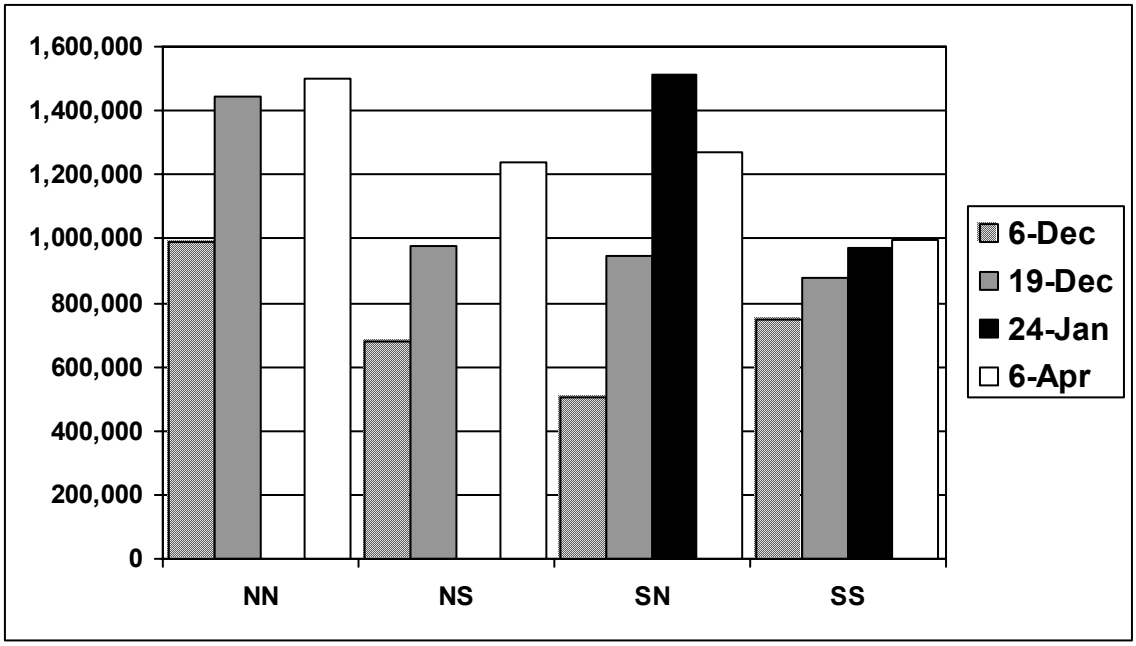

FIGURE 4.10: Average Backcalculated Asphalt Layer Modulus from FWD Deflections

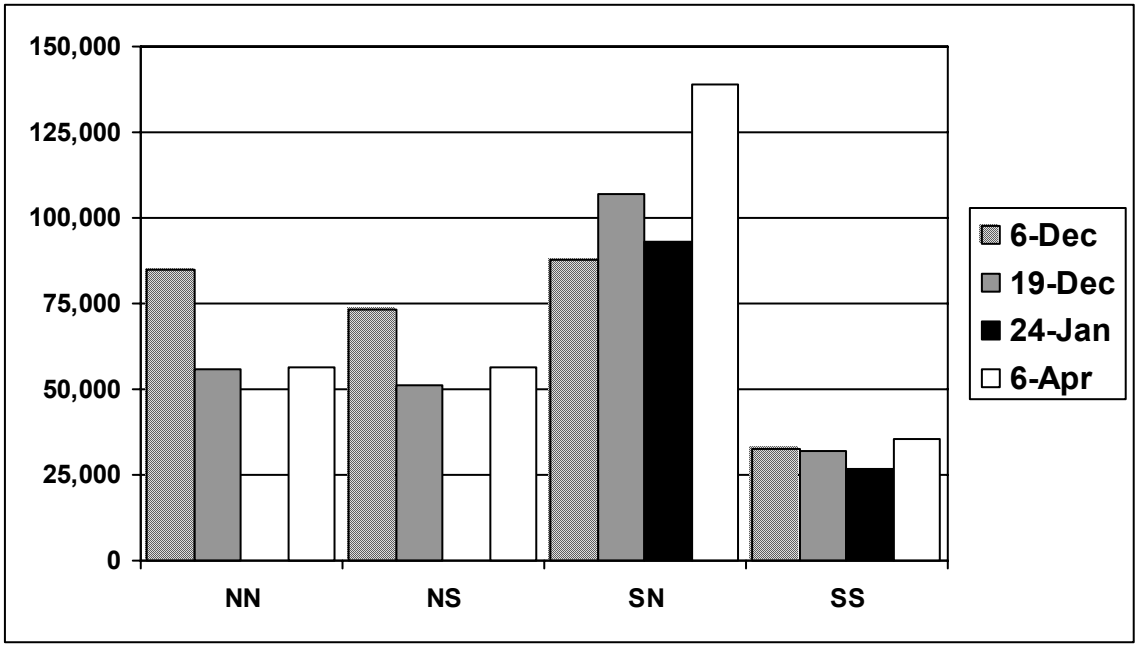

FIGURE 4.11: Average Backcalculated Base Layer Modulus from FWD Deflections

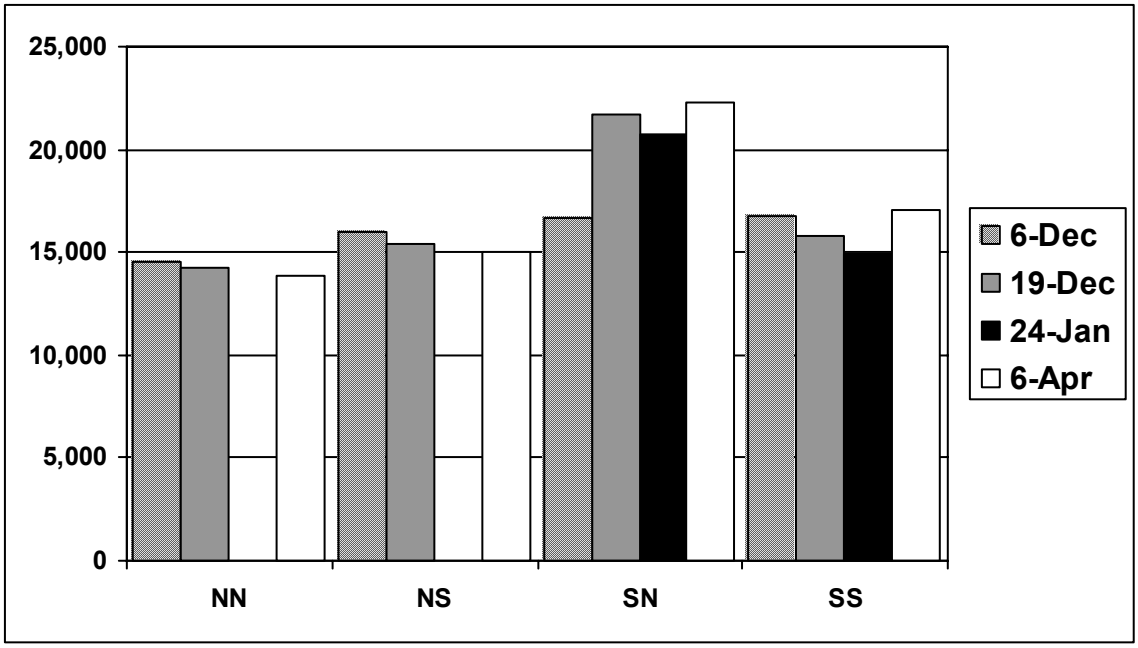

FIGURE 4.12: Average Backcalculated Subgrade Soil Modulus

4.6 Backcalculation of Layer Moduli from the Weight Drop Tests

The MODULUS 4.0 program was used to backcalculate the layer moduli. The analysis showed that for several weight drop tests, the beam supporting the LVDTs might have moved when the weight was dropped. Therefore, the deflections readings were inaccurate, and as a result, the backcalculated layer moduli were too high or too low. Modifications were later made to the weight drop device, to alleviate this problem for the CISL Experiment # 12.

Also, the weight drop measurements were difficult to perform toward the end of the ATL load assembly passes, when the asphalt concrete heaved between the tire paths. The circular loading plate was not seated properly on the uneven asphalt surface, even when sand was used to smooth out the unevenness.

For the cases when the backcalculation was deemed successful and reasonable layer moduli were obtained, the moduli values are listed in the Appendix G. The average

backcalculated moduli were plotted in Figures 4.13, 4.14, 4.15 and 4.16. Figure 4.13 shows that the asphalt concrete layer modulus varied significantly but had a decreasing trend. The average values computed from the weight drop deflections were almost always lower than the moduli backcalculated from the FWD deflection (Figure 4.10).

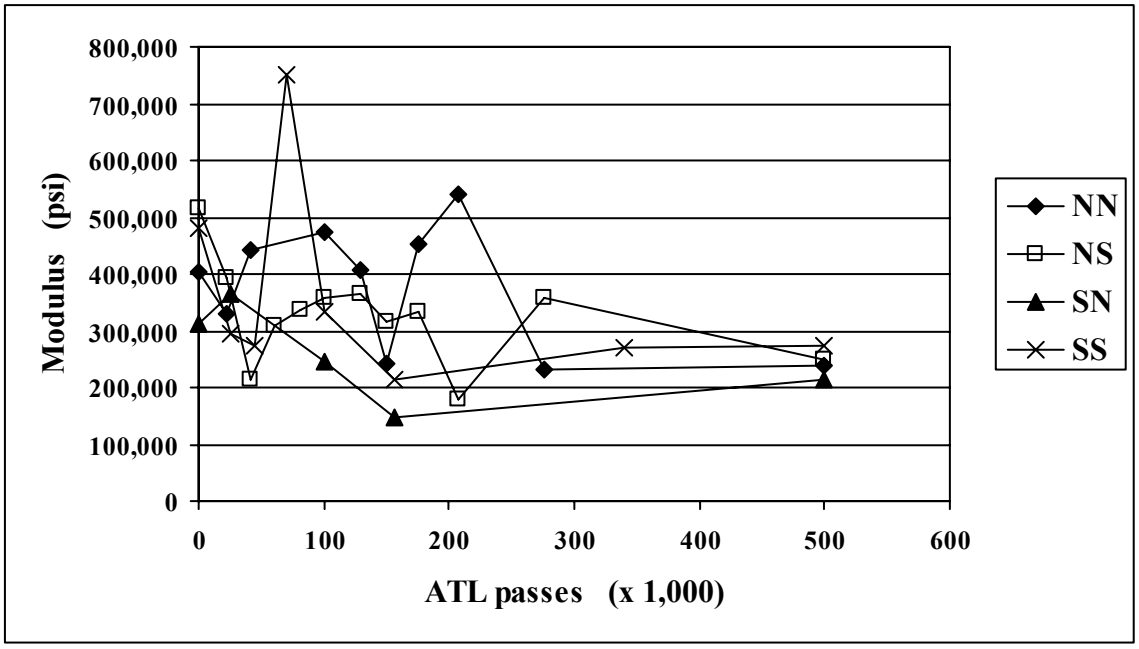

FIGURE 4.13: Backcalculated Asphalt Layer Modulus from the Weight Drop Deflections

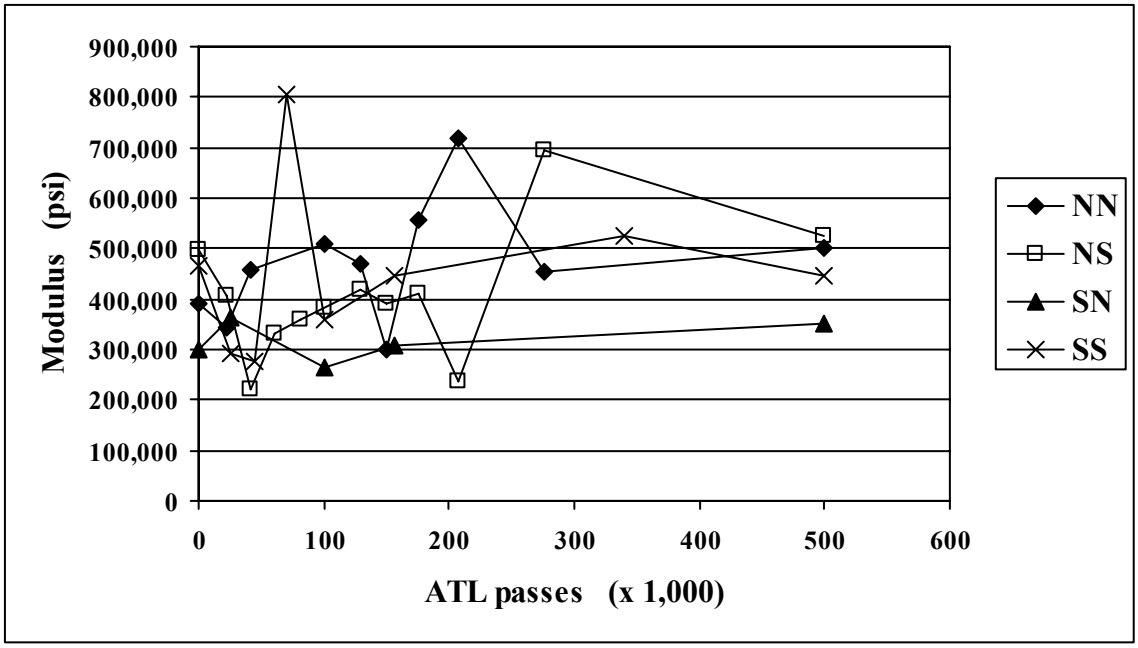

FIGURE 4.14: Temperature Corrected Asphalt Layer Modulus

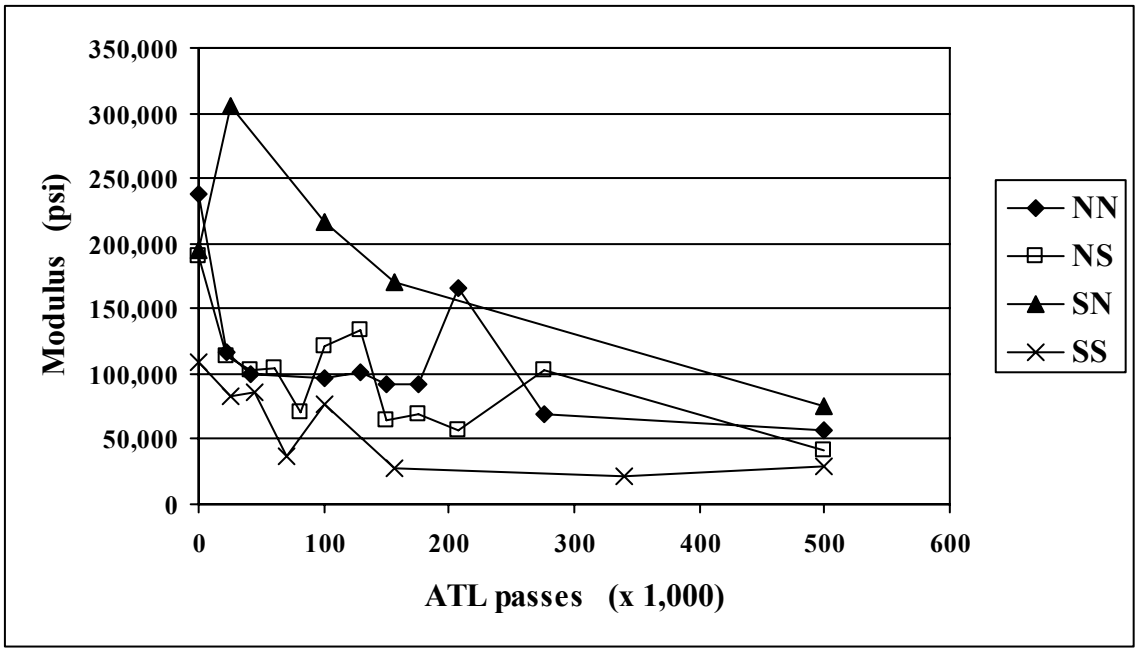

FIGURE 4.15: Backcalculated Base Layer Modulus from the Weight Drop Deflections

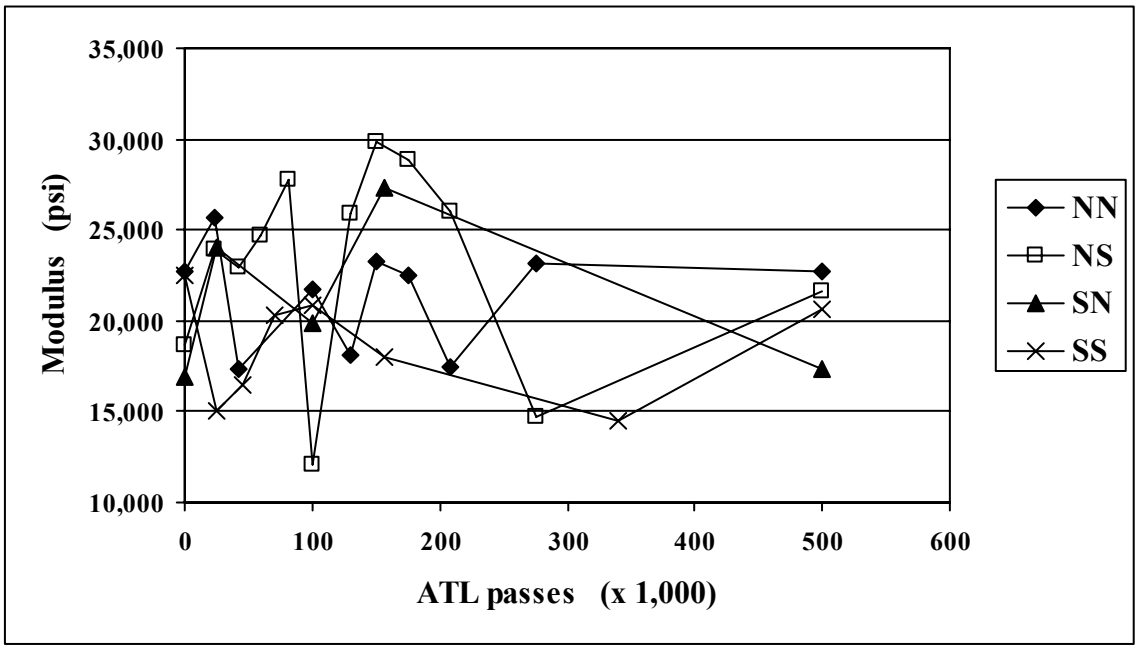

FIGURE 4.16: Backcalculated Subgrade Soil Modulus from the Weight Drop Deflections

The modulus of the asphalt concrete was corrected to the standard temperature of 68ºF (Figure 4.14) using the relationship recommended by Kim [21]:

$$E_{68} = E_T * 10^{0.0153(T - 68)} \quad (4.1)$$

Where:

E_{68}, E_T = backcalculated modulus of the asphalt concrete layer at temperature T (˚F) and the reference temperature of 68ºF

Figure 4.15 shows that the modulus of the foamed asphalt stabilized RAP base varied significantly, but overall, it had a decreasing trend with the values converging to below 100,000 psi toward the end of the experiment. The average moduli values computed from the weight drop deflections were lower than the moduli backcalculated from the FWD deflections (Figure 4.11). The backcalculated modulus of the crushed stone base decreased during the first 100,000 ATL load assembly passes but remained relatively unchanged after that. The average values computed

from the weight drop deflections were very similar to those backcalculated from the FWD deflections (Figure 4.11).

The backcalculated subgrade soil modulus varied between 15,000 and 30,000 psi (Figure 4.16). The average values computed from the weight drop deflections were always higher than those backcalculated from the FWD deflections (Figure 4.12). This can be explained by the higher load level used in the FWD tests that leads to larger stresses in the subgrade layer. The clayey, A-7-6 subgrade soil is stress sensitive; its modulus decreases when the stress level increases.

4.7 Pavement Cracking and Other Distresses

In this experiment, 500,000 ATL load repetitions were applied on each of the four pavement sections under study. All pavement sections exhibited only rutting in the wheel path. No cracking or other distresses were observed during the experiment.

4.8 Post-Mortem Evaluation

After 500,000 ATL load repetitions, loading was stopped. After consulting with the Project Monitor, Mr. Andy Gisi of KDOT, it was decided that the permanent deformation and rut depth values at the pavement surface reached levels that would allow comparison of performance of the four base layers. A destructive post-mortem evaluation was then conducted to further investigate the failure modes of the four pavement sections and to observe the degradation of the foundation layers.

4.8.1 Trenching and Coring

A transverse trench was cut in each of the two pairs of test sections at about the mid-lane location. The trenches were two feet wide. After the cuts were performed with a wet saw, the asphalt concrete was removed without disturbing the base layer (Figure 4.17). Underneath the

removed asphalt layer, the foamed asphalt stabilized RAP base was found to be a stiff layer without any cracks.

Both dry and wet coring was attempted in the foamed asphalt stabilized RAP base to extract sample for compressive modulus tests. Unfortunately, no intact core could be extracted. The FAS-FDR base material broke into two-three inch thick pieces (Figure 4.18). The failure plane at around two-three inches depth may be explained by the fact that the placement and compaction of the FAS-FDR base was done in approximately three-inch lifts. In normal pavement rehabilitation construction, the foamed asphalt stabilized RAP base would be placed and compacted in a single lift, especially if the layer is thinner than nine inches. In that case, the FAS-FDR base will not be 'laminated', as it was observed for the pavements tested in this experiment. Six-inch and four-inch diameter asphalt cores were extracted by a specialized crew from Kansas DOT, from the wheel path and outside the wheel path areas on each lane.

Square slabs (18 in. x 18 in.) were also sawn from the asphalt layer from the outside the wheel path areas (Figure 4.18). The sawn slabs were numbered and transported to the Advanced Asphalt Laboratory in Fiedler Hall on the KSU campus. The slabs were cut into smaller 10 in.x13 in. slabs and then set into metal forms. Ready-mix concrete was used to level the uneven bottom of the slabs so they could be tested in the Hamburg Wheel Tester.

After coring of the stabilized bases proved unsuccessful, the base material was removed to a depth of three inches so that the interface between the base and the asphalt concrete surface layers could be easily observed. More base material was removed in several areas so that dynamic cone penetrometer (DCP) tests could be performed on the subgrade soil.

4.8.2 Transverse Profiles and Layer Thickness

After the trenches were cut and three inches of base material were removed, transverse

profiles were first measured at the pavement surface right at the edge of the trenches using the profiler used during pavement condition monitoring. The transverse profiler measured the elevations at the pavement surface on two adjacent lanes at points spaced at 0.5 inches.

At the same locations where the elevation readings were taken, the asphalt concrete layer thickness was measured with a caliper. The elevation at the interface of the asphalt concrete and the base layers was computed at each point by subtracting the thickness from the elevation measured at the pavement surface.

FIGURE 4.17: Trench Cut on the Tested Pavements

FIGURE 4.18: Slabs and Cores Cut from the Tested Pavements

It is important to mention that, because of the similarity in color between the asphalt concrete layer and the FAS-FDR base layer, the interface between the two layers was difficult to discern. Therefore, the AC layer thicknesses may have not been accurately estimated. Figures 4.19 and 4.20 show the transverse profiles obtained at the post-mortem trenches. Figure 4.21 shows the measured thicknesses of the asphalt concrete layer. Figures 4.19 and 4.20 indicate that it is quite difficult to estimate, from the post-mortem profiles, the individual contribution of the base and surface layers to the permanent deformation at the pavement surface. Figure 4.21 indicates that the asphalt concrete layer thickness varied greatly in the transverse direction, between three and five inches. However, in the wheel path, the thickness of the asphalt layer varied only between three and four inches.

Because of the disturbances that are created during the digging of the trench, no post-mortem transverse profile can be measured at the surface of the subgrade soil layer. It is

therefore impossible to estimate the contribution of the subgrade layer to the permanent deformation at the pavement surface.

4.8.3 Estimation of the CBR of the Subgrade Soil

Dynamic Cone Penetrometer (DCP) tests were performed in the subgrade soil through the holes left by the extracted cores in the FAS-FDR base or in a hole dug in the crushed stone base. The relationship between the penetration vs. the number of drops of the DCP weight was used to estimate the CBR of the A-7-6 subgrade soil with the formula:

$$\log CBR = 2.20 - 0.71 \times (\log DCP)^{1.5} \quad (4.2)$$

Where: DCP is in mm per blow.

Figure 4.22 plots the computed CBR from the DCP tests. The results show that, with the exception of one value measured under the inside wheel path on lane SN, the CBR values of the compacted subgrade soil were similar for all four pavement test sections.

4.8.4 Rutting Characteristics of Asphalt Concrete

As mentioned earlier, the slabs sawn from the ATL pavements were trimmed to make specimens for the Hamburg Wheel Tester. The Hamburg wheel-tracking device used in this study has been manufactured by PMW, Inc. based out of Salina, Kansas and is capable of testing a pair of samples simultaneously. Figure 4.23 shows the Hamburg wheel tester at the Advanced Asphalt Test Laboratory of Kansas State University. The sample tested was usually 10.25 in. wide, 12.6 in. long and 1.6 in. deep. The samples were submerged under water at 122°F. The wheel of the tester is made of steel and is 4.7cm (1.85in) wide. The wheel applied a load of 158lbs and made 52 passes per minute. Each sample was tested for 20,000 passes or until 0.79 in. deformation occurs. Rut depth or deformation is measured at 11 different points along the length of each sample with a Linear Variable Differential Transformer (LVDT).

The various results that are obtained from the Hamburg Wheel Tester are creep slope, stripping slope and the stripping inflection point as depicted in Figure 4.24 [22]. The creep slope relates to rutting from plastic flow and is the inverse of the rate of deformation in the linear region of the deformation curve, after post compaction effects have been ended and before the onset of stripping. The stripping slope is the inverse of the rate of deformation in the linear region of the deformation curve, after stripping begins and until the end of the test. It is the number of passes required to create one mm impression from stripping, and is related to the severity of moisture damage. The stripping inflection point is the number of passes at the intersection of the creep slope and the stripping slope and is related to the resistance of the HMA to moisture damage. An acceptable mix is specified by the City of Hamburg to have less than 0.16 in. mm rut depth after 20,000 passes at a 122°F test temperature. However, this criterion was found to be very harsh in subsequent studies of the Colorado Department of Transportation [22].

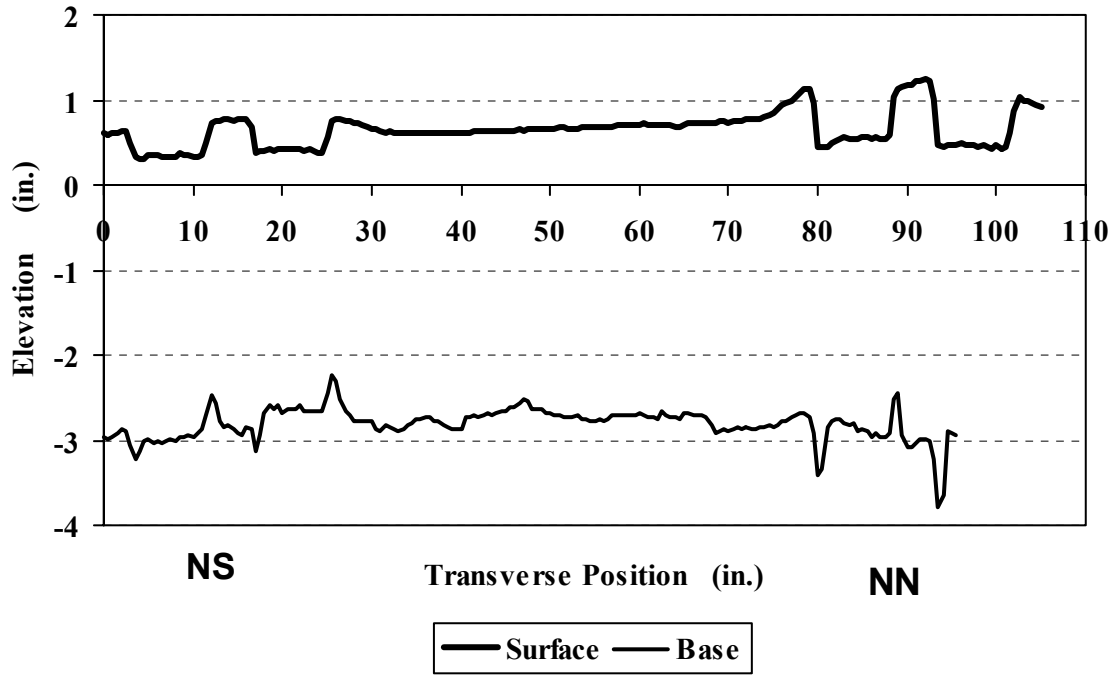

FIGURE 4.19: Transverse Post-Mortem Profile in the NN and NS Sections

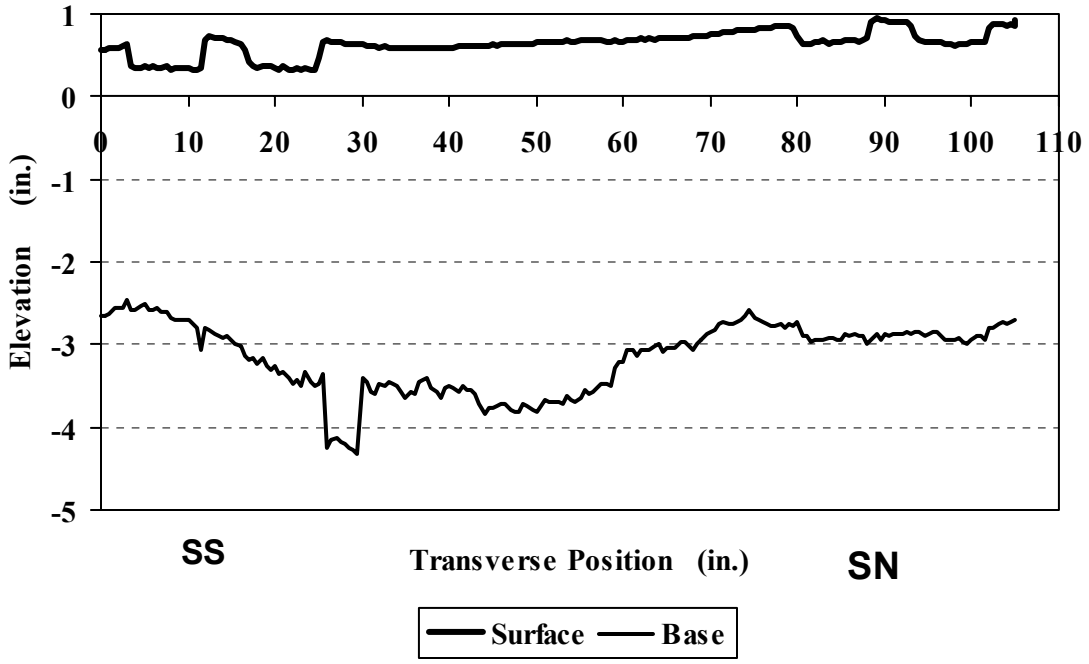

FIGURE 4.20: Transverse Post-Mortem Profile in the SN and SS Sections

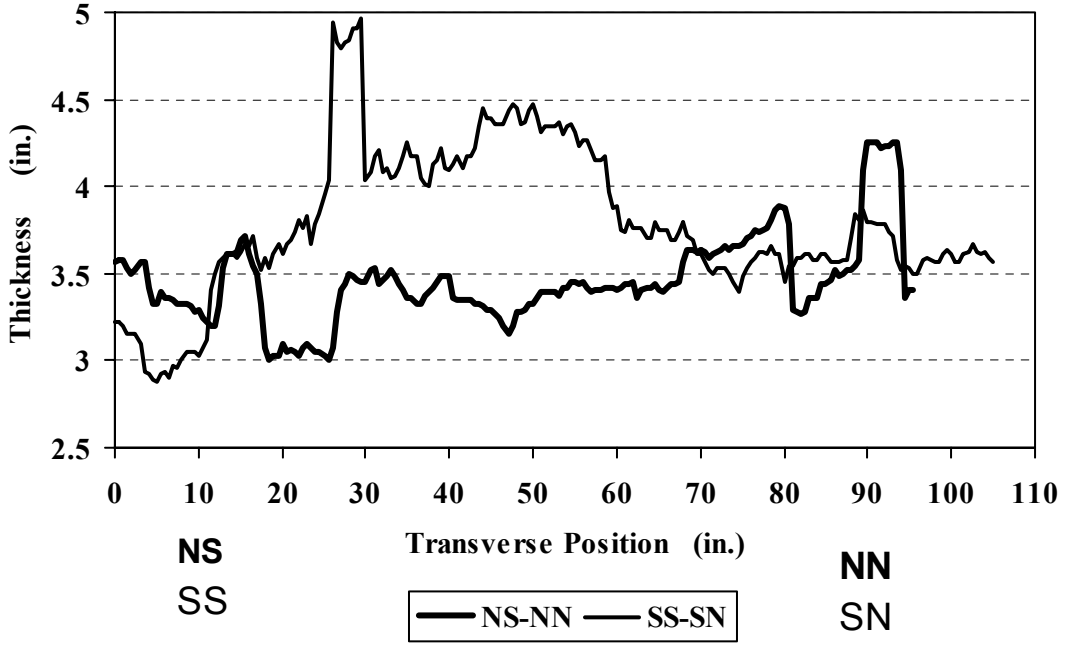

FIGURE 4.21: Asphalt Concrete Layer Thickness from the Post-Mortem Investigations

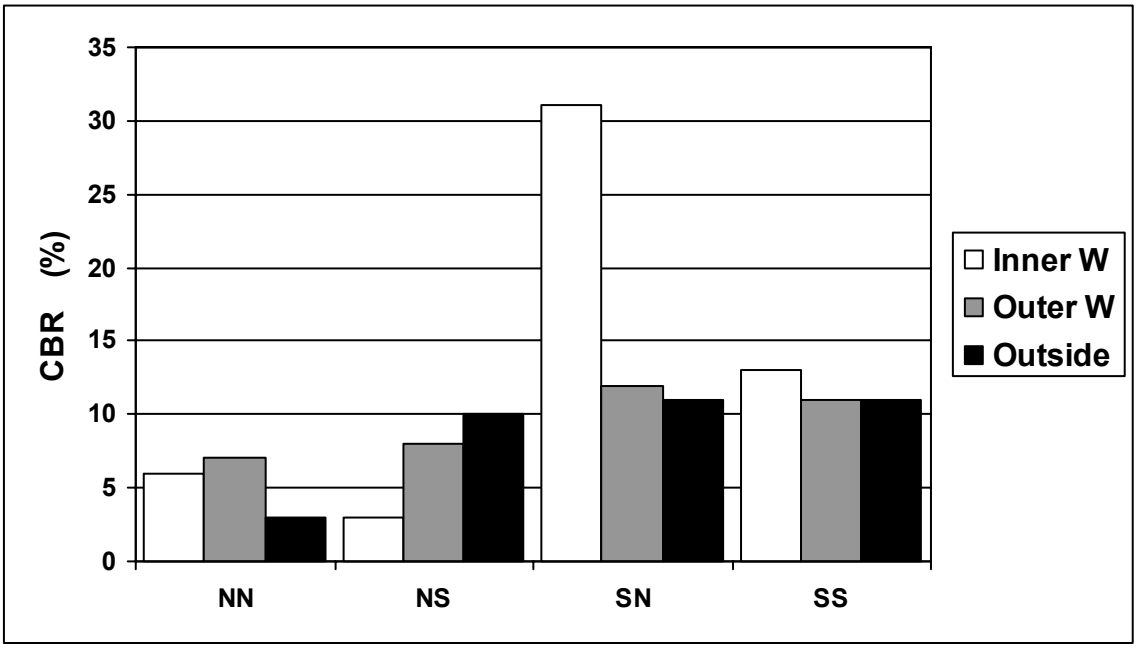

FIGURE 4.22: Estimated Subgrade Soil CBR from the DCP Measurements

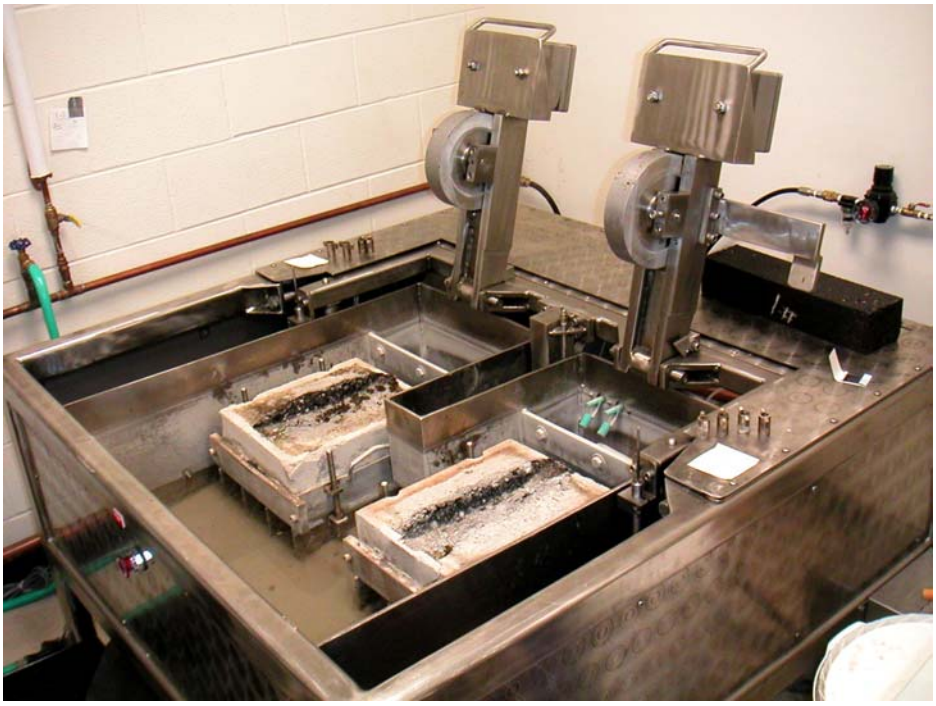

FIGURE 4.23: Hamburg Wheel Tester

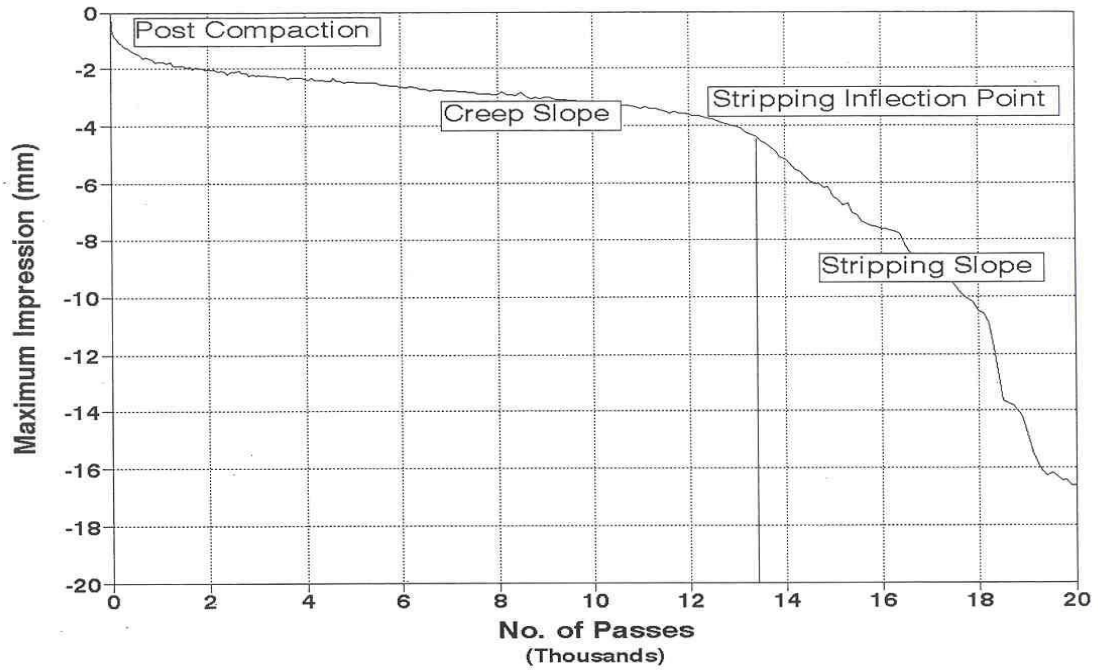

FIGURE 4.24: Interpretation of Results from the Hamburg Wheel Tester [21]

Only one pair of slab sample could be successfully tested in this study using the asphalt concrete slabs sawn from the ATL test pavements. Figure 4.25 shows the vertical deformation of the slabs under the Hamburg Wheel Tester and Table 4.9 tabulates and compares the results of this mixture with a number of Superpave mixtures tested under similar conditions at Kansas State University. Hamburg Wheel tests were also conducted on two sets of cores from the ATL test pavements. Figure 4.26 shows the typical vertical deformation results with the Hamburg wheel passes for one set of cores. Table 4.9 also tabulates the results for both sets of core. The slab and core results are quite comparable. The results show that the ATL test pavement asphalt concrete mixture (SM 12.5) outperformed similar size in-service Superpave mixtures tested earlier in terms of rutting. However, the stripping performance is similar to a Superpave mixture

designed by the Kansas Asphalt Pavement Association (KAPA) for an intersection project in Junction City, Kan. Overall, this is the third best performing mixture tested at KSU thus far.

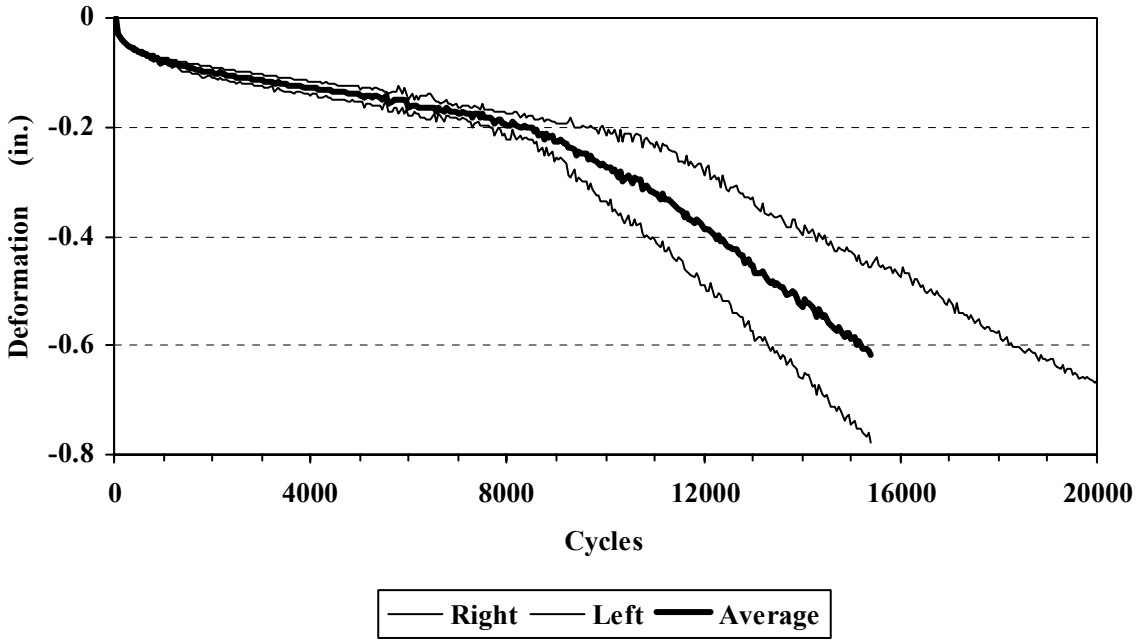

FIGURE 4.25: Measured Deformation in the Hamburg Wheel Rut Tester (Slabs)

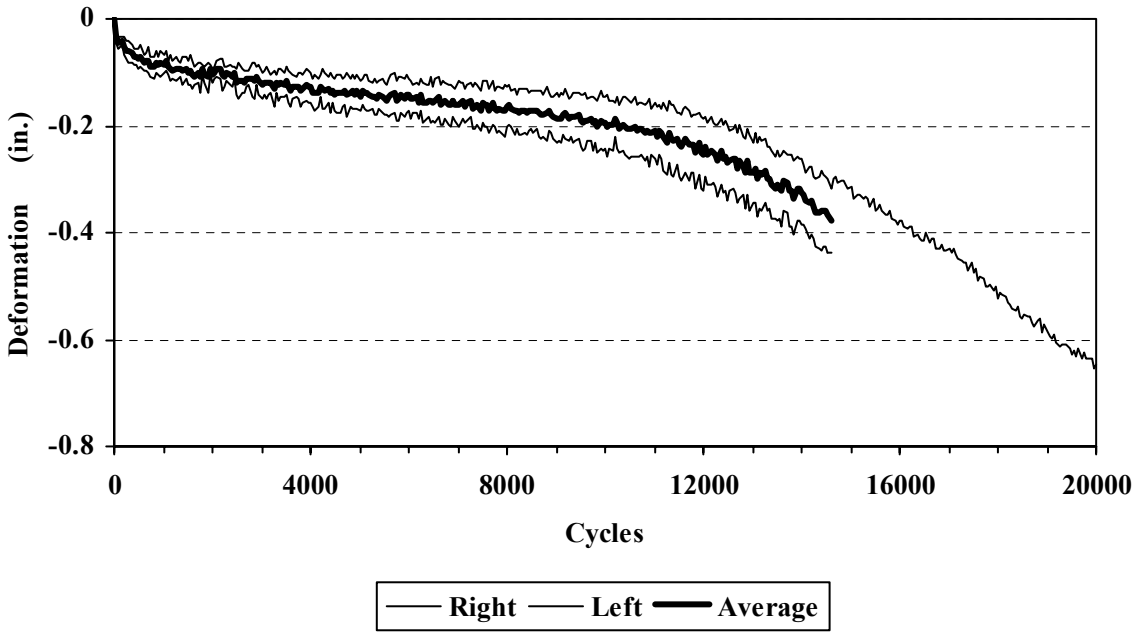

FIGURE 4.26: Measured Deformation in the Hamburg Wheel Rut Tester (Cores)

TABLE 4.9: Summary of Hamburg Wheel Test Results

(Ranked by Average Number of Passes)

Mix Type	Description	Number of Passes		Average Number of Passes to 20 mm (0.8 in.) Rut Depth	Average Creep Slope	Average Stripping Inflection Point	Average Stripping Slope
		Specimen 1 (Left)	Specimen 2 (Right)				
SM 19B	Ritchie K-42	1,440	1,320	1,380	117	755	66
SM 12.5A	Shilling K-4	5,421	5,890	5,656	544	3,696	430
SM 12.5A	Venture K-140	8,861	15,701	12,281	1,333	8,923	420
SM 12.5B	APAC Shears US 50	13,640	11,560	12,600	1,270	10,240	551
SM 12.5B	KAPA Junction City Intersection	13,120	12,321	12,721	954	10,311	788
SM 19A	Venture K-140_4A	12,941	13,721	13,331	1,214	8,347	501
SM 12.5 B	**ATL FAS-RAP Surface Layer (Slab)**	**20,000**	**15,330**	**17,675**	**2,250**	**10,112**	**667**
SM 12.5 B	**ATL FAS-RAP Surface Layer (Cores 1 & 2)**	**20,000**	**14,600**	**17,300**	**4,208**	**11,723**	**705**
SM 12.5 B	**ATL FAS-RAP Surface Layer (Cores 3 & 4)**	**19,241**	**15,640**	**17,440**	**2,719**	**9,104**	**668**
SM 19A	KDOT Research Special	20,000	16,161	18,081	2,667	14,521	1,333
SM 19 B	Shilling US 75 6C	19,981	20,000	19,991	12,413	14,614	6,667

Chapter 5

Base Layer Structural Performance Evaluation

5.1 Background

Currently, there is no standard method for the determination of layer coefficients. As mentioned earlier, the AASHTO guide [23] recommends the use of resilient modulus of the material in question to establish the required coefficient. Several methods have been used by different investigators to determine layer coefficients for certain paving materials. Another parameter, the layer thickness equivalency, has been used by several investigators mainly for the purpose of evaluating the support capacity of a given material as compared to a standard or commonly used material [24, 25]. This factor, however, is not usually used for design purposes. The layer thickness equivalency is determined as the thickness of the material in question required to replace 1 inch of the standard material.

Most of the methods used to evaluate either the layer coefficient or the layer thickness equivalency are based on the evaluation of limiting criteria at some points in the pavement structure (26). Three mechanistic responses to loads are generally considered in structural pavement analyses:

a) surface deflection,
b) maximum tensile strain at the bottom of the surface layer, and
c) vertical compressive strain (or deformation) on top of the subgrade.

The following is a brief summary of some of the evaluation methods reported in the literature:

1. AASHTO Performance Method: Kutz and Larson [27] used this method to determine the structural coefficients of two stabilized base course materials, which were included in the test track located at the Pennsylvania Transportation Research facility. The investigators used the following design equation, developed at the AASHO Road Test as the basis for their analysis.

$$G_t = b\ (\log W_t - \log g) \qquad (5.1)$$

Where:

G_t = a function of the ratio of loss in serviceability at time t to the potential loss taken at a point $p_t = 1.5$

b = a function of design and load variables that influence the shape of p versus W serviceability curve;

g = a function of design and load variables that denotes the expected number of axle applications to a $p_t = 1.5$;

W_t = axle load applications at the end of time t ;

p = present serviceability index ; and

p_t = serviceability at end of time t.

A statistical model similar to that utilized at the AASHO Road Test was selected to study the changes in b and g across levels of surface and base layer thicknesses for data collected at the test track. Terms related to the subbase were not included in the model since all test sections had a constant subbase thickness. The results of the statistical analysis were compared to the structural number equation and new layer coefficients were determined.

2. Limiting Criteria Approach: Wang et al. [28] used this method to determine the structural coefficients of two base courses constructed on the test track of the Pennsylvania Transportation Research facility. The same method has also been used by Hicks et al. [24].

Wang et al. [28] related rutting data collected from the test track to the compressive strain on top of the subgrade. The equivalent 18-kip axle load ($ESAL_{18}$) required to produce one inch of rutting for each section was compared to the maximum compressive strain on top of the subgrade. The strain associated with one million $ESAL_{18}$ was estimated and used as the limiting compressive strain in the determination of the structural layer coefficients of the two materials. A similar analysis was utilized for the criteria of surface deflection and tensile stain at the bottom of the surface layer. Both of these criteria were evaluated when significant surface cracking appeared.

The base layer thickness required to satisfy each limiting criteria was computed at different levels of surface and subbase layer thicknesses. The final base thickness was required to satisfy all three criteria simultaneously. The selected thickness was then plugged into the structural number equation and the corresponding layer coefficient was calculated.

3. AASHTO Factorial Design Approach: Little and Epps [29] utilized this method during the evaluation of certain structural characteristics of recycled pavement materials and later in the evaluation of foamed-asphalt aggregate mixtures [25]. The authors computed the maximum vertical subgrade deformation (W_s) for the pavement sections included in Loop 4 of the AASHO Road Test. A stress-sensitive layered elastic computer program was utilized to model the pavement sections. The elastic properties of the AASHO material were used as inputs. The subgrade deformation was related to the number of $ESAL_{18}$ applications required to bring the pavement to a terminal serviceability index of 2.5. The following correlation was established.

$$EAL_{18\,(2.5)} = 0.098\, e^{-3.39 \ln Ws} \qquad (5.2)$$

The elastic properties of the recycled asphalt concrete were substituted for the AASHO material properties, and changes in the pavement responses were evaluated. The new subgrade

deformations were inserted in the above equation to compute the $EAL_{18\,(2.5)}$ for the recycled pavement. The calculated allowable load applications were, in turn, used to estimate the required structural number (SN) from the AASHTO design equation. The structural layer coefficient (a_1) was finally calculated using the SN equation, where a_1 is the only unknown parameter.

4. AASHTO Design Nomograph Approach: Hicks et al. [30] used this method to compute layer equivalencies for open-graded emulsion mixtures. The researchers based their analysis on determining the $ESAL_{18}$ already carried by the pavement. The surface layer coefficient was backcalculated using the AASHTO interim design guide for a terminal serviceability of 2.0, the surface layer thickness, traffic ($ESAL_{18}$), regional factor, and soil support of the base. The weighted structural number was obtained from the design nomograph and divided by the surface thickness to determine the required layer coefficient.

5. Equal Mechanistic Response Approach: Several investigators have used this procedure to determine layer equivalencies [25] or structural layer coefficients [31] for different materials. Little et al. [25] used this method to compare the structural ability of foamed asphalt-aggregate mixture to an asphalt-treated base. The compressive strain on top of the subgrade was selected as the mechanistic response to be used in the comparison. Identical pavement structures, except for the layer in question, were analyzed using a layered elastic computer program. The thickness required to obtain an equal response for the two structures were calculated. The ratio of the thickness of the layer studied to that of the standard material is defined as the layer thickness equivalency of the material.

Majidzadeh and Elmitiny [31] used a similar approach to study the structural ability of open-graded asphalt stabilized base. The maximum compressive vertical deformation on top of the subgrade was used as the critical pavement response. The structural layer coefficient of the

open-graded base was then calculated by multiplying the inverse of the layer equivalency factor by the layer coefficient of the reference material.

5.2 Methodology Used in the Current Study

In this study, the AASHTO Design Method and the Equal Mechanistic Approach were followed to determine the structural layer coefficient of the foamed asphalt stabilized RAP base materials. In both approaches, backcalculated layer moduli values were used to determine the layer coefficient values.

5.2.1 AASHTO Design Guide Method

As mentioned earlier, AASHTO provides the following general equation for Structural Number reflecting the relative impact of the layer coefficients (a_i) and thickness (D_i) (assuming no effect of drainage):

$$SN = a_1 D_1 + a_2 D_2 + a_3 D_3 + a_4 D_4 \quad (5.4)$$

Because the pavements structures tested in the CISL Experiment # 11 had only two layers on top of the subgrade soil, and no drainage was required, the Structural Number can be computed as:

$$SN = a_1 D_1 + a_2 D_2 \quad (5.5)$$

Since the asphalt concrete layer had a thickness of h_1= 3 inches, and a typical structural layer coefficient for the asphalt concrete would be 0.42 (i.e. a_1=0.42), the structural layer coefficient for the base layer material can be computed as:

$$a_2 = [\ SN_{eff} - 0.42 * 3.0\ ] / D_2 \quad (5.6)$$

Where:

a_2 - the structural layer coefficient for the base layer material;

SN_{eff} - the effective structural number; and

D_2 - the thickness of the base layer, in inches

The effective structural number (SN_{eff}) can be computed from the following equation given in the 1993 AASHTO Design Guide [23]:

$$SN_{eff} = 0.0045 * D * E_p^{1/3} \quad (5.7)$$

Where: D = total thickness of all pavement layers above subgrade (inch), and

E_p = effective modulus of the pavement layers above subgrade (psi)

In equation (5.7), E_p is determined after computing the backcalculated subgrade modulus (M_r) value. The AASHTO algorithm for determining M_r suggests that M_r be calculated from a single deflection measurement at a distance sufficiently large enough so that the point falls outside the stress bulb at the subgrade-pavement interface and the measured deflection is solely due to the subgrade deformation. The following equation is used to calculate the M_r value:

$$M_r = (0.24\ P) / (d_r) * r \quad (5.8)$$

Where :

M_r = backcalculated subgrade resilient modulus

P = applied load

d_r = deflection at a distance r from the center of the load

r = distance from the center of the load

To use a particular sensor deflection for estimating the subgrade resilient modulus, the sensor location must be far enough so that it corresponds to the deflection of the subgrade only, but also be close enough so that it is not too small to be measured accurately. AASHTO further suggests that the minimum distance be determined by the radius of the stress bulb (a_e) at the subgrade-pavement interface. This is accomplished by choosing the 3rd or 4th sensor arbitrarily and checking whether it falls outside a radial distance of $0.7a_e$ from the center of the load or not.

The calculated M_r value is used to calculate the equivalent pavement modulus, E_p that satisfies the equation:

$$d_0 = 1.5 * p * a * \left\{ \frac{1}{M_R * [1+(D/a*(E_p/M_R)^{1/3})^2]^{0.5}} + \frac{1 - 1/\sqrt{[1+(D/a)^2]}}{E_p} \right\} \quad (5.9)$$

Where:

d_0 - the temperature corrected (68˚F) central deflection, in inches

p - load pressure, in psi

a - load plate radius, in inches

M_R - subgrade resilient modulus, in psi.

Tables 5.1 and 5.2 shows deflection data as well as the results of the calculations performed to estimate the structural layer coefficient for the base layer material. The deflections used in the calculations are those measured corresponding to the last drop at the 9,000 lbs load level, on December 6 and 19, 2001, before any ATL loading was applied. The calculations done are described as follows:

- The resilient modulus of the subgrade layer (AASHTO M_R) was computed with Equation (5.8) using the deflection measured by the geophone, placed at a distance r = 24 inches from the center of the loading plate. The estimated resilient modulus using Equation (5.8) was very similar to that backcalculated by the MODULUS program AASHTO ($BackM_R$).
- The effective modulus of the pavement layers above subgrade, E_p, was replaced in Equation (5.9) until the computed deflection d_0 matched the central deflection measured by the FWD.
- The effective Structural Number, SN_{eff}, was computed using Equation (5.7) with the effective modulus of the pavement layers above subgrade, E_p, computed in the previous step.
- The structural layer coefficient of the base layer material was computed using Equation (5.6) using the effective Structural Number, SN_{eff} computed in the previous step.

The estimated structural layer coefficients of the base layer material for all FWD test stations are tabulated in Tables 5.1 and 5.2, along with the computed average value for each lane. The average value of the layer coefficient for FAS-FDR base material is: NN – 0.1577; NS - 0.1501 and SN – 0.2166. The overall average computed for the three lanes is $a_2 = 0.1748$.

The average value of the computed structural layer coefficient for the AB-3 granular base is 0.1369, slightly lower that the value of 0.14 used by KDOT for the AB-3 granular base for the structural design of flexible pavements in Kansas. It is then reasonable to apply a simple linear correction to estimate the structural layer coefficient for the foamed asphalt stabilized RAP base as follows:

$$a_2 = 0.1748 \text{ x } (0.14 / 0.1369) = 0.1788 \qquad (5.10)$$

Thus, the Falling Weight Deflectometer tests performed on the constructed pavements before the load applications began resulted in recommended structural layer coefficient for the foamed asphalt stabilized RAP base of **0.18**.

TABLE 5.1: Estimation of the Structural Layer Coefficient for the Foamed Asphalt Stabilized RAP Base Material

Lane	Date	Station	Load (lbs)	D0 (mils)	D4 (mils)	BackMr (psi)	AASHTO M_R(psi)	D (in)	E_p (psi)	SN_{eff}	a_2
NN	Dec-06-2001	1	9355	14.54	6.52	14,880	14,348	9	217,402	2.435	0.1959
NN	Dec-06-2001	2	9347	14.67	6.45	14,956	14,491	9	211,238	2.412	0.1920
NN	Dec-06-2001	3	9323	16.92	6.54	14,783	14,255	9	147,550	2.140	0.1467
NN	Dec-06-2001	4	9347	16.93	6.56	14,826	14,248	9	147,135	2.138	0.1463
NN	Dec-06-2001	5	9319	17.17	6.61	14,702	14,098	9	142,440	2.115	0.1425
NN	Dec-06-2001	6	9331	17.17	6.65	14,609	14,032	9	144,515	2.125	0.1442
NN	Dec-19-2001	1	8794	13.96	6.38	14,467	13,784	9	212,713	2.418	0.1929
NN	Dec-19-2001	2	8786	14.15	6.35	14,552	13,836	9	202,515	2.378	0.1864
NN	Dec-19-2001	3	8743	16.61	6.54	14,020	13,369	9	140,925	2.108	0.1413
NN	Dec-19-2001	4	8926	16.93	6.56	14,243	13,607	9	138,412	2.095	0.1392
NN	Dec-19-2001	5	8942	17.44	6.65	14,170	13,447	9	129,195	2.047	0.1312
NN	Dec-19-2001	6	8926	17.37	6.65	14,079	13,423	9	131,796	2.061	0.1335
AVERAGE											**0.1577**
NS	0.1680	1	9350	14.34	5.83	15,875	16,038	12	135,243	2.772	0.1580
NS	0.1715	2	9355	14.11	5.84	15,883	16,019	12	139,881	2.803	0.1615
NS	0.1525	3	9342	15.19	5.59	16,428	16,712	12	115,831	2.632	0.1425
NS	0.1533	4	9435	15.39	5.82	16,074	16,211	12	116,817	2.640	0.1433
NS	0.1495	5	9427	15.89	5.93	15,698	15,897	12	112,378	2.606	0.1395
NS	0.1370	6	9411	16.76	5.82	15,973	16,170	12	98,441	2.493	0.1270
NS	0.1638	1	8934	14.15	5.82	15,351	15,351	12	129,835	2.734	0.1538
NS	0.1655	2	8894	14.03	5.75	15,351	15,468	12	131,967	2.749	0.1555
NS	0.1412	3	8871	15.49	5.69	15,657	15,591	12	102,974	2.531	0.1312
NS	0.1420	4	8913	15.66	5.72	15,492	15,582	12	103,860	2.538	0.1320
NS	0.1312	5	8890	16.41	5.93	15,326	14,992	12	92,297	2.440	0.1212
NS	0.1262	6	8942	17.09	5.89	15,302	15,182	12	87,369	2.396	0.1162
AVERAGE											**0.1501**
SN	Dec-06-2001	1	9509	9.38	3.87	22,066	24,571	15	200,876	3.953	0.2244
SN	Dec-06-2001	2	9501	9.52	3.91	21,941	24,299	15	194,860	3.913	0.2211
SN	Dec-06-2001	3	9466	9.45	3.94	21,963	24,025	15	193,666	3.905	0.2204
SN	Dec-06-2001	4	9490	9.44	3.95	21,641	24,025	15	200,681	3.952	0.2243
SN	Dec-06-2001	5	9470	10.17	3.85	22,573	24,597	15	163,838	3.694	0.2028
SN	Dec-06-2001	6	9470	10.39	3.74	23,259	25,321	15	153,348	3.613	0.1961
SN	Dec-19-2001	1	9156	8.88	3.80	21,589	24,095	15	212,460	4.028	0.2306
SN	Dec-19-2001	2	9125	8.98	3.81	21,724	23,950	15	202,759	3.965	0.2255
SN	Dec-19-2001	3	9125	9.07	3.88	21,715	23,518	15	195,435	3.917	0.2214
SN	Dec-19-2001	4	9207	9.14	3.87	21,530	23,791	15	201,512	3.957	0.2248
SN	Dec-19-2001	5	9183	9.87	3.90	21,642	23,546	15	169,504	3.736	0.2063
SN	Dec-19-2001	6	9152	10.02	3.83	21,944	23,896	15	161,854	3.679	0.2015
AVERAGE											**0.2166**

TABLE 5.2: Estimation of the Structural Layer Coefficient for the AB-3 Granular Base Material

Lane	Date	Station	Load (lbs)	D0 (mils)	D4 (mils)	BackMr (psi)	AASHTO M_R(psi)	D (in)	E_p (psi)	SN_{eff}	a_2
SS	Dec-06-2001	1	9334	16.67	5.57	16,528	16,758	12	94,648	2.461	0.1334
SS	Dec-06-2001	2	9319	16.33	5.50	16,663	16,944	12	97,821	2.488	0.1365
SS	Dec-06-2001	3	9323	16.41	5.45	16,638	17,106	12	98,172	2.491	0.1368
SS	Dec-06-2001	4	9342	16.63	5.41	17,087	17,268	12	91,838	2.436	0.1307
SS	Dec-06-2001	5	9311	16.31	5.46	16,926	17,053	12	95,462	2.468	0.1342
SS	Dec-06-2001	6	9342	16.70	5.57	16,732	16,772	12	92,248	2.440	0.1311
SS	Dec-19-2001	1	8998	15.94	5.67	15,831	15,869	12	99,460	2.502	0.1380
SS	Dec-19-2001	2	8990	15.72	5.58	15,806	16,111	12	104,048	2.540	0.1422
SS	Dec-19-2001	3	8958	15.70	5.60	15,525	15,996	12	106,699	2.561	0.1446
SS	Dec-19-2001	4	9093	16.22	5.69	15,834	15,981	12	98,713	2.496	0.1373
SS	Dec-19-2001	5	9049	15.94	5.65	15,813	16,016	12	101,787	2.521	0.1401
SS	Dec-19-2001	6	9069	16.17	5.74	15,673	15,800	12	99,750	2.504	0.1383
AVERAGE											**0.1369**

Chapter 6

Conclusions and Recommendations

The major conclusions resulting from this research are:

1. Foamed asphalt stabilized RAP material is a uniform material that can be placed and compacted easily, and can be efficiently used as base material in flexible pavements.

This conclusion is supported by the following:

- During manufacturing, the FAS-FDR was a uniform blend of crushed stone, RAP and soil, and was uniformly stabilized with foamed asphalt
- The placing and compaction could be easily done. Good compaction was achieved with a tamper.
- During the post-mortem analysis, the FAS-FDR base material was found to be very compact, crack free and stiff.
- The permanent deformation at the pavement surface on the pavements with the FAS-FDR base was between 0.25 and 0.5 inches and was comparable to that of Kansas AB-3 granular base, after 100,000 passes of 17,000-lb single axle and 400,000 passes of 32,000-lb tandem axle.

Considering these observations, the use of foamed asphalt stabilized RAP as a base material for flexible pavements is recommended. The FAS-FDR base performed well under moderate moisture conditions. The foamed asphalt technology allows an efficient use of the RAP material contaminated with soil and aggregates during full-depth reclamation process. The materials cannot be recycled through other established methods.

2. When used as a base material, one inch of foamed asphalt stabilized RAP material is equivalent to 1.0 to 1.25 inches of conventional Kansas AB-3 granular base.

This conclusion is supported by the following:

- The permanent deformation and the rut depth values measured at the surface of the flexible pavement with nine inches of granular base were in between those measured on the pavements with nine and 12 inches of FAS-FDR bases.
- The vertical compressive stress measured at the top of the subgrade on the pavement with nine inches of granular base was close to the stress measured in the pavement with nine inch of FAS-FDR base.
- The effective structural number computed from the FWD deflections measured on the as-constructed pavements suggested a structural layer coefficient of 0.18 for the FAS-FDR base material.

REFERENCES

1. Melhem, H.G., *Development of an Accelerated Testing Laboratory for Highway Research in Kansas*, Report No. FHWA-KS-97/5, Kansas Department of Transportation, Topeka, KS, November 1997.

2. Melhem, H.G., *Accelerated Testing for Studying Pavement Design and Performance*; FY97-98, Report No. FHWA-KS-99-2, Kansas Department of Transportation, Topeka, KS, May 1999.

3. Melhem, H.G., Sheffield, F., *Accelerated Testing for Studying Pavement Design and Performance*; FY99, Report No. FHWA-KS-99-7, Kansas Department of Transportation, Topeka, KS, July 2000.

4. Swart, R., Melhem, H.G., *Accelerated Testing for Studying Pavement Design and Performance*; FY2000, Report No. FHWA-KS-02-6, Kansas Department of Transportation, Topeka, KS, March 2001.

5. "*Standard Specifications for State Road and Bridge Construction*" Kansas Department of Transportation, Topeka, KS, Edition 1990.

6. Roberts F.L., Kandhal P.S., Brown E.R., Lee D.Y. and T. Kennedy. *Hot Mix Asphalt Materials, Mixture Design and Construction*. Second Edition, NAPA Research and Education Foundation, Lanham, MD, 1996.

7. Csanyi L.H., Foamed Asphalt in Bituminous Paving Mixtures. Highway Research Records No. 160, National Research Council, Washington, DC, 1957, pp. 108-122.

8. Wirtgen GmbH, *Wirtgen Cold Recycling Manual*, Windhagen, Germany, ISBN 3-00-003577-X, 1998.

9. Bowering, R.H. Properties and Behavior of Foamed Bitumen Mixtures for Road Building. *Proceedings of the 5th Australian Road Research Board Conference*, Canberra, Australia, 1970.

10. Soter - Foamstab In : http://www.soter.com/foam_asphalt.html. (2001).

11. Roberts, F.L., Engelbrecht, J.C. and T.W. Kennedy. Evaluation of Recycled Mixtures Using Foamed Asphalt. Transportation Research Record No. 968, Washington, DC, Transportation Research Board. 1984, pp 78_85.

12. Maccarrone, S., Holleran, G., Leonard. D.J. & Hey, S. 1994. Pavement Recycling using Foamed Bitumen. In: 17th ARRB Conference, Proceedings held in Gold Coast, Queensland, 15_19 August, 1994, Volume 17, Part 3, pp 349_365.

13. Maccarrone, S., Holleran, G, & Leonard, D.J. 1993. Bitumen Stabilisation - A New Approach To Recycling Pavements. In: AAPA Members Conference, 1993.

14. Lancaster. J., McArthur, L. & Warwick, R. 1994. VICROADS experience with foamed bitumen stabilisation. In: 17th ARRB Conference, Proceedings held in Gold Coast, Queensland, 15-19 August, 1994, Volume 17, Part 3, pp193_211.

15. Ramanujam, J.M. & Fernando, D.P. 1997. Foam Bitumen Trial at Gladfield_Cunningham Highway. In: Proceedings of the Southern Region Symposium, Australia, 1997.

16. Muthen K.M., *Foamed Asphalt Mixes - Mix Design Procedure*. Contract Report CR-98/077. CSAIT Transportek, Pretoria, South Africa, 1999.

17. Lewis A.J.N. and D.C. Collings, Cold in Place Recycling: a Relevant Process for Road Rehabilitation and Upgrading. *Seventh Conference on Asphalt Pavements for South Africa*, Pretoria, South Africa, 1999.

18. Van der Walt N., Botha P., Semmelink C., Engelbrecht F. and N. Salminen. "The Use of Foamed Bitumen in Full_depth In_place Recycling of Pavement Layers Illustrating the Basic Concept of Water Saturation in the Foam Process". *Seventh Conference on Asphalt Pavements for South Africa*, Pretoria, South Africa, 1999.

19. Van Wyk, A., Yoder, E.J. & Wood, L.E.. Determination of structural equivalency factors of recycled layers by using field data. *Low_volume roads: Third International Conference*. (Transportation Research Record No. 898), Transportation Research Board, Washington, DC, 1983, pp 122_132.

20. Van Wijk, A. & Wood, L.E. Use of Foamed Asphalt in Recycling of an Asphalt Pavement. *Transportation Research Record No. 911*, Transportation Research Board. Washington, DC, 1983., pp 96-103.

21. Kim R and E. Inge. (1995) "Prediction of Effective Asphalt Layer Temperature" *Transportation Research Record No. 1473*, National Academy Press, Washington, D.C., pp. 93-100.

22. Aschenbrener, T. Influence of Refining Processes and Crude Oil Sources Used in Colorado on Results from the Hamburg Wheel-Tracking Device. *Final Report No. CDOT-DTD-R-94-7*, Colorado Department of Transportation, April 1994.

23. AASHTO, *AASHTO Guide for Design of Pavement Structures*, American Association of State Highway and Transportation Officials, Washington, D.C., 1993.

24. Hicks, R.G., Gatch, D.R., Williamson, R., and Stewart, J. Open-Graded Emulsion Mixes For Use As Road Surfaces. In *Transportation Research Record 702*, Transportation Research Board, Washington, D.C., 1979, pp. 64-72.

25. Little, D.N., Button, J.N., and Epps, J.A. Structural Properties of Laboratory Mixtures Containing Foamed Asphalt and Marginal Aggregates. In *Transportation Research Record 911*, Transportation Research Board, Washington D.C., 1983, pp. 104-113.

26. Van Til, C.J., McCullough, B.F., Vallerga, B.A., and Hicks, R.G. *Evaluation of AASHO Interim Guide for Design of Pavement Structures*. NCHRP Report 128, Highway Research Board.

27. Kutz, S.A. and Larson, T .D. *Determination of the Structural Coefficients of Two Stabilized Base Course Materials Using the AASHTO Performance Method*. Report PTI 7712, The Pennsylvania Transportation Institute, The Pennsylvania State University, July 1977.

28. Wang, M.C., Larson, T.D., and Kilareski, W.P. *Structural Coefficients of Bituminous Concrete and Aggregate Cement Base Materials By the Limiting Criteria Approach*. Report PTI 7713, The Pennsylvania Transportation Institute, The Pennsylvania State University, July 1977.

29. Little, D. N. and Epps. *Evaluation of Certain Structural Characteristics of Recycled Pavement Materials.* Proceedings of the Association of Asphalt Paving Technologists, Louisville, KY, Vol 49, 1980, pp. 219-251.

30. Hicks, R.G., Santucci, L.E., Fink, D.G., and Williamson, Ronald. Performance Evaluation of Open-Graded Emulsified Asphalt Pavement. *Proceedings of the Association of Asphalt Paving Technologists*, Atlanta, Georgia, February, 1983, pp. 441-473.

31. Majidzadeh, K. and Elmitiny, R. *Development and Implementation of Pavement Drainage Design Guidelines in Ohio.* Report FHWA/OH-81/007, Ohio Department of Transportation, March, 1981.

APPENDIX A

FOAMED ASPHALT BIBLIOGRAPHY

Foamed Asphalt Reference Documents

Acott, S.M. & Myburgh, P.A. 1983. Design and performance study of sand bases treated with foamed asphalt. In: Low-volume roads: third international conference. Washington, DC: (Transportation Research Record; 898), pp 290-296.

Acott, S.M.1979. Sand stabilisation using foamed bitumen. In: 3rd Conference on Asphalt Pavements for Southern Africa, 3rd, 1979, Durban, pp.155-172.

Akeroyd, F.M.L. & Hicks, B.J. 1988. Foamed Bitumen Road Recycling. Highways, Volume 56, Number 1933, pp 42, 43, 45.

Akeroyd, F.M.M. 1989. Advances in foamed bitumen technology. In: Fifth conference on asphalt pavements for Southern Africa; CAPSA 89, held in Swaziland, 5-9 June 1989, Section 8, pp 1-4

Bissada, A.F. 1987. Structural response of foamed-asphalt-sand mixtures in hot environments. In: Asphalt materials and mixtures. Washington, DC: Transportation Research Board. (Transportation Research Record, 1115), pp 134-149.

Bowering, R.H. & Martin, C.L. 1976. Foamed bitumen production and application of mixtures, evaluation and performance of pavements. in: Proceedings of the Association of Asphalt Paving Technologists, Vol. 45, pp. 453-477.

Bowering, R.H. 1970. Properties and behaviour of foamed bitumen mixtures for road building. In: Proceedings of the 5th Australian Road Research Board Conference, held in Canberra, Australia, 1970, pp. 38-57.

Bowering, R.H. & Martin, C.L. 1976. Performance of newly constructed full depth foamed bitumen pavements. In: Proceedings of the 8th Australian Road Research Board Conference, held in Perth, Australia, 1976.

Brennen, M., Tia, M., Altschaeffl, A.G. & Wood, L.E. 1983. Laboratory investigation of the use of foamed asphalt for recycled bituminous pavements. In: Asphalt materials, mixtures, construction, moisture effects and sulfur. Washington, DC: Transportation Research Board. (Transportation Research Record; 911), pp 80-87.

Castedo-Franco, L.H., Beaudoin, C.C., Wood, E.L. & Altschaeffl, A.G. 1984. Durability characteristics of foamed asphalt mixtures. In: Proceedings of the 29th Annual Canadian Technical Asphalt Association Conference, held in Montreal, Canada, 1984.

Castedo-Franco, L.H. & Wood, E.L. 1983. Stabilisation with foamed asphalt of aggregates commonly used in low volume roads. In: Low-volume roads: 3rd international conference. Washington, DC: Transportation Research Board. (Transportation Research Record; 898), pp 297-302.

Collings, D. 1997. Through foaming it's possible to mix hot asphalt with cold, damp aggregate. Asphalt Contractor, June 1997 (Article based on the presentation at the 1997 ARRA annual meeting, San Antonio, TX).

Engelbrecht, J.C., Roberts, F.L. & Kennedy, T.W. 1985. Cold recycled mixtures, with emphasis on the curing of foamed specimens - a laboratory study. In: Annual Transportation Convention, Session - Maintenance of the Transport Infrasture, held in Pretoria, 1985, vol. S.350 TI, paper 7.

Flynn, L. 1995. 'Foamstab' process rehabilitates Montreal residential thoroughfares. In: Roads and Bridges Magazine, Volume 33, Number 5, pp 40-41.

Joubert, G., Poolman, S. & Strauss, P.J. 1989. Foam bitumen stabilised sand as an alternative to gravel bases for low volume roads. In: 5th Conference on Asphalt Pavements for South Africa (CAPSA 89), Proceedings held in Swaziland, 5-9 June, 1989, Section 8, pp21-5.

Lancaster. J., McArthur, L. & Warwick, R. 1994. VICROADS experience with foamed bitumen stabilisation. In: 17th ARRB Conference, Proceedings held in Gold Coast, Queensland, 15-19 August, 1994, Volume 17, Part 3, pp193-211.

Lee, D.Y. 1981. Treating marginal aggregates and soil with foamed asphalt. In: Proceedings of the Association of Asphalt Paving Technologists, Vol. 50, pp 211-150.

Little, D.N., Button, J.W. & Epps, J.A. 1983. Structural properties of laboratory mixtures containing foamed asphalt and marginal aggregates. In: Asphalt materials, mixtures, construction, moisture effects, and sulfur. Washington, DC: Transportation Research Board. (Transportation Research Record; 911), pp 104-113.

Maccarrone, S., Holleran, G., Leonard. D.J. & Hey, S. 1994. Pavement Recycling using Foamed Bitumen. In: 17th ARRB Conference, Proceedings held in Gold Coast, Queensland, 15-19 August, 1994, Volume 17, Part 3, pp 349-365.

Maccarrone, S., Holleran, G, & Leonard, D.J. 1993. Bitumen Stabilisation - A New Approach To Recycling Pavements. In: AAPA Members Conference, 1993.

Maccarrone, S., Holleran, G. & Ky, A. 1995. Cold Asphalt Systems as an Alternative to Hot Mix. In: 9th AAPA International Asphalt Conference.

Ramanujam, J.M. & Fernando, D.P. 1997. Foam Bitumen Trial at Gladfield-Cunningham Highway. In: Proceedings of the Southern Region Symposium, Australia, 1997.

Roberts, F.L., Engelbrecht, J.C. & Kennedy, T.W. 1984. Evaluation of recycled mixtures using foamed asphalt. In: Asphalt mixtures and performance. Washington, DC: Transportation Research Board. (Transportation Research Record; 968), pp 78-85.

Ruckel, P.J. et al Foamix Asphalt Advances. In: Asphalt Pavement Construction: New

Materials and Techniques. Philadelphia, PA: American Society for Testing and Materials (ASTM STP; 724), pp. 93-109.

Ruckel, P.J., Acott, S.M. & Bowering, R.H. 1982. Foamed-asphalt paving mixtures: preparation of design mixes and treatment of test specimens. In: Asphalt materials, mixtures, construction, moisture effects and sulfur. Washington, DC: Transportation Research Board. (Transportation Research Record; 911), pp 88-95.

Sakr, H.A. & Manke, P.G. 1985. Innovations in Oklahoma foamix design procedures. In: Asphalt materials, mixes, construction and quality. Washingtong, DC: Transportation Research Board. (Transportation Research Record;1034), pp 26-34.

Tia, M. & Wood, L.E. 1983. Use of asphalt emulsion and foamed asphalt in cold-recycled asphalt paving mixtures. In: Low-volume roads: third international conference. Washington, DC: Transportation Research Board. (Transportation Research Record; 898), pp 315-322.

Van Wyk, A., Yoder, E.J. & Wood, L.E. 1983. Determination of structural equivalency factors of recycled layers by using field data. In: Low-volume roads: third international conference. Washington, DC: Transportation Research Board. (Transportation Research Record; 898), pp 122-132.

Van Wijk, A.J. 1984. Structural comparison of two cold recycled pavement layers. In: Design, evaluation, and performance of pavements. Washington, DC: Transportation Research Board. (Transportation Research Record; 954), pp 70-77.

Van Wijk, A. & Wood, L.E. 1983. Use of foamed asphalt in recycling of an asphalt pavement. In: Asphalt materials, mixtures, construction, moisture effects and sulfur. Washington, DC: Transportation Research Board. (Transportation Research Record; 911), pp 96-103.

Van Wijk. A. & Wood, L.E. 1982. Construction of a recycled pavement using foamed asphalt. In: Proceedings of the Twenty-seventh Annual Conference of Canadian Technical Asphalt Association, edited by P Turcotte, held in Edmonton, Alberta, Canada, 1982.

CAPSA'99 - Muthen et al: Foamed Asphalt Mixes Mix Design Procedure

CAPSA'99 - Engelbrecht: Manufacturing Foam Bitumen In A Standard Drum Mixing Asphalt Plant

CAPSA'99 - Lewis: Cold In Place Recycling: A Relevant Process For Road Rehabilitation And Upgrading

CAPSA'99 - Jenkins et al: Characterization Of Foamed Bitumen

CAPSA'99 - Jenkins et al: Half-Warm Foamed Bitumen Treatment, A New Process

CAPSA'99 - van der Walt et al: The Use Of Foamed Bitumen In Full-Depth In-Place Recycling Of Pavement Layers Illustrating The Basic Concept Of Water Saturation In The Foam Process

Daniel C. Brown: Wisconsin Demo Explores In-place Asphalt Rehabilitation

CMI News 1

CMI News 2

Paige-Green: An innovative solution for township roads in sandy areas

APPENDIX B

INDIRECT TENSILE STRENGTH RESULTS

TABLE B1. Indirect Tensile Strength Results – Additive: Portland Cement

Sample	Type	Water	Height (in.)	Weight (g)	Gmb	Load (lbf)	ITS (psi)
1	2% AC, 1% PC	dry	2.54	1122.6	2.147	1330	86.07
2	2% AC, 1% PC	dry	2.52	1134.4	2.187	1435	92.13
3	2% AC, 1% PC	dry	2.53	1128.6	2.167	1385	89.28
Avg.							**89.16**
4	2% AC, 1% PC	wet	2.53	1133.9	2.178	520	33.52
5	2% AC, 1% PC	wet	2.49	1106.1	2.158	725	45.99
6	2% AC, 1% PC	wet	2.55	1137.1	2.167	655	42.55
Avg.							**40.69**
1	3% AC, 1% PC	dry	2.47	1094.6	2.153	1505	94.71
2	3% AC, 1% PC	dry	2.58	1135.1	2.138	1500	98.6
3	3% AC, 1% PC	dry	2.55	1135.4	2.163	1555	101.03
Avg.							**98.11**
4	3% AC, 1% PC	wet	2.57	1120.3	2.118	1050	68.75
5	3% AC, 1% PC	wet	2.55	1136.9	2.166	945	61.39
6	3% AC, 1% PC	wet	2.51	1112.3	2.153	995	63.63
Avg.							**64.59**
1	3.5% AC, 1% PC	dry	2.56	1125.5	2.136	1435	93.59
2	3.5% AC, 1% PC	dry	2.58	1132.2	2.132	1440	94.65
3	3.5% AC, 1% PC	dry	2.55	1129.3	2.152	1440	93.55
Avg.							**93.93**
4	3.5% AC, 1% PC	wet	2.54	1141.3	2.183	675	43.68
5	3.5% AC, 1% PC	wet	2.59	1137.6	2.134	735	48.5
6	3.5% AC, 1% PC	wet	2.58	1116.3	2.102	770	50.61
Avg.							**47.60**
1	4% AC, 1% PC	dry	2.49	1100.4	2.147	1460	92.62
2	4% AC, 1% PC	dry	2.51	1091.6	2.113	1455	93.05
3	4% AC, 1% PC	dry	2.49	1089.2	2.125	1305	82.79
Avg.							**89.49**
4	4% AC, 1% PC	wet	2.50	1092.3	2.123	765	48.73
5	4% AC, 1% PC	wet	2.52	1108.0	2.136	725	46.55
6	4% AC, 1% PC	wet	2.51	1103.6	2.136	750	47.96
Avg.							**47.75**

AC = Asphalt Cement, PC = Portland Cement, HL = Hydrated Lime

TABLE B2. Indirect Tensile Strength Results – Additive: Hydrated Lime

Sample	Type	Water	Height (in.)	Weight (g)	Gmb	Load (lbf)	ITS (psi)
1	2% AC, 2% HL	dry	2.49	1102.7	2.152	950	60.27
2	2% AC, 2% HL	dry	2.48	1084.7	2.125	800	50.55
3	2% AC, 2% HL	dry	2.46	1082.6	2.138	800	50.14
Avg.							**53.65**
4	2% AC, 2% HL	wet	2.44	1093.2	2.177	420	26.11
5	2% AC, 2% HL	wet	2.49	1096.9	2.14	360	22.84
6	2% AC, 2% HL	wet	2.47	1070.4	2.106	350	22.03
Avg.							**23.66**
1	3% AC, 2% HL	dry	2.50	1095.7	2.130	1005	64.01
2	3% AC, 2% HL	dry	2.48	1077.0	2.110	900	56.87
3	3% AC, 2% HL	dry	2.50	1089.7	2.118	950	60.51
Avg.							**60.46**
4	3% AC, 2% HL	wet	2.47	1084.9	2.134	405	25.49
5	3% AC, 2% HL	wet	2.48	1082.0	2.120	460	29.06
6	3% AC, 2% HL	wet	2.49	1080.7	2.109	360	22.84
Avg.							**25.80**
1	3.5% AC, 2% HL	dry	2.50	1083.6	2.106	905	57.64
2	3.5% AC, 2% HL	dry	2.50	1080.4	2.100	960	61.15
3	3.5% AC, 2% HL	dry	2.51	1100.4	2.130	1125	71.94
Avg.							**63.58**
4	3.5% AC, 2% HL	wet	2.47	1093.7	2.151	685	43.11
5	3.5% AC, 2% HL	wet	2.49	1059.6	2.068	535	33.94
6	3.5% AC, 2% HL	wet	2.51	1085.6	2.101	550	35.17
Avg.							**37.41**
1	4% AC, 2% HL	dry	2.51	1082.3	2.095	950	60.75
2	4% AC, 2% HL	dry	2.52	1101.5	2.124	1060	68.06
3	4% AC, 2% HL	dry	2.51	1078.4	2.088	950	60.75
Avg.							**63.19**
4	4% AC, 2% HL	wet	2.50	1087.4	2.113	500	31.85
5	4% AC, 2% HL	wet	2.54	1090.5	2.086	500	32.36
6	4% AC, 2% HL	wet	2.55	1101.1	2.098	540	35.08
Avg.							**33.10**

AC = Asphalt Cement, PC = Portland Cement, HL = Hydrated Lime

TABLE B3. Indirect Tensile Strength Results – No Additive

Sample	Type	Water	Height (in.)	Weight (g)	Gmb	Load (lbf)	ITS (psi)
1	2% AC	dry	2.49	1117.8	2.181	1515	96.11
2	2% AC	dry	2.51	1120.1	2.168	1670	106.79
3	2% AC	dry	2.46	1105.2	2.183	1765	110.62
Avg.							**104.51**
4	2% AC	wet	2.48	1098.2	2.152	190	12.01
5	2% AC	wet	2.48	1122.5	2.199	285	18.01
6	2% AC	wet	2.46	1108.9	2.190	285	17.86
Avg.							**15.96**
1	3% AC	dry	2.56	1119.1	2.124	1355	88.38
2	3% AC	dry	2.5	1123.0	2.183	1355	86.31
3	3% AC	dry	2.51	1117.2	2.163	1450	92.73
Avg.							**89.14**
4	3% AC	wet	2.49	1118.2	2.182	325	20.62
5	3% AC	wet	2.54	1123.5	2.149	435	28.15
6	3% AC	wet	2.52	1116.4	2.153	305	19.58
Avg.							**22.78**
1	3.5% AC	dry	2.49	1113.8	2.173	1245	78.98
2	3.5% AC	dry	2.55	1117.8	2.130	1200	77.96
3	3.5% AC	dry	2.53	1109.2	2.130	1150	74.13
Avg.							**77.02**
4	3.5% AC	wet	2.53	1119.1	2.149	500	32.23
5	3.5% AC	wet	2.52	1125.7	2.170	360	23.11
6	3.5% AC	wet	2.55	1114.6	2.124	505	32.81
Avg.							**29.38**
1	4% AC	dry	2.57	1118.3	2.114	1245	81.52
2	4% AC	dry	2.55	1117.8	2.130	1320	85.76
3	4% AC	dry	2.59	1119.6	2.100	1235	81.49
Avg.							**82.92**
4	4% AC	wet	2.57	1116.0	2.110	540	35.36
5	4% AC	wet	2.58	1121.5	2.112	485	31.88
6	4% AC	wet	2.53	1108.4	2.129	445	28.68
Avg.							**31.97**

AC = Asphalt Cement, PC = Portland Cement, HL = Hydrated Lime

APPENDIX C

LONGITUDINAL PROFILE ELEVATION DATA

TABLE C1. Elevation Data for the Longitudinal Profile Lane NN

Station	ATL Passes (x 1,000) / Date														
	0	23	42	60	82	100	130	150	176	208	276	341	408	460	500
	12/14/01	02/15/02	02/22/02	03/01/02	03/08/02	03/14/02	04/05/02	04/12/02	04/19/02	04/26/02	06/10/02	06/20/02	07/01/02	07/10/02	07/17/02
1	0.080	0.078	0.080	0.080	0.080	0.083	0.049	0.045	0.049	0.052	0.053	0.056	0.063	0.065	0.065
2	0.080	0.081	0.083	0.081	0.084	0.085	0.051	0.047	0.052	0.053	0.056	0.057	0.062	0.063	0.064
3	0.080	0.081	0.082	0.080	0.080	0.082	0.053	0.045	0.049	0.051	0.052	0.054	0.060	0.059	0.061
4	0.070	0.083	0.082	0.079	0.080	0.081	0.052	0.044	0.046	0.049	0.049	0.053	0.058	0.058	0.060
5	0.060	0.074	0.071	0.070	0.072	0.073	0.040	0.036	0.039	0.040	0.042	0.046	0.051	0.049	0.052
6	0.060	0.066	0.067	0.066	0.068	0.068	0.036	0.031	0.034	0.035	0.037	0.041	0.045	0.045	0.048
7	0.070	0.062	0.060	0.060	0.064	0.063	0.029	0.024	0.028	0.030	0.031	0.035	0.040	0.040	0.040
8	0.060	0.058	0.060	0.057	0.058	0.060	0.025	0.039	0.024	0.026	0.027	0.032	0.037	0.038	0.038
9	0.060	0.054	0.054	0.053	0.054	0.056	0.025	0.018	0.021	0.021	0.024	0.026	0.032	0.033	0.033
10	0.050	0.053	0.053	0.052	0.055	0.055	0.022	0.016	0.020	0.020	0.023	0.025	0.033	0.031	0.034
11	0.050	0.057	0.058	0.057	0.058	0.060	0.028	0.021	0.024	0.026	0.027	0.031	0.036	0.035	0.039
12	0.060	0.065	0.066	0.064	0.067	0.067	0.030	0.027	0.031	0.032	0.032	0.035	0.041	0.041	0.044
13	0.080	0.073	0.085	0.070	0.073	0.074	0.032	0.035	0.038	0.039	0.040	0.044	0.049	0.047	0.050
14	0.080	0.075	0.086	0.074	0.076	0.075	0.045	0.038	0.041	0.042	0.042	0.046	0.054	0.051	0.055
15	0.070	0.080	0.090	0.077	0.080	0.082	0.050	0.042	0.044	0.047	0.046	0.051	0.055	0.055	0.058
16	0.090	0.085	0.096	0.083	0.085	0.086	0.053	0.047	0.049	0.051	0.051	0.055	0.068	0.058	0.062
17	0.100	0.095	0.100	0.090	0.095	0.096	0.062	0.056	0.059	0.061	0.059	0.062	0.072	0.066	0.068
18	0.100	0.101	0.109	0.098	0.102	0.102	0.067	0.063	0.064	0.068	0.066	0.069	0.085	0.071	0.075
19	0.110	0.112	0.115	0.114	0.115	0.116	0.080	0.078	0.079	0.081	0.079	0.082	0.090	0.084	0.086
SV	0.917	0.332	0.445	0.354	0.337	0.341	0.395	0.715	0.344	0.347	0.314	0.319	0.342	0.302	0.279

TABLE C2. Elevation Data for the Longitudinal Profile Lane NS

Station	ATL Passes (x 1,000) / Date														
	0	23	42	60	82	100	130	150	176	208	276	341	408	460	500
	12/14/01	02/15/02	02/22/02	03/01/02	03/08/02	03/14/02	04/05/02	04/12/02	04/19/02	04/26/02	06/10/02	06/20/02	07/01/02	07/10/02	07/17/02
1	0.100	0.116	0.119	0.118	0.117	0.119	0.084	0.081	0.081	0.084	0.084	0.085	0.091	0.092	0.090
2	0.110	0.118	0.118	0.120	0.120	0.118	0.082	0.082	0.081	0.085	0.084	0.084	0.086	0.088	0.087
3	0.110	0.115	0.147	0.117	0.116	0.117	0.078	0.046	0.078	0.082	0.079	0.081	0.085	0.084	0.082
4	0.100	0.108	0.112	0.110	0.113	0.113	0.076	0.073	0.075	0.076	0.075	0.076	0.080	0.079	0.078
5	0.100	0.100	0.106	0.105	0.103	0.106	0.069	0.068	0.068	0.069	0.067	0.070	0.073	0.073	0.073
6	0.100	0.098	0.099	0.099	0.100	0.100	0.064	0.061	0.064	0.065	0.063	0.064	0.067	0.067	0.066
7	0.090	0.092	0.095	0.093	0.095	0.095	0.059	0.057	0.057	0.058	0.057	0.059	0.061	0.060	0.060
8	0.080	0.084	0.088	0.086	0.088	0.088	0.052	0.050	0.050	0.052	0.050	0.052	0.056	0.056	0.054
9	0.080	0.110	0.083	0.080	0.090	0.081	0.046	0.044	0.045	0.046	0.044	0.047	0.048	0.047	0.048
10	0.080	0.080	0.080	0.080	0.080	0.080	0.044	0.043	0.044	0.044	0.042	0.041	0.046	0.047	0.047
11	0.080	0.081	0.087	0.085	0.084	0.087	0.048	0.048	0.048	0.049	0.047	0.050	0.054	0.053	0.052
12	0.090	0.086	0.090	0.089	0.087	0.088	0.053	0.053	0.052	0.053	0.051	0.054	0.058	0.057	0.059
13	0.090	0.084	0.090	0.087	0.086	0.089	0.053	0.051	0.051	0.052	0.051	0.053	0.057	0.057	0.057
14	0.080	0.077	0.079	0.080	0.078	0.080	0.044	0.045	0.045	0.045	0.045	0.047	0.053	0.053	0.053
15	0.080	0.080	0.077	0.080	0.080	0.078	0.047	0.043	0.044	0.047	0.047	0.050	0.054	0.054	0.055
16	0.080	0.080	0.083	0.083	0.084	0.085	0.050	0.047	0.048	0.049	0.049	0.051	0.056	0.058	0.058
17	0.090	0.085	0.090	0.087	0.088	0.087	0.053	0.052	0.052	0.055	0.054	0.057	0.060	0.063	0.062
18	0.100	0.099	0.099	0.100	0.098	0.100	0.066	0.064	0.064	0.065	0.065	0.067	0.071	0.072	0.072
19	0.090	0.092	0.096	0.113	0.094	0.096	0.062	0.060	0.061	0.062	0.064	0.066	0.075	0.078	0.077
SV	0.497	1.184	1.433	0.389	0.296	0.318	0.288	1.374	0.244	0.252	0.253	0.279	0.281	0.273	0.262

TABLE C3. Elevation Data for the Longitudinal Profile Lane SN

Station	ATL Passes (x 1,000) / Date											
	0	25	45	71	100	157	201	246	328	420	468	500
	11/11/01	01/04/02	01/11/02	01/25/02	02/07/02	07/25/02	08/02/02	08/12/02	09/04/02	09/17/02	09/25/02	10/01/02
1	0.110	0.110	0.110	0.106	0.110	0.074	0.074	0.074	0.074	0.074	0.075	0.076
2	0.120	0.110	0.110	0.104	0.110	0.072	0.071	0.070	0.070	0.072	0.072	0.072
3	0.110	0.110	0.110	0.095	0.104	0.066	0.063	0.066	0.066	0.065	0.066	0.065
4	0.100	0.100	0.100	0.087	0.090	0.049	0.049	0.049	0.048	0.049	0.050	0.048
5	0.080	0.080	0.070	0.081	0.071	0.031	0.030	0.031	0.029	0.031	0.028	0.030
6	0.060	0.060	0.060	0.075	0.057	0.016	0.017	0.016	0.016	0.016	0.017	0.017
7	0.050	0.050	0.050	0.070	0.047	0.008	0.007	0.008	0.007	0.007	0.008	0.007
8	0.050	0.050	0.040	0.068	0.044	0.002	0.002	0.003	0.001	0.003	0.004	0.002
9	0.040	0.040	0.040	0.065	0.040	-0.002	-0.002	-0.002	-0.002	-0.002	0.000	-0.002
10	0.040	0.040	0.040	0.069	0.035	-0.007	-0.007	-0.006	-0.007	-0.006	-0.004	-0.006
11	0.030	0.030	0.030	0.063	0.032	-0.013	-0.012	-0.011	-0.012	-0.012	-0.011	-0.012
12	0.040	0.040	0.040	0.061	0.036	-0.010	-0.008	-0.009	-0.010	-0.010	-0.008	-0.010
13	0.030	0.040	0.040	0.061	0.035	-0.009	-0.008	-0.009	-0.009	-0.008	-0.007	-0.008
14	0.030	0.040	0.040	0.065	0.034	-0.010	-0.009	-0.008	-0.009	-0.009	-0.007	-0.009
15	0.040	0.040	0.040	0.059	0.040	-0.004	-0.002	-0.004	-0.003	-0.004	-0.002	-0.003
16	0.050	0.050	0.050	0.067	0.051	0.010	0.009	0.009	0.010	0.008	0.011	0.009
17	0.060	0.060	0.060	0.087	0.054	0.017	0.018	0.018	0.019	0.018	0.021	0.019
18	0.070	0.080	0.080	0.112	0.075	0.038	0.039	0.035	0.037	0.039	0.039	0.040
19	0.100	0.110	0.100	0.120	0.105	0.069	0.067	0.067	0.067	0.068	0.070	0.069
SV	1.608	1.556	1.386	0.838	1.373	1.526	1.378	1.448	1.430	1.439	1.484	1.449

TABLE C4. Elevation Data for the Longitudinal Profile Lane SS

Station	ATL Passes (x 1,000) / Date											
	0	25	45	71	100	157	201	246	328	420	468	500
	11/11/01	01/04/02	01/11/02	01/25/02	02/07/02	07/25/02	08/02/02	08/12/02	09/04/02	09/17/02	09/25/02	10/01/02
1	0.100	0.100	0.110	0.114	0.104	0.070	0.069	0.069	0.069	0.070	0.070	0.072
2	0.100	0.100	0.100	0.114	0.101	0.064	0.062	0.063	0.063	0.063	0.063	0.064
3	0.090	0.090	0.100	0.110	0.092	0.053	0.052	0.052	0.053	0.053	0.063	0.055
4	0.080	0.080	0.090	0.094	0.082	0.042	0.041	0.041	0.042	0.042	0.055	0.042
5	0.070	0.080	0.080	0.076	0.075	0.036	0.035	0.034	0.036	0.035	0.042	0.037
6	0.070	0.070	0.080	0.093	0.072	0.031	0.030	0.030	0.030	0.030	0.036	0.031
7	0.060	0.070	0.070	0.051	0.068	0.024	0.023	0.023	0.022	0.023	0.031	0.023
8	0.060	0.070	0.070	0.046	0.065	0.023	0.022	0.023	0.023	0.023	0.024	0.022
9	0.060	0.060	0.060	0.044	0.062	0.018	0.018	0.018	0.020	0.019	0.021	0.020
10	0.060	0.060	0.070	0.039	0.064	0.020	0.020	0.020	0.020	0.021	0.022	0.020
11	0.060	0.060	0.060	0.033	0.060	0.015	0.015	0.016	0.017	0.016	0.017	0.015
12	0.050	0.060	0.060	0.034	0.057	0.013	0.013	0.013	0.013	0.013	0.016	0.013
13	0.050	0.060	0.060	0.034	0.060	0.015	0.014	0.016	0.016	0.016	0.018	0.016
14	0.050	0.060	0.070	0.035	0.063	0.019	0.019	0.020	0.020	0.021	0.022	0.022
15	0.050	0.060	0.060	0.039	0.054	0.015	0.017	0.017	0.018	0.017	0.020	0.019
16	0.060	0.060	0.070	0.051	0.060	0.022	0.023	0.024	0.024	0.024	0.025	0.027
17	0.080	0.090	0.090	0.057	0.083	0.057	0.050	0.051	0.049	0.051	0.052	0.052
18	0.110	0.110	0.110	0.076	0.106	0.074	0.075	0.076	0.077	0.079	0.079	0.078
19	0.120	0.120	0.120	0.105	0.115	0.084	0.084	0.085	0.087	0.085	0.087	0.086
SV	1.099	0.988	1.052	2.297	0.877	1.186	1.066	1.083	1.102	1.157	1.102	1.081

APPENDIX D

HORIZONTAL STRAINS AT THE BOTTOM OF THE ASPHALT CONCRETE LAYER

TABLE D1. Longitudinal Strains at the Bottom of the Asphalt Layer – Lane NN (microstrain)

Lane	Location	L/T	Date	Passes (1000)	Signal Type	A	B	C	D	E	F	G	Strain
NN	W	L	17-Dec-01	0	3	1718	1522	644	450	336	412	468	976
NN	E	L	17-Dec-01	0	3	5341	5308	4629	4517	4413	4385	4479	696
NN	W	L	15-Feb-02	23	3	1439	1346	441	221	44	152	187	952
NN	E	L	15-Feb-02	23	3	5071	4945	4348	4268	4005	3992	4216	660
NN	W	L	19-Feb-02	26	3	1900	1782	1005	810	604	738	767	836
NN	E	L	19-Feb-02	26	3	5820	5688	5177	5100	4850	4833	5030	577
NN	W	L	25-Feb-02	42	3	1348	1232	473	278	120	217	265	817
NN	E	L	25-Feb-02	42	3	5268	5160	4624	4545	4366	4340	4515	590
NN	W	L	26-Feb-02	47	3	1969	1847	1058	875	738	799	877	850
NN	E	L	26-Feb-02	47	3	4491	4388	3821	3759	3595	3562	3751	619
NN	W	L	1-Mar-02	60	3	2292	2187	1449	1253	1083	1191	1226	791
NN	E	L	1-Mar-02	60	3	6355	6256	5739	5655	5460	5437	5623	567
NN	W	L	5-Mar-02	67	3	2187	2091	1345	1158	966	1100	1122	794
NN	E	L	5-Mar-02	67	3	6390	6297	5778	5693	5478	5461	5652	566
NN	W	L	8-Mar-02	82	3	3188	3095	2357	2159	1977	2108	2123	785
NN	E	L	8-Mar-02	82	3	7880	7773	7244	7162	6938	6919	7184	583
NN	W	L	15-Mar-02	100	3	3339	3262	2525	2332	2162	2276	2310	776
NN	E	L	15-Mar-02	100	3	8547	8441	7991	7828	7629	7590	7803	503
NN	W	L	5-Apr-02	130	6	4953	4841	4856	4818	4200			667
NN	E	L	5-Apr-02	130	6	1726	1703	1603	1575	1182			470
NN	W	L	12-Mar-02	150	6	5191	5092	5096	5074	4438			675
NN	E	L	12-Mar-02	150	6	3207	3151	3052	3048	2603			512
NN	W	L	19-Mar-02	176	6	7694	7588	7573	7545	6904			696
NN	E	L	19-Mar-02	176	6	7722	7684	7595	7582	7070			576
NN	W	L	26-Apr-02	208	6	7209	7127	7082	7073	6383			740
NN	E	L	26-Apr-02	208	6	8988	8943	8828	8826	8333			563
NN	W	L	10-Jun-02	276	6	5990	5911	5886	5853	5269			641
NN	E	L	10-Jun-02	276	6	950	912	859	843	401			490
NN	W	L	20-Jun-02	341	6	1784	1731	1655	1619	1114			583
NN	E	L	20-Jun-02	341	6	8331	8298	8240	8236	7806			470
NN	W	L	10-Jul-02	460	6	9471	9413	9375	9344	8821			580
NN	E	L	10-Jul-02	460	6	8506	8479	8467	8458	7915			563
NN	W	L	17-Jul-02	500	6	4235	4178	4120	4092	3487			669

TABLE D2. Transverse Strains at the Bottom of the Asphalt Layer – Lane NN (microstrain)

Lane	Location	Direction	Date	Passes (K rep.)	Signal Type	A	B	C	D	E	Strain
NN	W	T	17-Dec-01	0	2	5162	5139	4873			278
NN	E	T	17-Dec-01	0	2	5837	5858	5580			268
NN	W	T	15-Feb-02	23	2	7533	7548	7249			292
NN	E	T	15-Feb-02	23	2	6460	6479	6201			269
NN	W	T	19-Feb-02	26	2	8308	8309	8088			221
NN	E	T	19-Feb-02	26	2	7867	7875	7640			231
NN	W	T	25-Feb-02	42	2	8361	8359	8097			263
NN	E	T	25-Feb-02	42	2	8018	8041	7761			269
NN	W	T	26-Feb-02	47	2	7951	7934	7644			299
NN	E	T	26-Feb-02	47	2	6832	6868	6571			279
NN	W	T	1-Mar-02	60	2	9589	9576	9343			240
NN	E	T	1-Mar-02	60	2	8858	8894	8628			248
NN	W	T	5-Mar-02	67	2	9797	9798	9573			225
NN	E	T	5-Mar-02	67	2	9450	9458	9216			238
NN	W	T	8-Mar-02	82	2	1045	1044	839			206
NN	E	T	8-Mar-02	82	2	643	667	438			217
NN	W	T	15-Mar-02	100	2	1836	1836	1610			226
NN	E	T	15-Mar-02	100	2	1608	1640	1409			215
NN	W	T	5-Apr-02	130	6	4789	4718	4800	4709	4707	47
NN	E	T	5-Apr-02	130	6	4279	4223	4265	4164	4142	91
NN	W	T	12-Mar-02	150	6	5968	5906	5995	5889	5875	65
NN	E	T	12-Mar-02	150	6	4647	4611	4673	4581	4490	138
NN	W	T	19-Mar-02	176	6	212	158	232	98	132	43
NN	E	T	19-Mar-02	176	6	9021	8999	9086	8968	8858	161
NN	W	T	26-Apr-02	208	6	1001	940	1033	931	916	60
NN	E	T	26-Apr-02	208	6	2334	2297	2346	2258	2194	115
NN	E	T	10-Jun-02	276	6	6709	6659	6674	6558	6607	43
NN	E	T	20-Jun-02	341	6	3524	3456	3493	3305	3451	7

TABLE D3. Longitudinal Strains at the Bottom of the Asphalt Layer – Lane NS (microstrain)

Lane	Location	Direction	Date	Passes (K rep.)	Signal Type	A	B	C	D	E	F	G	Strain
NS	W	L	17-Dec-01	0	3	6278	6234	5110	4855	4883	4749	4942	1146
NS	E	L	17-Dec-01	0	3	5824	5850	4608	4320	4416	4177	4440	1229
NS	W	L	15-Feb-02	23	3	4338	4153	3173	2985	2895	2785	2981	1073
NS	E	L	15-Feb-02	23	3	4822	4904	3636	3320	3410	3276	3389	1227
NS	W	L	19-Feb-02	26	3	5588	5378	4479	4346	4226	4119	4306	1004
NS	E	L	19-Feb-02	26	3	5786	5880	4692	4385	4473	4359	4449	1141
NS	W	L	25-Feb-02	42	3	5214	5026	4150	4011	3915	3815	4011	970
NS	E	L	25-Feb-02	42	3	5317	5397	4234	3944	4038	3916	4003	1123
NS	W	L	26-Feb-02	47	3	4208	4041	3119	2992	2894	2789	3021	1006
NS	E	L	26-Feb-02	47	3	4565	4648	3484	3192	3296	3169	3265	1123
NS	W	L	1-Mar-02	60	3	5810	5691	4815	4665	4550	4477	4658	936
NS	E	L	1-Mar-02	60	3	6587	6664	5494	5215	5289	5176	5267	1132
NS	W	L	5-Mar-02	67	3	6435	6261	5403	5284	5143	5068	5251	945
NS	E	L	5-Mar-02	67	3	6828	6935	5761	5484	5560	5456	5532	1121
NS	W	L	8-Mar-02	82	3	7349	7238	6381	6233	6083	6033	6194	913
NS	E	L	8-Mar-02	82	3	8342	8414	7243	6948	7018	6926	6986	1135
NS	W	L	15-Mar-02	100	3	8308	8190	7366	7220	7083	6999	7203	883
NS	E	L	15-Mar-02	100	3	9055	9130	7988	7695	7779	7689	7756	1105
NS	W	L	5-Apr-02	130	5	1212	1194	1138	1068	418			735
NS	E	L	5-Apr-02	130	6	2719	2784	2901	2775	1813			982
NS	W	L	12-Mar-02	150	6	1364	1360	1289	1229	583			728
NS	E	L	12-Mar-02	150	6	3518	3545	3652	3558	2616			952
NS	W	L	19-Mar-02	176	6	4349	4368	4241	4216	3514			780
NS	E	L	19-Mar-02	176	6	7449	7476	7657	7574	6454			1085
NS	W	L	26-Apr-02	208	6	4633	4621	4542	4523	3822			758
NS	E	L	26-Apr-02	208	6	8153	8200	8318	8278	7123			1114
NS	W	L	10-Jun-02	276	6	4149	4134	3979	3991	3452			611
NS	E	L	10-Jun-02	276	6	3590	3583	3778	3672	2749			907
NS	W	L	20-Jun-02	341	6	7897	7919	7734	7743	7287			536
NS	E	L	20-Jun-02	341	6	9770	9759	9861	9815	9074			727
NS	W	L	10-Jul-02	460	6	2394	2403	2205	2235	1722			587
NS	E	L	10-Jul-02	460	6	7219	7229	7307	7258	6446			807
NS	W	L	17-Jul-02	500	6	8546	8546	8367	8405	7863			603
NS	E	L	17-Jul-02	500	6	9672	9658	9720	9691	8854			831

TABLE D4. Transverse Strains at the Bottom of the Asphalt Layer – Lane NS (microstrain)

Lane	Location	Direction	Date	Passes (x 1,000)	Signal Type	A	B	C	D	E	Strain
NS	E	T	17-Dec-01	0	4	4476	4693	4588			109
NS	E	T	15-Feb-02	23	4	2172	2327	2257			78
NS	E	T	19-Feb-02	26	4	3228	3372	3301			72
NS	E	T	25-Feb-02	42	4	2813	2917	2866			52
NS	E	T	26-Feb-02	47	4	1850	1913	1875			32
NS	E	T	1-Mar-02	60	4	3637	3746	3695			55
NS	E	T	5-Mar-02	67	4	3924	4049	3998			63
NS	E	T	8-Mar-02	82	4	5012	5133	5078			61
NS	E	T	15-Mar-02	100	4	5502	5605	5555			52
NS	E	T	20-Jun-02	341	5	495	368	477	271	1099	696
NS	E	T	10-Jul-02	460	5	69	3	68	133	620	618
NS	E	T	17-Jul-02	500	5	456	389	435	247	938	556

TABLE D5. Longitudinal Strains at the Bottom of the Asphalt Layer – Lane SN (microstrain)

Lane	Location	Direction	Date	Passes (x 1,000)	Signal Type	A	B	C	D	E	Strain
SN	W	L		0	2	877	623	0			750
SN	E	L		0	2	537	505	-70			591
SN	W	L		25	2	402	462	0			432
SN	E	L		25	2	331	271	3			298
SN	E	L		45	2	167	241	4			200
SN	E	L		71	2	217	205	4			207
SN	E	L		100	2	237	240	-1			240
SN	E	L		150	6	136	159	114	103	29	99
SN	E	L		171	6	196	202	116	123	15	144
SN	W	L		201	6	234	242	147	96	68	112
SN	E	L		201	6	198	193	106	126	11	145
SN	W	L		224	6	224	265	187	171	0	212
SN	E	L		224	6	211	215	116	123	9	157
SN	E	L		247	6	135	141	83	87	5	107
SN	E	L		273	6	139	131	70	82	9	97
SN	E	L		328	6	175	168	76	89	16	111
SN	E	L		386	6	142	142	83	98	5	111
SN	E	L		420	6	159	132	149	156	1	148
SN	E	L		468	6	126	93	105	117	3	107
SN	E	L		500	6	107	91	110	119	-8	115

TABLE D6. Transverse Strains at the Bottom of the Asphalt Layer – Lane SS (microstrain)

Lane	Location	Direction	Date	Passes (x 1,000)	Signal Type	A	B	C	Strain
SS	W	T		0	2	374	405	34	356
SS	E	T		0	2	365	436	0	401
SS	W	T		25	2	349	354	29	323
SS	E	T		25	2	400	439	-20	440
SS	W	T		45	2	373	391	31	351
SS	E	T		45	2	434	467	-15	466
SS	W	T		71	2	363	375	18	351
SS	E	T		71	2	428	473	-18	469
SS	W	T		100	2	356	356	34	322
SS	E	T		100	2	391	434	-21	434

APPENDIX E

VERTICAL COMPRESSIVE STRESS AT THE TOP OF THE SOIL SUBGRADE

TABLE E1. Vertical Stress at the Top of the Soil Subgrade Layer

Lane	Location	Date	Passes (K rep.)	Signal Type	A	B	C	D	E	Stress (psi)
NS	W	17-Dec-01	0	1	1.70	1.02	0.03			1.33
NS	E			1	3.32	4.35	-1.12			4.955
NN	E			2	-8.24	-8.99	-1.58			7.035
NN	W			2	-8.77	-7.75	-1.91			6.35
NS	W	15-Feb-02	23	1	2.30	1.56	0.19			1.74
NS	E			1	3.69	3.71	-0.96			4.66
NN	E			2	-8.54	-9.42	-1.74			7.24
NN	W			2	-10.6	-9.48	-2.11			7.925
NS	W	19-Feb-02	26	1	1.82	1.30	-0.09			1.65
NS	E			1	2.10	2.92	-1.22			3.73
NN	E			2	-7.38	-8.30	-1.47			6.37
NN	W			1	7.62	6.37	-0.21			7.205
NS	W	25-Feb-02	42	1	2.03	1.43	0.22			1.51
NS	E			1	1.70	2.45	-0.91			2.985
NN	E			2	-7.07	-7.95	-1.77			5.74
NN	W			1	7.46	6.16	0.11			6.7
NS	W	26-Feb-02	47	1	2.11	1.62	0.37			1.495
NS	E			1	1.55	2.39	-0.80			2.77
NN	E			2	-7.04	-7.95	-2.03			5.465
NN	W			1	7.48	6.35	0.32			6.595
NS	W	1-Mar-02	60	1	1.42	0.95	0.06			1.125
NS	E			1	0.82	1.63	-1.11			2.335
NN	E			2	-6.11	-7.11	-1.60			5.01
NN	W			1	6.88	5.71	-0.04			6.335
NS	W	5-Mar-02	67	1	1.83	1.28	0.16			1.395
NS	E			1	1.26	2.14	-1.00			2.7
NN	E			2	-6.56	-7.50	-1.74			5.29
NN	W			1	7.21	5.95	0.03			6.55
NS	W	8-Mar-02	82	1	1.48	1.01	-0.11			1.355
NS	E			1	0.98	1.76	-1.29			2.66
NN	E			2	-6.57	-7.55	-1.46			5.6
NN	W			1	7.10	5.92	-2.50			9.01
NS	W	15-Mar-02	100	1	1.61	1.18	0.11			1.285
NS	E			1	0.93	1.76	-1.01			2.355
NN	E			2	-6.62	-7.43	-1.66			5.365
NN	W			1	7.33	6.30	-0.01			6.825

TABLE E1. Vertical Stress at the Top of the Soil Subgrade Layer (continued)

Lane	Location	Date	Passes (K rep.)	Signal Type	A	B	C	D	E	Stress (psi)
NS	W	5-Apr-02	130	5	1.43	2.36	1.25	1.17	0.20	1.3525
NS	E			5	0.40	1.34	1.36	1.60	-0.93	2.105
NN	E			6	-6.42	-6.15	-6.52	-7.58	-1.78	4.8875
NN	W			5	7.32	7.16	6.15	6.58	0.12	6.6825
NS	W	12-Mar-02	150	5	1.43	2.35	1.23	1.19	1.13	0.42
NS	E			5	0.76	1.61	1.67	1.88	-1.01	2.49
NN	E			6	-7.21	-6.77	-7.19	-8.16	-1.71	5.6225
NN	W			5	7.38	7.25	6.28	6.70	0.03	6.8725
NS	W	19-Mar-02	176	5	2.23	3.16	2.06	1.91	0.00	2.34
NS	E			5	1.33	2.26	2.28	2.66	-1.04	3.1725
NN	E			6	-7.87	-7.62	-8.07	-8.88	-1.56	6.55
NN	W			5	8.94	8.66	7.95	8.16	0.00	8.4275
NS	W	26-Apr-02	208	5	1.77	2.68	1.58	1.52	0.09	1.7975
NS	E			5	0.40	1.23	1.29	1.46	-1.00	2.095
NN	E			6	-7.10	-6.67	-7.14	-7.90	-1.62	5.5825
NN	W			5	8.50	8.24	7.33	7.75	0.04	7.915
NS	W	10-Jun-02	276	5	3.12	3.97	2.83	2.61	-0.30	3.4325
NS	E			5	1.91	2.82	2.82	3.04	-1.23	3.8775
NN	E			6	-9.35	-8.84	-9.41	-10.2	-1.22	8.23
NN	W			5	10.05	9.70	8.65	9.06	-0.20	9.565
NS	W	20-Jun-02	341	5	3.42	4.49	3.29	3.03	-0.35	3.9075
NS	E			5	3.63	4.48	4.24	4.67	-1.10	5.355
NN	E			6	-10.8	-10.3	-10.5	-11.6	-1.26	9.5325
NN	W			5	11.25	10.95	9.51	10.07	-0.08	10.525
NS	W	10-Jul-02	460	5	3.88	4.84	3.75	3.40	-0.41	4.3775
NS	E			5	3.68	4.41	4.24	4.82	-1.07	5.3575
NN	E			6	-11.1	-10.5	-10.8	-12.1	-1.21	9.945
NN	W			5	11.86	11.14	9.91	10.45	-0.11	10.95
NS	W	17-Jul-02	500	5	3.28	4.13	3.03	2.77	-0.29	3.5925
NS	E			5	2.53	3.36	3.13	3.62	-1.05	4.21
NN	E			6	-10.9	-10.2	-10.4	-11.8	-1.30	9.5575
NN	W			5	11.33	10.78	9.36	10.00	-0.04	10.4075
SN	W		0	1	0.09	0.07	0.00			0.08
SS	E			1	0.19	0.30	-0.01			0.255
SN	E			1	0.18	0.29	-0.02			0.255
SN	W		25	1	0.10	0.08	-0.01			0.1
SS	E			1	0.69	1.17	-0.06			0.99
SN	E			1	0.12	0.18	-0.02			0.17

TABLE E1. Vertical Stress at the Top of the Soil Subgrade Layer (continued)

Lane	Location	Date	Passes (K rep.)	Signal Type	A	B	C	D	E	Stress (psi)
SN	W		45	1	0.26	0.10	-0.01			0.19
SS	E		45	1	1.99	2.64	-0.13			2.445
SN	E		45	1	0.24	0.45	-0.02			0.365
SN	W		71	1	0.23	0.09	-0.01			0.17
SS	E		71	1	1.49	2.02	-0.10			1.855
SN	E		71	1	0.20	0.36	-0.02			0.3
SN	W		100	1	0.24	0.09	-0.02			0.185
SS	E		100	1	1.67	2.29	-0.15			2.13
SN	E		100	1	0.18	0.35	-0.03			0.295
SN	W		150	5	1.24	1.35	0.19	0.41	-0.07	0.8675
SS	E		150	5	3.08	3.87	4.03	4.14	-0.39	4.17
SN	E		150	5	0.76	0.75	0.90	1.46	-0.09	1.0575
SN	W		171	5	1.24	1.41	0.20	0.45	-0.08	0.905
SS	E		171	5	3.07	3.78	3.90	4.17	-0.39	4.12
SN	E		171	5	0.64	0.61	0.80	1.36	-0.04	0.8925
SN	W		201	5	1.69	1.77	0.32	0.70	-0.11	1.23
SS	E		201	5	2.44	2.98	3.18	3.36	-0.31	3.3
SN	E		201	5	0.75	0.71	0.94	1.50	-0.09	1.065
SN	W		224	5	1.72	1.79	0.35	0.72	-0.11	1.255
SS	E		224	5	2.47	3.00	3.19	3.36	-0.31	3.315
SN	E		224	5	0.75	0.71	0.92	1.52	-0.09	1.065
SN	W		247	5	1.54	1.57	0.30	0.66	0.10	0.9175
SS	E		247	5	3.63	4.25	4.64	4.76	-0.47	4.79
SN	E		247	5	0.62	0.63	0.82	1.36	-0.07	0.9275
SN	W		273	5	1.58	1.66	0.34	0.68	-0.10	1.165
SS	E		273	5	3.65	4.25	4.67	4.84	-0.47	4.8225
SN	E		273	5	0.64	0.62	0.84	1.41	-0.08	0.9575
SN	W		328	5	1.51	1.60	0.25	0.58	-0.10	1.085
SS	E		328	5	3.19	3.63	4.23	4.27	-0.43	4.26
SN	E		328	5	0.58	0.51	0.78	1.33	-0.07	0.87
SN	W		386	5	1.36	1.40	0.28	0.58	-0.09	0.995
SS	E		386	5	1.81	2.17	2.63	2.69	-0.25	2.575
SN	E		386	5	0.53	0.54	0.76	1.19	-0.07	0.825
SN	W		420	5	0.69	0.76	0.11	0.20	-0.05	0.49
SS	E		420	5	1.26	1.57	2.04	2.15	-0.21	1.965
SN	E		420	5	0.16	0.16	0.30	0.64	-0.03	0.345
SN	W		468	5	1.19	1.20	0.20	0.43	-0.08	0.835
SS	E		468	5	2.11	2.47	3.11	3.11	-0.30	3
SN	E		468	5	0.32	0.28	0.48	0.89	-0.05	0.5425
SN	W		500	5	0.85	0.93	0.12	0.25	-0.05	0.5875
SS	E		500	5	1.35	1.60	2.10	2.34	-0.22	2.0675
SN	E		500	5	0.16	0.13	0.25	0.60	-0.04	0.325

APPENDIX F

FALLING WEIGHT DEFLECTOMETER DATA

TABLE F1. FWD deflection data and corresponding backcalculated moduli

Lane	Date	Passes (x1,000)	Station	Drop Nr.	Load (lbs)	D0 (mils)	D1 (mils)	D2 (mils)	D3 (mils)	D4 (mils)	D5 (mils)	D6 (mils)	E(AC) (psi)	E(Base) (psi)	Mr (psi)
NN	1	0	1	1	6280	9.19	7.65	6.56	5.23	4.15	2.57	1.32	1,898,250	87,796	15,831
NN	1	0	1	2	9363	14.56	12.05	10.33	8.24	6.54	4.09	2.13	1,509,779	97,102	14,873
NN	1	0	1	3	9355	14.54	12.02	10.31	8.22	6.52	4.08	2.12	1,466,621	99,761	14,880
NN	1	0	2	1	6252	9.24	7.73	6.64	5.23	4.09	2.60	1.33	1,886,760	83,108	15,792
NN	1	0	2	2	9339	14.64	12.18	10.48	8.24	6.44	4.09	2.10	1,662,900	83,093	14,955
NN	1	0	2	3	9347	14.67	12.20	10.50	8.25	6.45	4.09	2.12	1,664,273	82,385	14,956
NN	1	0	3	1	6217	10.95	8.79	7.21	5.46	4.20	2.61	1.35	927,284	72,775	15,409
NN	1	0	3	2	9319	16.94	13.54	11.17	8.47	6.54	4.11	2.18	788,076	80,168	14,759
NN	1	0	3	3	9323	16.92	13.52	11.16	8.46	6.54	4.10	2.18	794,320	79,990	14,783
NN	1	0	4	1	6212	10.62	8.30	6.88	5.31	4.13	2.57	1.28	600,001	107,630	15,662
NN	1	0	4	2	9327	16.89	13.25	10.99	8.41	6.52	4.03	2.08	658,670	90,738	14,916
NN	1	0	4	3	9347	16.93	13.28	11.03	8.45	6.56	4.07	2.10	604,185	96,493	14,826
NN	1	0	5	1	6196	11.18	8.79	7.31	5.54	4.24	2.59	1.30	799,289	76,043	15,253
NN	1	0	5	2	9358	17.19	13.57	11.32	8.59	6.61	4.05	2.11	796,603	76,799	14,766
NN	1	0	5	3	9319	17.17	13.56	11.31	8.58	6.61	4.06	2.11	791,633	76,949	14,702
NN	1	0	6	1	6280	10.85	8.57	7.11	5.47	4.20	2.61	1.33	752,962	91,359	15,510
NN	1	0	6	2	9347	17.21	13.57	11.28	8.65	6.66	4.10	2.11	685,222	86,607	14,595
NN	1	0	6	3	9331	17.17	13.54	11.27	8.64	6.65	4.10	2.11	739,434	82,748	14,609
NN	2	5	1	1	6037	9.32	7.85	6.70	5.37	4.24	2.65	1.39	2,015,266	75,367	14,859
NN	2	5	1	2	8791	13.98	11.83	10.14	8.10	6.40	4.00	2.09	2,183,317	63,944	14,398
NN	2	5	1	3	8794	13.96	11.81	10.13	8.09	6.38	3.98	2.07	2,199,995	62,528	14,467
NN	2	5	2	1	5998	9.54	8.03	6.88	5.42	4.25	2.66	1.38	2,046,547	63,158	14,765
NN	2	5	2	2	8775	14.18	12.02	10.33	8.12	6.37	3.96	2.09	2,199,995	54,707	14,502
NN	2	5	2	3	8786	14.15	12.00	10.31	8.10	6.35	3.96	2.07	2,199,995	54,906	14,552
NN	2	5	3	1	5971	11.17	9.00	7.49	5.66	4.33	2.67	1.38	1,047,100	60,060	14,396
NN	2	5	3	2	8755	16.65	13.50	11.28	8.54	6.55	4.01	2.14	1,181,500	53,015	14,047
NN	2	5	3	3	8743	16.61	13.47	11.25	8.53	6.54	4.01	2.15	1,159,546	54,635	14,020
NN	2	5	4	1	6153	11.34	8.98	7.42	5.67	4.34	2.68	1.41	762,966	78,155	14,735
NN	2	5	4	2	8918	16.94	13.58	11.28	8.60	6.55	4.00	2.10	1,023,687	59,089	14,253
NN	2	5	4	3	8926	16.93	13.57	11.30	8.61	6.56	4.00	2.10	1,033,350	59,159	14,243
NN	2	5	5	1	6188	11.85	9.37	7.72	5.81	4.45	2.73	1.42	759,400	69,297	14,491
NN	2	5	5	2	8921	17.43	13.94	11.54	8.68	6.64	4.02	2.15	982,721	54,787	14,131
NN	2	5	5	3	8942	17.44	14.00	11.57	8.70	6.65	4.02	2.15	1,033,920	52,067	14,170
NN	2	5	6	1	6244	11.76	9.39	7.77	5.86	4.47	2.76	1.45	909,708	63,950	14,545
NN	2	5	6	2	8929	17.37	13.97	11.61	8.76	6.66	4.05	2.14	1,062,731	52,382	14,068
NN	2	5	6	3	8926	17.37	13.97	11.61	8.75	6.65	4.04	2.13	1,056,204	52,423	14,079
NN	4	149	1	1	6320	9.64	8.26	7.11	5.64	4.39	2.67	1.41	1,999,995	60,000	15,476
NN	4	149	1	2	8961	14.42	12.20	10.56	8.42	6.61	4.13	2.13	1,999,995	68,559	14,141
NN	4	149	1	3	8977	14.48	12.25	10.60	8.45	6.67	4.16	2.13	1,999,995	69,921	14,060
NN	4	149	2	1	6260	9.75	8.34	7.19	5.58	4.22	2.63	1.35	1,999,995	41,991	16,043
NN	4	149	2	2	8982	14.57	12.36	10.70	8.38	6.44	4.06	2.08	1,999,995	59,547	14,456
NN	4	149	2	3	8966	14.56	12.35	10.69	8.38	6.46	4.07	2.08	1,999,995	60,165	14,395
NN	4	149	3	1	6204	11.43	9.43	7.87	5.93	4.54	2.81	1.49	1,485,719	43,845	14,422

NN	4	149	3	2	8966	16.95	14.07	11.83	8.99	6.88	4.27	2.22	1,572,459	41,260	13,753
NN	4	149	3	3	8937	16.93	14.06	11.83	8.99	6.87	4.27	2.22	1,576,328	40,894	13,718
NN	4	149	4	1	6188	11.27	9.13	7.63	5.74	4.34	2.65	1.42	1,291,113	49,304	14,967
NN	4	149	4	2	8937	16.88	13.77	11.57	8.75	6.67	4.09	2.13	1,406,642	44,190	14,146
NN	4	149	4	3	8961	16.94	13.79	11.59	8.80	6.71	4.12	2.13	1,337,851	47,719	14,054
NN	4	149	5	1	6260	11.94	9.60	7.99	5.97	4.54	2.82	1.42	1,019,422	56,512	14,338
NN	4	149	5	2	8942	17.44	14.11	11.83	8.94	6.91	4.30	2.20	1,030,158	60,345	13,491
NN	4	149	5	3	8926	17.38	14.06	11.78	8.93	6.91	4.30	2.20	990,655	63,504	13,449
NN	4	149	6	1	6339	11.70	9.41	7.81	5.83	4.41	2.74	1.40	1,080,305	55,760	14,937
NN	4	149	6	2	8926	17.44	14.11	11.85	8.94	6.85	4.25	2.17	1,093,171	55,435	13,585
NN	4	149	6	3	8953	17.41	14.11	11.86	8.96	6.86	4.30	2.26	1,095,927	56,854	13,559
NS	1	0	1	1	6284	8.96	7.05	5.83	4.62	3.71	2.40	1.23	846,775	90,503	16,722
NS	1	0	1	2	9342	14.35	11.30	9.29	7.26	5.83	3.78	1.98	817,513	79,408	15,868
NS	1	0	1	3	9350	14.34	11.30	9.29	7.26	5.83	3.79	1.98	814,250	79,745	15,875
NS	1	0	2	1	6225	8.90	7.10	5.87	4.60	3.72	2.39	1.24	1,021,527	81,973	16,662
NS	1	0	2	2	9350	14.11	11.22	9.29	7.23	5.84	3.79	2.01	936,240	78,263	15,878
NS	1	0	2	3	9355	14.11	11.24	9.30	7.24	5.84	3.79	2.01	954,782	77,554	15,883
NS	1	0	3	1	6241	9.90	7.61	6.07	4.52	3.58	2.36	1.24	661,137	68,494	17,323
NS	1	0	3	2	9363	15.26	11.81	9.50	7.13	5.59	3.76	2.04	679,067	67,679	16,439
NS	1	0	3	3	9342	15.19	11.76	9.45	7.09	5.59	3.74	2.03	654,088	69,424	16,428
NS	1	0	4	1	6296	9.63	7.19	5.90	4.61	3.68	2.38	1.22	457,651	94,802	16,956
NS	1	0	4	2	9443	15.41	11.58	9.47	7.31	5.82	3.79	1.99	500,603	81,803	16,070
NS	1	0	4	3	9435	15.39	11.58	9.46	7.30	5.82	3.78	1.99	505,584	81,465	16,074
NS	1	0	5	1	6304	10.09	7.76	6.26	4.75	3.76	2.50	1.30	615,337	74,758	16,506
NS	1	0	5	2	9403	15.86	12.28	9.91	7.46	5.90	3.91	2.06	668,284	65,753	15,754
NS	1	0	5	3	9427	15.89	12.31	9.94	7.49	5.93	3.93	2.07	666,317	66,452	15,698
NS	1	0	6	1	6360	10.55	7.90	6.34	4.76	3.74	2.49	1.31	496,736	72,749	16,768
NS	1	0	6	2	9427	16.70	12.55	10.05	7.46	5.85	3.87	2.09	513,827	63,372	15,947
NS	1	0	6	3	9411	16.76	12.53	10.04	7.45	5.82	3.86	2.07	493,972	63,477	15,973
NS	2	5	1	1	6180	9.39	7.62	6.31	4.88	3.91	2.56	1.34	1,129,225	70,271	15,644
NS	2	5	1	2	8942	14.13	11.48	9.50	7.31	5.80	3.75	2.02	1,214,052	60,245	15,405
NS	2	5	1	3	8934	14.15	11.48	9.52	7.33	5.82	3.76	2.00	1,214,564	60,163	15,351
NS	2	5	2	1	6133	9.39	7.59	6.25	4.92	3.89	2.52	1.35	1,177,548	66,830	15,688
NS	2	5	2	2	8910	14.06	11.35	9.40	7.37	5.76	3.74	2.01	1,213,021	61,368	15,375
NS	2	5	2	3	8894	14.03	11.34	9.38	7.35	5.75	3.73	2.01	1,174,081	62,590	15,351
NS	2	5	3	1	6045	10.50	8.25	6.65	4.96	3.78	2.46	1.36	899,869	48,773	15,950
NS	2	5	3	2	8866	15.50	12.27	9.98	7.45	5.70	3.67	2.08	995,791	46,301	15,620
NS	2	5	3	3	8871	15.49	12.26	9.98	7.44	5.69	3.66	2.08	998,732	46,176	15,657
NS	2	5	4	1	6106	10.42	7.91	6.40	4.84	3.80	2.51	1.34	567,900	68,445	15,856
NS	2	5	4	2	8945	15.68	11.97	9.76	7.35	5.72	3.70	1.96	679,351	59,295	15,560
NS	2	5	4	3	8913	15.66	11.96	9.75	7.34	5.72	3.70	1.96	656,704	60,179	15,492
NS	2	5	5	1	6090	11.07	8.75	7.06	5.20	3.99	2.55	1.37	932,673	42,887	15,419
NS	2	5	5	2	8894	16.41	12.98	10.57	7.76	5.92	3.70	2.02	1,040,158	37,694	15,380
NS	2	5	5	3	8890	16.41	12.96	10.57	7.77	5.93	3.71	2.00	1,027,315	38,280	15,326
NS	2	5	6	1	6141	11.56	8.85	7.02	5.17	3.94	2.56	1.37	645,757	48,078	15,508
NS	2	5	6	2	8910	17.09	13.19	10.63	7.76	5.87	3.73	2.02	786,377	40,818	15,292
NS	2	5	6	3	8942	17.09	13.20	10.66	7.78	5.89	3.74	2.03	797,728	40,861	15,302
NS	4	149	1	1	6145	9.00	7.42	6.26	4.93	3.80	2.57	1.33	1,596,074	63,810	15,749
NS	4	149	1	2	9117	13.22	10.85	9.21	7.33	5.82	3.88	2.02	1,425,733	76,765	15,261

NS	4	149	1	3	9101	13.18	10.80	9.16	7.30	5.81	3.84	2.02	1,497,737	74,144	15,369
NS	4	149	2	1	6257	8.78	7.20	6.17	4.88	3.87	2.56	1.33	1,626,957	73,631	15,861
NS	4	149	2	2	9136	13.07	10.76	9.25	7.37	5.87	3.89	2.02	1,669,644	73,538	15,225
NS	4	149	2	3	9144	13.07	10.73	9.22	7.35	5.92	3.89	2.01	1,563,479	77,889	15,149
NS	4	149	3	1	6172	10.35	8.42	6.93	5.13	3.91	2.51	1.34	1,275,523	42,603	15,921
NS	4	149	3	2	9093	15.09	12.35	10.30	7.80	5.97	3.87	2.06	1,398,177	45,363	15,274
NS	4	149	3	3	9093	15.09	12.38	10.33	7.80	5.96	3.88	2.06	1,417,438	44,774	15,274
NS	4	149	4	1	6193	10.40	8.05	6.65	5.09	3.91	2.54	1.36	778,269	63,239	15,615
NS	4	149	4	2	9136	15.41	12.00	10.02	7.67	5.97	3.86	2.05	837,659	63,242	15,152
NS	4	149	4	3	9077	15.31	11.93	9.97	7.63	5.98	3.84	2.03	853,398	63,181	15,096
NS	4	149	5	1	6201	11.06	8.93	7.29	5.41	4.02	2.50	1.39	1,259,070	34,025	15,815
NS	4	149	5	2	8937	16.39	13.19	10.86	8.19	6.15	3.79	2.06	1,257,824	34,826	14,955
NS	4	149	5	3	8953	16.38	13.20	10.88	8.20	6.21	3.80	2.06	1,271,880	35,103	14,904
NS	4	149	6	1	6363	11.71	9.04	7.33	5.33	4.01	2.59	1.41	776,412	44,917	15,798
NS	4	149	6	2	8926	17.11	13.32	10.96	8.12	6.13	3.93	2.08	841,863	43,257	14,548
NS	4	149	6	3	8890	17.06	13.28	10.93	8.13	6.13	3.93	2.08	842,532	43,403	14,486
SN	1	0	1	1	6344	5.95	4.46	3.68	2.97	2.49	1.79	0.97	519,535	156,334	22,822
SN	1	0	1	2	9525	9.44	7.09	5.83	4.66	3.89	2.78	1.54	541,165	138,798	22,035
SN	1	0	1	3	9509	9.38	7.08	5.81	4.65	3.87	2.77	1.53	560,531	138,245	22,066
SN	1	0	2	1	6331	6.11	4.54	3.74	2.98	2.53	1.78	0.96	503,563	147,197	22,801
SN	1	0	2	2	9490	9.51	7.17	5.89	4.67	3.91	2.77	1.52	589,109	131,045	21,977
SN	1	0	2	3	9501	9.52	7.17	5.90	4.69	3.91	2.78	1.53	586,136	131,626	21,941
SN	1	0	3	1	6272	6.04	4.80	3.93	3.07	2.51	1.75	0.93	1,087,173	106,682	22,880
SN	1	0	3	2	9474	9.41	7.44	6.14	4.80	3.93	2.75	1.49	1,034,907	106,220	21,971
SN	1	0	3	3	9466	9.45	7.44	6.14	4.81	3.94	2.74	1.50	1,007,605	106,092	21,963
SN	1	0	4	1	6347	5.94	4.57	3.78	3.04	2.54	1.79	0.94	718,343	141,037	22,430
SN	1	0	4	2	9522	9.46	7.27	6.01	4.76	3.96	2.80	1.50	724,132	125,297	21,694
SN	1	0	4	3	9490	9.44	7.24	6.00	4.77	3.95	2.79	1.50	717,908	125,773	21,641
SN	1	0	5	1	6280	6.47	4.81	3.84	2.97	2.45	1.77	0.98	526,930	117,685	23,427
SN	1	0	5	2	9466	10.20	7.65	6.13	4.70	3.85	2.74	1.55	574,757	105,338	22,564
SN	1	0	5	3	9470	10.17	7.65	6.14	4.70	3.85	2.74	1.55	601,373	104,387	22,573
SN	1	0	6	1	6336	6.54	4.81	3.82	2.93	2.41	1.76	0.97	500,001	116,221	24,065
SN	1	0	6	2	9474	10.40	7.72	6.13	4.64	3.75	2.72	1.54	547,509	99,460	23,172
SN	1	0	6	3	9470	10.39	7.72	6.13	4.64	3.74	2.70	1.53	561,135	98,144	23,259
SN	2	5	1	1	6304	5.92	4.61	3.78	3.06	2.58	1.84	1.02	715,922	144,617	21,816
SN	2	5	1	2	9180	8.89	6.89	5.70	4.57	3.80	2.69	1.50	773,277	131,210	21,662
SN	2	5	1	3	9156	8.88	6.89	5.70	4.57	3.80	2.69	1.50	760,041	131,653	21,589
SN	2	5	2	1	6257	5.95	4.62	3.81	3.07	2.55	1.81	1.00	764,539	135,849	21,931
SN	2	5	2	2	9149	9.02	7.01	5.84	4.64	3.81	2.65	1.48	909,006	116,711	21,770
SN	2	5	2	3	9125	8.98	7.00	5.82	4.63	3.81	2.65	1.49	921,148	116,909	21,724
SN	2	5	3	1	6304	6.15	4.93	4.07	3.22	2.63	1.83	1.01	1,197,766	105,083	21,869
SN	2	5	3	2	9117	9.09	7.29	6.08	4.80	3.89	2.66	1.46	1,330,464	95,615	21,611
SN	2	5	3	3	9125	9.07	7.27	6.08	4.79	3.88	2.65	1.46	1,343,135	95,231	21,715
SN	2	5	4	1	6315	6.06	4.78	3.98	3.15	2.62	1.88	1.03	918,663	126,674	21,478
SN	2	5	4	2	9199	9.14	7.22	6.04	4.73	3.86	2.72	1.52	1,050,721	108,419	21,528
SN	2	5	4	3	9207	9.14	7.23	6.05	4.74	3.87	2.72	1.52	1,078,745	107,539	21,530
SN	2	5	5	1	6363	6.70	5.12	4.18	3.22	2.63	1.89	1.08	691,912	107,338	21,928
SN	2	5	5	2	9152	9.86	7.59	6.24	4.80	3.89	2.71	1.56	820,071	95,966	21,635
SN	2	5	5	3	9183	9.87	7.61	6.25	4.81	3.90	2.72	1.57	818,686	96,420	21,642

SN	2	5	6	1	6347	6.78	5.10	4.14	3.19	2.59	1.88	1.09	615,051	107,438	22,186
SN	2	5	6	2	9168	10.06	7.66	6.26	4.79	3.84	2.70	1.56	740,161	93,623	21,918
SN	2	5	6	3	9152	10.02	7.64	6.24	4.78	3.83	2.69	1.55	752,204	93,478	21,944
SN	3	71	1	1	6355	5.96	4.70	4.14	3.25	2.65	1.89	1.07	1,319,091	119,075	21,223
SN	3	71	1	2	9756	9.31	7.46	6.44	5.15	4.24	2.94	1.61	1,478,531	110,818	20,754
SN	3	71	1	3	9763	9.29	7.45	6.42	5.13	4.26	2.95	1.62	1,430,716	114,216	20,655
SN	3	71	2	1	6400	6.24	4.87	4.32	3.33	2.75	1.90	1.10	1,291,028	108,875	21,093
SN	3	71	2	2	9752	9.53	7.66	6.69	5.26	4.32	2.96	1.65	1,688,221	96,974	20,680
SN	3	71	2	3	9772	9.51	7.65	6.70	5.26	4.31	2.95	1.64	1,699,996	96,664	20,784
SN	3	71	3	1	6296	6.31	5.11	4.38	3.55	2.84	1.96	1.07	1,698,564	92,586	20,195
SN	3	71	3	2	9700	9.82	7.92	6.88	5.48	4.38	3.00	1.61	1,699,996	88,189	20,327
SN	3	71	3	3	9668	9.79	7.91	6.86	5.44	4.38	3.00	1.64	1,699,996	88,618	20,271
SN	3	71	4	1	6284	6.33	5.04	4.29	3.37	2.68	1.92	1.04	1,246,134	100,154	20,967
SN	3	71	4	2	9700	9.93	7.98	6.80	5.31	4.25	2.98	1.66	1,428,907	90,368	20,776
SN	3	71	4	3	9713	9.91	7.99	6.80	5.33	4.26	2.99	1.67	1,464,856	90,244	20,739
SN	3	71	5	1	6284	6.54	5.17	4.42	3.43	2.73	1.90	1.11	1,282,868	89,690	21,028
SN	3	71	5	2	9620	10.03	7.98	6.83	5.29	4.22	2.89	1.63	1,437,954	83,306	21,136
SN	3	71	5	3	9636	10.02	7.99	6.85	5.29	4.21	2.90	1.64	1,467,630	82,613	21,178
SN	3	71	6	1	6312	6.69	5.22	4.46	3.44	2.70	1.91	1.12	1,137,059	89,539	21,179
SN	3	71	6	2	9689	10.24	8.10	6.85	5.35	4.20	2.92	1.62	1,263,027	85,470	21,135
SN	3	71	6	3	9708	10.23	8.10	6.88	5.37	4.23	2.94	1.65	1,312,098	85,337	21,045
SN	4	100	1	1	6566	5.09	4.06	3.48	2.92	2.52	1.86	1.07	894,454	221,576	22,008
SN	4	100	1	2	9454	7.61	6.06	5.19	4.34	3.74	2.73	1.57	836,170	210,255	21,531
SN	4	100	1	3	9430	7.59	6.06	5.20	4.32	3.68	2.72	1.57	950,975	198,010	21,759
SN	4	100	2	1	6442	5.32	4.17	3.61	2.98	2.52	1.87	1.09	801,519	197,140	21,787
SN	4	100	2	2	9482	7.81	6.23	5.37	4.46	3.77	2.74	1.59	1,034,595	182,775	21,531
SN	4	100	2	3	9454	7.83	6.26	5.41	4.47	3.77	2.75	1.61	1,073,149	177,954	21,454
SN	4	100	3	1	6411	5.38	4.47	3.80	3.04	2.46	1.82	1.04	1,699,996	126,739	22,676
SN	4	100	3	1	6355	5.45	4.47	3.75	3.08	2.51	1.83	1.05	1,423,583	136,106	22,076
SN	4	100	3	2	9355	8.11	6.62	5.64	4.57	3.78	2.73	1.54	1,477,327	133,596	21,701
SN	4	100	3	2	9347	8.10	6.71	5.72	4.56	3.70	2.67	1.48	1,699,996	117,543	22,345
SN	4	100	3	3	9403	8.12	6.64	5.65	4.63	3.80	2.72	1.52	1,555,869	131,029	21,774
SN	4	100	3	3	9366	8.10	6.71	5.73	4.56	3.69	2.66	1.48	1,699,996	115,234	22,594
SN	4	100	4	1	6466	5.40	4.27	3.61	3.00	2.56	1.87	1.07	800,676	189,874	21,855
SN	4	100	4	1	6315	5.31	4.23	3.60	2.97	2.48	1.81	0.94	1,018,352	168,482	22,009
SN	4	100	4	2	9366	8.04	6.50	5.52	4.53	3.68	2.75	1.47	1,234,448	147,904	21,812
SN	4	100	4	2	9342	8.07	6.48	5.49	4.42	3.69	2.74	1.55	1,079,041	152,966	21,931
SN	4	100	4	3	9358	8.09	6.50	5.50	4.41	3.67	2.73	1.52	1,086,798	150,108	22,123
SN	4	100	4	3	9311	8.02	6.48	5.49	4.48	3.66	2.73	1.43	1,178,324	148,586	21,871
SN	4	100	5	1	6435	5.46	4.32	3.67	2.93	2.40	1.78	1.06	1,048,141	148,790	23,438
SN	4	100	5	2	9334	8.11	6.47	5.50	4.39	3.61	2.66	1.59	1,118,146	141,972	22,629
SN	4	100	5	3	9363	8.13	6.48	5.50	4.41	3.62	2.67	1.57	1,113,196	142,980	22,603
SN	4	100	6	1	6415	5.46	4.38	3.60	2.93	2.36	1.78	1.09	1,034,984	145,633	23,656
SN	4	100	6	2	9382	8.13	6.48	5.43	4.35	3.54	2.65	1.60	1,046,396	143,054	23,106
SN	4	100	6	3	9379	8.12	6.46	5.41	4.37	3.54	2.66	1.60	998,584	147,020	22,994
SS	1	0	1	1	6209	10.61	8.12	6.48	4.70	3.47	2.06	1.11	655,895	38,743	17,489
SS	1	0	1	2	9355	16.71	12.89	10.36	7.54	5.56	3.26	1.80	684,970	35,100	16,564
SS	1	0	1	3	9334	16.67	12.88	10.36	7.54	5.57	3.27	1.81	703,239	34,570	16,528
SS	1	0	2	1	6212	10.56	8.18	6.56	4.72	3.45	2.07	1.13	714,588	36,194	17,558

SS	1	0	2	2	9350	16.37	12.80	10.35	7.50	5.53	3.29	1.83	757,026	34,243	16,611
SS	1	0	2	3	9319	16.33	12.76	10.32	7.48	5.50	3.27	1.81	766,176	33,640	16,663
SS	1	0	3	1	6185	10.77	8.28	6.59	4.69	3.43	2.10	1.14	633,497	37,129	17,407
SS	1	0	3	2	9323	16.44	12.75	10.26	7.39	5.44	3.30	1.80	675,238	36,720	16,617
SS	1	0	3	3	9323	16.41	12.74	10.27	7.39	5.45	3.30	1.80	690,185	36,204	16,638
SS	1	0	4	1	6244	10.74	8.20	6.49	4.58	3.34	2.00	1.04	647,934	35,030	18,266
SS	1	0	4	2	9331	16.70	12.98	10.41	7.42	5.41	3.18	1.68	731,171	30,679	17,069
SS	1	0	4	3	9342	16.63	12.94	10.38	7.41	5.41	3.18	1.67	737,515	31,043	17,087
SS	1	0	5	1	6244	10.77	8.39	6.69	4.78	3.46	2.04	1.11	754,479	31,554	17,813
SS	1	0	5	2	9339	16.33	12.81	10.34	7.43	5.45	3.20	1.77	802,998	30,993	17,016
SS	1	0	5	3	9311	16.31	12.81	10.33	7.44	5.46	3.21	1.78	800,298	31,141	16,926
SS	1	0	6	1	6272	11.19	8.71	6.97	4.94	3.57	2.06	1.11	779,845	27,386	17,631
SS	1	0	6	2	9334	16.68	13.05	10.55	7.55	5.56	3.25	1.77	778,359	30,353	16,718
SS	1	0	6	3	9342	16.70	13.06	10.56	7.56	5.57	3.24	1.77	781,479	30,194	16,732
SS	2	5	1	1	6252	11.02	8.71	7.05	5.17	3.81	2.27	1.21	811,670	32,990	16,166
SS	2	5	1	2	9001	16.00	12.79	10.40	7.70	5.70	3.37	1.86	892,537	31,050	15,674
SS	2	5	1	3	8998	15.94	12.74	10.36	7.69	5.67	3.34	1.85	922,727	29,822	15,831
SS	2	5	2	1	6225	10.80	8.65	7.00	5.10	3.76	2.29	1.24	834,900	33,910	16,138
SS	2	5	2	2	8993	15.71	12.57	10.28	7.52	5.56	3.37	1.82	871,549	33,180	15,824
SS	2	5	2	3	8990	15.72	12.59	10.29	7.54	5.58	3.37	1.82	880,967	32,810	15,806
SS	2	5	3	1	6180	10.88	8.69	6.98	5.07	3.78	2.32	1.22	753,055	36,400	15,850
SS	2	5	3	2	8993	15.76	12.61	10.25	7.51	5.62	3.45	1.81	805,879	36,650	15,521
SS	2	5	3	3	8958	15.70	12.57	10.22	7.50	5.60	3.43	1.80	811,682	36,367	15,525
SS	2	5	4	1	6276	11.06	8.74	7.01	5.07	3.77	2.26	1.19	756,069	34,275	16,346
SS	2	5	4	2	9093	16.24	12.91	10.48	7.65	5.68	3.36	1.75	847,473	30,988	15,905
SS	2	5	4	3	9093	16.22	12.91	10.49	7.67	5.69	3.37	1.76	845,523	31,446	15,834
SS	2	5	5	1	6315	11.16	8.92	7.21	5.24	3.87	2.33	1.25	829,642	32,159	16,030
SS	2	5	5	2	9049	15.96	12.80	10.45	7.65	5.66	3.41	1.84	871,922	32,345	15,697
SS	2	5	5	3	9049	15.94	12.79	10.44	7.64	5.65	3.39	1.84	904,088	30,971	15,813
SS	2	5	6	1	6312	11.39	9.15	7.43	5.38	3.97	2.35	1.26	888,217	28,194	15,846
SS	2	5	6	2	9085	16.22	12.99	10.66	7.77	5.74	3.42	1.84	907,894	29,706	15,687
SS	2	5	6	3	9069	16.17	12.97	10.63	7.76	5.74	3.42	1.85	915,570	29,631	15,673
SS	3	71	1	1	6130	11.49	9.10	7.55	5.39	3.94	2.37	1.29	839,127	27,592	15,342
SS	3	71	1	2	9501	17.51	14.07	11.72	8.56	6.33	3.77	2.01	974,646	26,765	14,969
SS	3	71	1	3	9485	17.47	14.07	11.70	8.56	6.33	3.74	2.00	1,022,371	24,868	15,108
SS	3	71	2	1	6180	11.38	9.16	7.52	5.35	3.84	2.36	1.24	891,401	25,647	15,797
SS	3	71	2	2	9490	17.31	14.05	11.61	8.46	6.17	3.71	1.91	1,025,177	24,515	15,374
SS	3	71	2	3	9490	17.28	14.02	11.59	8.44	6.15	3.71	1.89	1,009,966	25,100	15,369
SS	3	71	3	1	6141	11.56	9.28	7.57	5.41	3.94	2.43	1.29	798,114	28,750	15,156
SS	3	71	3	2	9517	17.58	14.22	11.84	8.60	6.33	3.86	1.97	972,807	26,799	14,845
SS	3	71	3	3	9501	17.58	14.19	11.83	8.58	6.30	3.87	1.93	948,135	27,531	14,806
SS	3	71	4	1	6148	11.69	9.36	7.62	5.48	4.01	2.44	1.32	799,795	28,238	15,022
SS	3	71	4	2	9530	17.59	14.16	11.80	8.55	6.31	3.81	2.06	962,014	26,720	14,989
SS	3	71	4	3	9490	17.52	14.10	11.76	8.55	6.27	3.80	2.04	963,839	26,748	14,966
SS	3	71	5	1	6156	11.69	9.31	7.67	5.63	4.11	2.47	1.26	857,350	27,945	14,763
SS	3	71	5	2	9514	17.67	14.18	11.81	8.69	6.44	3.87	1.89	951,734	28,040	14,647
SS	3	71	5	3	9501	17.60	14.19	11.81	8.58	6.34	3.85	2.06	947,535	27,502	14,800
SS	3	71	6	1	6117	11.78	9.41	7.78	5.53	3.99	2.40	1.24	863,325	24,041	15,206
SS	3	71	6	2	9549	17.57	14.18	11.80	8.58	6.33	3.82	2.05	975,880	26,748	14,969

SS	3	71	6	3	9522	17.65	14.17	11.82	8.69	6.47	3.90	1.95	945,545	28,909	14,554
SS	4	100	1	1	6188	9.96	7.97	6.57	4.89	3.54	2.27	1.24	965,475	35,829	17,635
SS	4	100	1	2	9144	14.73	11.85	9.81	7.33	5.40	3.44	1.93	1,026,639	35,612	17,229
SS	4	100	1	3	9096	14.68	11.78	9.78	7.33	5.43	3.42	1.96	1,012,684	36,453	17,099
SS	4	100	2	1	6236	10.07	8.17	6.54	4.87	3.53	2.29	1.24	910,385	36,376	17,736
SS	4	100	2	2	9093	14.61	11.87	9.67	7.22	5.35	3.41	1.93	987,207	36,657	17,274
SS	4	100	2	3	9180	14.68	11.93	9.72	7.28	5.42	3.44	1.94	998,497	37,254	17,248
SS	4	100	3	1	6284	10.52	8.41	6.75	4.97	3.65	2.28	1.24	848,736	34,341	17,611
SS	4	100	3	1	6212	10.46	8.43	6.84	5.03	3.72	2.33	1.24	905,811	33,403	17,119
SS	4	100	3	2	9165	15.07	12.17	9.99	7.42	5.58	3.54	1.93	929,510	38,297	16,691
SS	4	100	3	2	9149	15.31	12.19	9.94	7.40	5.54	3.49	1.93	831,934	39,359	16,767
SS	4	100	3	3	9176	15.28	12.18	9.96	7.39	5.52	3.48	1.87	853,936	38,607	16,882
SS	4	100	3	3	9149	15.05	12.19	9.99	7.39	5.57	3.54	1.91	944,307	37,322	16,738
SS	4	100	4	1	6185	10.11	8.11	6.57	4.79	3.52	2.22	1.21	896,870	34,374	17,939
SS	4	100	4	1	6276	10.20	8.05	6.54	4.83	3.61	2.20	1.21	882,080	36,264	18,023
SS	4	100	4	2	9136	14.91	12.08	9.90	7.27	5.39	3.41	1.79	978,366	34,284	17,328
SS	4	100	4	2	9176	15.05	11.94	9.83	7.29	5.48	3.40	1.79	875,242	38,975	17,143
SS	4	100	4	3	9141	14.90	12.09	9.91	7.25	5.38	3.40	1.78	984,563	33,935	17,381
SS	4	100	4	3	9196	15.08	12.00	9.86	7.30	5.51	3.39	1.74	896,129	37,931	17,191
SS	4	100	5	1	6133	10.20	8.17	6.66	4.89	3.66	2.28	1.27	891,792	35,543	17,209
SS	4	100	5	2	9069	14.89	12.03	9.92	7.34	5.52	3.45	1.91	1,002,290	34,809	16,923
SS	4	100	5	3	9033	14.84	11.99	9.89	7.32	5.52	3.44	1.91	1,008,850	34,709	16,888
SS	4	100	6	1	6204	10.25	8.20	6.72	4.90	3.64	2.23	1.24	949,548	32,334	17,697
SS	4	100	6	2	9093	14.68	11.83	9.79	7.26	5.41	3.38	1.90	1,050,252	33,959	17,329
SS	4	100	6	3	9088	14.68	11.81	9.80	7.26	5.44	3.39	1.91	1,041,664	34,611	17,243

Note:

Date 1 – December 06, 2001
Date 2 – December 19, 2001
Date 3 – January 24, 2002
Date 4 – April 09, 2002

APPENDIX G

WEIGHT DROP DATA

TABLE G1. Weight Drop Device - Deflection data – Lane NN

Lane	ATL Passes (x 1,000)	Station	Load (lbs)	D0 (mils)	D6 (mils)	D12 (mils)	D18 (mils)	D24 (mils)	D30 (mils)	D36 (mils)
NN	**0**	**W**	2183	2.54	1.91	1.24	0.74	0.66	0.65	0.77
NN	**0**	**V**	2100	2.40	1.45	0.72	0.63	0.50	0.36	0.64
NN	**0**	**M**	2192	2.51	1.48	0.76	0.49	0.39	0.59	0.76
NN	**0**	**E**	2283	2.50	2.00	1.31	0.60	0.36	0.20	0.75
NN	**23**	**W**	2558	2.78	1.79	1.06	0.41	0.19	0.32	0.93
NN	**23**	**V**	2275	3.45	2.63	1.76	0.89	0.63	0.49	0.87
NN	**23**	**M**	2458	3.86	2.61	1.50	0.89	0.73	0.70	0.86
NN	**23**	**E**	2567	3.45	2.20	1.28	0.75	0.65	0.54	0.87
NN	**42**	**W**	2492	3.55	2.93	2.06	1.21	0.86	0.68	0.89
NN	**42**	**V**	2250	4.49	3.38	2.18	1.26	0.95	0.86	1.00
NN	**42**	**M**	2508	3.71	3.04	2.13	1.28	0.99	0.79	0.95
NN	**42**	**E**	2250	4.55	3.26	1.86	0.94	0.71	0.64	0.91
NN	**60**	**W**	2500	2.96	2.45	1.73	0.98	0.73	0.66	0.94
NN	**60**	**V**	2442	3.55	2.76	1.83	0.88	0.43	0.46	0.85
NN	**60**	**M**	2117	2.61	2.31	1.86	1.40	1.26	1.11	1.06
NN	**60**	**E**	2525	2.86	1.34	1.06	0.69	0.49	0.50	0.84
NN	**82**	**W**	2633	2.76	1.90	1.45	0.95	0.86	0.84	0.97
NN	**82**	**V**	2533	3.50	2.10	1.08	0.38	0.54	0.54	0.94
NN	**82**	**M**	2358	4.04	2.94	1.85	0.89	0.79	0.84	0.99
NN	**82**	**E**	2542	4.89	3.76	2.39	1.06	0.70	0.49	0.94
NN	**100**	**W**	2500	3.73	2.89	2.00	1.26	1.25	1.09	1.04
NN	**100**	**V**	2517	3.85	2.71	1.68	0.86	0.68	0.59	0.89
NN	**100**	**M**	2500	3.31	2.39	1.45	0.67	0.28	0.46	0.91
NN	**100**	**E**	2608	4.66	3.25	2.06	1.15	0.99	0.89	1.05
NN	**130**	**W**	2708	3.10	2.25	1.23	0.84	0.49	0.59	0.96
NN	**130**	**V**	2375	4.66	3.54	2.19	1.15	0.67	0.56	0.89
NN	**130**	**M**	2600	3.63	2.28	1.21	0.79	0.78	0.45	0.74
NN	**130**	**E**	2850	4.41	3.39	2.31	1.38	1.16	0.95	1.04
NN	**150**	**W**	2208	3.36	2.30	1.33	0.78	0.65	0.49	0.86
NN	**150**	**V**	2517	2.65	2.09	1.46	1.03	0.80	0.71	0.94
NN	**150**	**M**	2358	2.74	1.95	1.55	1.09	0.94	0.78	0.96
NN	**150**	**E**	2592	4.85	3.45	2.04	1.00	0.86	0.64	0.93
NN	**176**	**W**	2617	3.68	2.99	2.09	1.09	0.90	0.70	0.91
NN	**176**	**V**	2275	4.76	3.21	2.04	1.24	0.92	0.73	0.89
NN	**176**	**M**	2617	4.24	3.06	1.70	0.85	0.69	0.63	0.95
NN	**176**	**E**	2400	4.65	3.21	1.78	0.88	0.71	0.74	0.99
NN	**208**	**W**	2475	3.30	2.90	2.11	1.36	1.08	0.89	1.04
NN	**208**	**V**	2617	4.19	2.90	1.80	1.03	0.90	0.81	0.94
NN	**208**	**M**	2542	4.29	2.99	1.75	0.96	0.61	0.65	1.01
NN	**208**	**E**	2750	4.10	2.81	1.63	0.88	0.68	0.71	0.96
NN	**276**	**W**	2492	4.30	3.93	3.43	1.75	1.58	1.68	0.85
NN	**276**	**V**	2275	4.15	2.95	1.45	1.03	0.61	0.45	0.80
NN	**276**	**M**	2475	5.68	3.69	3.28	2.60	2.53	2.16	1.09
NN	**276**	**E**	1692	4.94	2.94	1.31	0.73	0.45	0.34	0.64
NN	**500**	**W**	2492	5.46	3.78	2.06	0.87	0.55	0.41	0.71
NN	**500**	**V**	2608	5.10	3.28	1.98	1.24	0.95	0.73	0.91
NN	**500**	**M**	2400	4.76	3.03	2.04	1.20	0.73	0.44	0.95
NN	**500**	**E**	2333	5.94	3.65	3.05	2.18	1.70	1.09	0.70

TABLE G2. Weight Drop Device - Deflection data – Lane NS

Lane	ATL Passes (x 1,000)	Station	Load (lbs)	D0 (mils)	D6 (mils)	D12 (mils)	D18 (mils)	D24 (mils)	D30 (mils)	D36 (mils)
NS	**0**	**V**	2283	3.01	2.06	1.38	0.95	0.85	0.76	0.70
NS	**0**	**M**	1633	2.33	1.64	0.81	0.29	0.30	0.27	0.64
NS	**0**	**E**	2508	2.56	1.94	1.39	0.91	0.68	0.60	0.76
NS	**23**	**W**	2650	3.09	2.41	2.09	1.28	1.11	0.76	0.89
NS	**23**	**V**	2133	3.01	2.19	1.46	0.94	0.69	0.55	0.92
NS	**23**	**M**	2800	2.90	1.81	0.93	0.45	0.41	0.40	0.75
NS	**23**	**E**	1983	3.93	2.56	1.46	0.71	0.55	0.39	0.76
NS	**42**	**W**	2475	3.20	2.23	1.31	0.88	0.75	0.66	0.94
NS	**42**	**V**	2475	2.93	1.68	0.98	0.38	0.66	0.56	0.80
NS	**42**	**M**	2567	2.33	1.94	1.30	0.89	0.59	0.51	0.80
NS	**42**	**E**	2267	4.30	2.75	1.41	0.65	0.55	0.54	0.76
NS	**60**	**W**	2392	3.05	1.89	1.33	1.00	0.98	0.97	0.96
NS	**60**	**V**	2283	3.93	2.58	1.73	1.10	1.03	0.84	1.00
NS	**60**	**M**	2517	3.26	2.18	1.45	0.76	0.61	0.45	0.77
NS	**60**	**E**	2558	4.43	2.99	1.41	0.66	0.80	0.51	0.85
NS	**82**	**W**	2558	2.01	1.58	1.09	0.72	0.75	0.69	0.85
NS	**82**	**V**	2617	3.88	2.81	1.70	0.89	0.78	0.61	0.94
NS	**82**	**M**	2600	3.60	2.35	1.29	0.65	0.41	0.28	0.75
NS	**82**	**E**	2283	4.68	3.28	1.80	1.84	0.76	0.35	0.75
NS	**100**	**W**	2575	2.68	2.10	1.30	0.60	0.34	0.31	0.84
NS	**100**	**V**	2467	3.16	2.19	1.43	0.90	0.73	0.76	0.95
NS	**100**	**M**	2542	3.98	3.11	2.13	1.30	1.15	0.96	0.95
NS	**100**	**E**	2467	4.53	2.96	1.95	1.24	1.06	0.98	0.99
NS	**130**	**W**	2475	2.54	1.65	0.99	0.65	0.51	0.44	0.74
NS	**130**	**V**	2475	3.68	2.59	1.39	0.55	0.49	0.51	0.84
NS	**130**	**M**	2450	3.63	2.84	1.59	0.75	0.53	0.56	0.88
NS	**130**	**E**	2583	3.58	2.73	1.66	0.91	0.60	0.59	0.89
NS	**150**	**W**	2392	3.04	2.09	1.13	0.56	0.43	0.19	0.71
NS	**150**	**V**	2575	3.40	2.28	1.30	0.85	0.58	0.58	0.86
NS	**150**	**M**	2642	3.65	2.23	1.13	0.60	0.50	0.50	0.81
NS	**150**	**E**	2517	4.24	2.79	1.50	0.78	0.66	0.55	0.84
NS	**176**	**W**	2667	3.48	2.44	1.46	0.75	0.65	0.64	0.96
NS	**176**	**V**	2725	3.69	2.44	1.30	0.64	0.55	0.53	0.89
NS	**176**	**M**	2542	4.05	2.99	1.83	0.93	0.73	0.64	0.94
NS	**176**	**E**	2758	4.50	3.11	1.48	0.55	0.38	0.28	0.73
NS	**208**	**W**	2692	2.63	2.35	1.76	1.21	1.00	0.88	0.98
NS	**208**	**V**	2450	4.40	3.31	2.10	1.05	0.94	0.94	0.97
NS	**208**	**M**	2508	3.60	2.24	1.20	0.74	0.48	0.52	0.81
NS	**208**	**E**	2583	4.76	3.00	1.51	0.75	0.64	0.54	0.84
NS	**276**	**W**	2517	3.61	2.81	1.85	1.06	1.00	0.94	1.04
NS	**276**	**V**	2375	5.15	2.83	1.28	0.51	0.47	0.46	0.75
NS	**276**	**M**	2533	4.33	3.28	2.13	1.25	0.94	0.76	0.75
NS	**276**	**E**	2317	6.11	4.25	2.29	1.34	1.29	0.91	0.74
NS	**500**	**W**	2425	5.09	3.14	1.89	1.25	1.10	0.90	0.95
NS	**500**	**V**	2550	5.69	4.06	2.54	1.33	1.10	0.83	0.99
NS	**500**	**M**	2375	5.03	2.64	2.24	1.84	1.19	0.94	1.16
NS	**500**	**E**	2492	5.05	3.35	1.69	0.65	0.49	0.39	0.73

TABLE G3. Weight Drop Device - Deflection data – Lane SN

Lane	ATL Passes (x 1,000)	Station	Load (lbs)	D0 (mils)	D6 (mils)	D12 (mils)	D18 (mils)	D24 (mils)	D30 (mils)	D36 (mils)
SN	**0**	**V**	2083	1.91	1.25	0.69	0.53	0.49	0.56	0.65
SN	**0**	**M**	2108	1.53	0.93	0.42	0.36	0.18	0.33	0.59
SN	**0**	**E**	2042	1.44	0.85	0.45	0.43	0.26	0.18	0.50
SN	**25**	**W**	2867	1.41	0.91	0.69	0.51	0.44	0.40	0.63
SN	**25**	**V**	2642	1.63	1.19	0.65	0.36	0.44	0.48	0.67
SN	**25**	**M**	2558	1.88	1.08	0.66	0.46	0.50	0.54	0.63
SN	**25**	**E**	2825	1.93	1.34	0.85	0.74	0.60	0.49	0.66
SN	**45**	**W**	2750	1.33	1.28	0.95	0.73	0.54	0.61	0.78
SN	**45**	**V**	2608	1.65	1.09	0.64	0.55	0.44	0.49	0.61
SN	**45**	**M**	2750	1.80	1.11	0.65	0.45	0.46	0.39	0.58
SN	**45**	**E**	2625	2.24	1.30	0.59	0.36	0.41	0.36	0.59
SN	**71**	**W**	2633	1.71	1.11	0.65	0.48	0.21	0.24	0.61
SN	**71**	**V**	2725	0.99	0.46	0.30	0.28	0.30	0.24	0.48
SN	**71**	**M**	2483	1.98	1.49	1.00	0.61	0.61	0.65	0.70
SN	**71**	**E**	2717	2.04	0.91	0.35	0.10	0.23	0.25	0.56
SN	**100**	**W**	2608	1.70	0.91	0.41	0.34	0.28	0.21	0.55
SN	**100**	**V**	2642	1.78	1.19	0.73	0.49	0.39	0.40	0.65
SN	**100**	**M**	2758	1.51	1.06	0.69	0.74	0.46	0.50	0.63
SN	**100**	**E**	2575	1.79	1.03	0.63	0.51	0.51	0.58	0.60
SN	**157**	**W**	2458	3.06	1.85	1.08	0.85	0.81	0.63	0.74
SN	**157**	**V**	2525	2.76	1.56	0.73	0.49	0.25	0.34	0.76
SN	**157**	**M**	2292	2.91	1.69	1.59	1.14	0.81	0.50	0.77
SN	**157**	**E**	2583	2.79	1.56	0.74	0.38	0.28	0.37	0.71
SN	**340**	**W**	2667	3.24	2.03	0.81	0.36	0.25	0.26	0.38
SN	**340**	**V**	2567	2.65	2.09	1.08	0.58	0.86	0.58	0.95
SN	**340**	**M**	2408	2.83	1.41	0.68	0.61	0.41	0.57	0.66
SN	**340**	**E**	2392	2.11	1.40	0.76	0.33	0.19	0.29	0.71
SN	**500**	**W**	2483	2.86	1.94	0.91	0.43	0.36	0.38	0.64
SN	**500**	**V**	2583	2.44	1.35	0.63	0.46	0.40	0.49	0.71
SN	**500**	**M**	2500	2.79	1.80	0.83	0.90	0.79	0.61	0.57
SN	**500**	**E**	2342	2.74	1.56	0.65	0.35	0.32	0.31	0.65

TABLE G4. Weight Drop Device - Deflection data – Lane SS

Lane	ATL Passes (x 1,000)	Station	Load (lbs)	D0 (mils)	D6 (mils)	D12 (mils)	D18 (mils)	D24 (mils)	D30 (mils)	D36 (mils)
SS	**0**	**V**	2325	2.40	1.81	0.91	0.90	0.39	0.36	0.54
SS	**0**	**M**	2383	2.38	1.56	0.87	0.55	0.29	0.29	0.53
SS	**0**	**E**	2258	2.51	1.86	1.08	0.65	0.47	0.38	0.51
SS	**25**	**W**	2683	4.29	2.98	1.75	0.84	0.60	0.42	0.66
SS	**25**	**V**	2642	4.43	3.19	1.89	1.05	1.00	0.85	0.80
SS	**25**	**M**	2817	3.89	3.31	2.28	1.39	1.14	0.96	0.90
SS	**25**	**E**	2625	4.69	3.63	2.36	1.33	1.06	0.85	0.89
SS	**45**	**W**	2633	4.81	3.73	2.40	1.44	1.09	0.88	0.85
SS	**45**	**V**	2617	3.80	2.66	1.64	0.95	0.78	0.59	0.75
SS	**45**	**M**	2875	4.55	3.25	1.55	0.68	0.63	0.45	0.73
SS	**45**	**E**	2567	4.36	3.08	1.95	1.05	0.86	0.74	0.78
SS	**71**	**W**	2608	4.20	3.24	2.08	1.03	0.65	0.49	0.71
SS	**71**	**V**	2533	3.24	1.44	0.88	0.25	0.23	0.34	0.71
SS	**71**	**M**	2475	4.75	4.11	2.66	1.34	0.71	0.48	0.75
SS	**71**	**E**	2625	3.50	2.70	1.56	0.80	0.46	0.10	0.68
SS	**100**	**W**	2633	4.19	3.28	2.23	1.40	0.95	0.79	0.83
SS	**100**	**V**	2517	4.00	2.79	1.58	0.86	0.79	0.65	0.78
SS	**100**	**M**	2358	4.38	3.15	1.64	0.73	0.38	0.48	0.80
SS	**100**	**E**	2808	4.45	2.83	1.50	0.53	0.35	0.29	0.69
SS	**157**	**W**	2567	5.46	3.49	1.88	0.82	0.44	0.41	0.86
SS	**157**	**V**	2383	6.55	4.34	2.15	1.10	0.70	0.54	0.84
SS	**157**	**M**	2350	6.40	4.43	2.28	0.89	0.57	0.50	0.89
SS	**157**	**E**	2492	7.08	4.98	2.65	1.39	0.55	0.36	0.86
SS	**340**	**W**	2417	6.10	4.61	2.64	0.99	0.59	0.45	0.78
SS	**340**	**V**	2542	6.05	4.39	2.44	1.04	0.41	0.54	0.90
SS	**340**	**M**	2450	6.43	4.49	2.45	0.91	0.34	0.39	0.74
SS	**340**	**E**	2175	6.89	4.96	2.84	1.30	0.75	0.71	0.94
SS	**500**	**W**	2558	5.90	3.86	1.89	0.71	0.45	0.29	0.54
SS	**500**	**V**	2475	5.43	4.05	2.54	1.19	0.74	0.59	0.80
SS	**500**	**M**	2708	5.33	4.09	1.95	0.59	0.40	0.24	0.56
SS	**500**	**E**	2242	5.93	4.13	2.11	1.05	0.70	0.42	0.75

TABLE G5. Backcalculated Layer Moduli (psi)

Lane	Station	Passes	AC	Temp*	AC-Corrected*	BASE	SUBGRADE
NN	W	0	404160	67	390,170	237873	22700
NN	V	23	588653	69	609,761	67898	22604
NN	M	23	211149	69	218,720	120502	24309
NN	E	23	189825	69	196,632	163373	30085
NN	W	42	700470	69	725,587	108879	17757
NN	V	42	275813	69	285,703	92302	15280
NN	M	42	556925	69	576,895	137867	16033
NN	E	42	234233	69	242,632	58952	20461
NN	W	60	756894	70	812,148	146822	20970
NN	E	82	643258	70	690,216	22228	22231
NN	V	100	295932	70	317,535	94688	24905
NN	E	100	201130	70	215,813	120955	18798
NN	V	130	453437	72	522,056	40212	19794
NN	E	130	359504	72	413,908	161974	16444
NN	W	150	233884	74	288,935	116159	25071
NN	E	150	252638	74	312,104	68074	21410
NN	W	176	625259	74	772,431	109078	19243
NN	M	176	278979	74	344,645	74792	25666
NN	W	208	871374	76	1,155,060	190205	13669
NN	V	208	210632	76	279,206	139877	21183
NN	V	276	231743	87	452,592	69523	23174
NN	W	500	316766	89	663,802	24775	25185
NN	M	500	161863	89	339,194	88659	20281
NS	E	0	516798	67	498,908	190828	18618
NS	W	23	742542	69	769,168	179254	11956
NS	V	23	327797	69	339,551	117655	16950
NS	M	23	294750	69	305,319	107485	45034
NS	E	23	212541	69	220,162	49058	21715
NS	W	42	230582	69	238,850	156550	19990
NS	E	42	194943	69	201,933	49621	25805
NS	M	60	307595	70	330,050	104830	24703
NS	V	82	327229	70	351,117	82508	21053
NS	M	82	345822	70	371,067	58358	34575
NS	M	100	358229	70	384,380	121387	12100
NS	W	130	225440	72	259,556	198055	29294
NS	E	130	501506	72	577,399	69696	22609
NS	W	150	427560	74	528,198	61291	35531
NS	E	150	206503	74	255,109	67850	24122
NS	W	176	319890	74	395,185	97597	25188
NS	V	176	269021	74	332,343	79191	31207
NS	M	176	363328	74	448,848	66127	20249
NS	E	176	374544	74	462,704	31184	38901
NS	E	208	178571	76	236,707	56083	26029
NS	W	276	358867	87	700,864	128419	14306
NS	M	276	353447	87	690,278	76679	15072
NS	V	500	221505	89	464,177	53841	14108
NS	E	500	279541	89	585,795	29091	29093

TABLE G5. Backcalculated Layer Moduli (psi) - continued

Lane	Station	Passes	AC	Temp*	AC-Corrected*	BASE	SUBGRADE
SN	E	0	311864	67	301,068	194917	16916
SN	E	25	363315	68	363,315	305416	24053
SN	W	100	246682	70	264,690	216445	19919
SN	M	157	164288	89	344,275	169239	24076
SN	W	157	130290	89	273,030	172353	30509
SN	E	500	214072	82	350,558	74961	17357
SS	W	0	590295	67	569,861	52221	23483
SS	V	0	424145	67	409,463	146529	22366
SS	E	0	427838	67	413,028	126794	21612
SS	W	25	306356	68	306,356	64116	20638
SS	V	25	235485	68	235,485	102029	13387
SS	E	25	338260	68	338,260	83103	11063
SS	W	45	327478	68	327,478	83510	10529
SS	V	45	267694	68	267,694	113524	16037
SS	M	45	254806	68	254,806	57443	25485
SS	E	45	247430	68	247,430	92065	13872
SS	W	71	502750	70	539,451	54405	17100
SS	M	71	725851	70	778,839	26635	14422
SS	E	71	1022093	70	1,096,706	27752	29363
SS	W	100	438754	70	470,783	94468	11187
SS	V	100	225607	70	242,076	97257	16450
SS	E	100	336735	70	361,317	39103	34768
SS	W	157	228138	89	478,077	34375	22818
SS	V	157	148984	89	312,205	32956	15396
SS	M	157	197501	89	413,875	24042	17739
SS	E	157	277307	89	581,113	19073	15991
SS	W	340	340411	87	664,819	19671	17173
SS	E	340	198026	87	386,743	24225	11722
SS	W	500	246250	82	403,252	24625	24625
SS	V	500	331931	82	543,560	38166	14084
SS	M	500	337690	82	552,991	22667	28981
SS	E	500	177860	82	291,258	32992	14874